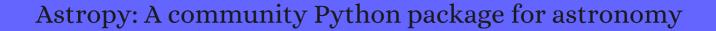
# CITATION REPORT List of articles citing



DOI: 10.1051/0004-6361/201322068 Astronomy and Astrophysics, 2013, 558, A33.

Source: https://exaly.com/paper-pdf/56579368/citation-report.pdf

Version: 2024-04-28

This report has been generated based on the citations recorded by exaly.com for the above article. For the latest version of this publication list, visit the link given above.

The third column is the impact factor (IF) of the journal, and the fourth column is the number of citations of the article.

#	Paper	IF	Citations
2212	A MEASUREMENT OF THE TURBULENCE-DRIVEN DENSITY DISTRIBUTION IN A NON-STAR-FORMING MOLECULAR CLOUD. <b>2013</b> , 779, 50		33
2211	DISCOVERY AND REDSHIFT OF AN OPTICAL AFTERGLOW IN 71 deg 2 : iPTF13bxl AND GRB 130702A. <b>2013</b> , 776, L34		49
2210	2MASS wide-field extinction maps. <i>Astronomy and Astrophysics</i> , <b>2014</b> , 565, A18	5.1	28
2209	An edge-on translucent dust disk around the nearest AGB star, L2Puppis. <i>Astronomy and Astrophysics</i> , <b>2014</b> , 564, A88	5.1	31
2208	Astrometric planet search around southern ultracool dwarfs. <i>Astronomy and Astrophysics</i> , <b>2014</b> , 565, A20	5.1	32
2207	The dynamics and star-forming potential of the massive Galactic centre cloud G0.253+0.016. <i>Astronomy and Astrophysics</i> , <b>2014</b> , 568, A56	5.1	45
2206	CORRECTING FOR TELLURIC ABSORPTION: METHODS, CASE STUDIES, AND RELEASE OF THE TelFit CODE. <b>2014</b> , 148, 53		50
2205	VERY LATE PHOTOMETRY OF SN 2011fe. <b>2014</b> , 796, L26		31
2204	TYPE Ia SUPERNOVA RATE MEASUREMENTS TO REDSHIFT 2.5 FROM CANDELS: SEARCHING FOR PROMPT EXPLOSIONS IN THE EARLY UNIVERSE. <b>2014</b> , 148, 13		97
2203	YSOVAR: MID-INFRARED VARIABILITY IN THE STAR-FORMING REGION LYNDS 1688. <b>2014</b> , 148, 122		35
2202	THE MASS DISTRIBUTION OF COMPANIONS TO LOW-MASS WHITE DWARFS. <b>2014</b> , 797, L32		17
2201	CONSTRAINING THE DUST COMA PROPERTIES OF COMET C/SIDING SPRING (2013 A1) AT LARGE HELIOCENTRIC DISTANCES. <b>2014</b> , 797, L8		21
2200	DISCOVERY OF EIGHTz~ 6 QUASARS FROM Pan-STARRS1. <b>2014</b> , 148, 14		112
2199	THE MILKY WAY PROJECT: LEVERAGING CITIZEN SCIENCE AND MACHINE LEARNING TO DETECT INTERSTELLAR BUBBLES. <b>2014</b> , 214, 3		27
2198	A PARAMETRIC MODELING APPROACH TO MEASURING THE GAS MASSES OF CIRCUMSTELLAR DISKS. <b>2014</b> , 788, 59		188
2197	VARYING [C II]/[N II] LINE RATIOS IN THE INTERACTING SYSTEM BR1202-0725 AT $z = 4.7$ . <b>2014</b> , 782, L17	7	42
2196	TIRSPEC: TIFR Near Infrared Spectrometer and Imager. <b>2014</b> , 03, 1450006		23

2195	EXPANDING SHELL AND STAR FORMATION IN THE INFRARED DUST BUBBLE N6. <b>2014</b> , 797, 40	13
2194	Updated point spread function simulations for JWST with WebbPSF. <b>2014</b> ,	18
2193	13CO filaments in the Taurus molecular cloud. <b>2014</b> , 444, 2507-2524	40
2192	The second data release of the INT Photometric H&urvey of the Northern Galactic Plane (IPHAS DR2). <b>2014</b> , 444, 3230-3257	99
2191	A measurement of the millimetre emission and the Sunyaev Zel'dovich effect associated with low-frequency radio sources. <b>2014</b> , 445, 460-478	32
2190	Signatures of warm carbon monoxide in protoplanetary discs observed with Herschel SPIRE?. <b>2014</b> , 444, 3911-3925	16
2189	The RoboPol pipeline and control system. <b>2014</b> , 442, 1706-1717	37
2188	Reference image selection for difference imaging analysis*. <b>2014</b> , 442, 259-272	3
2187	A compact, metal-rich, kpc-scale outflow in FBQS J02090438: detailed diagnostics from HST/COS extreme UV observations. <b>2014</b> , 440, 3317-3340	25
2186	A spectral synthesis code for rapid modelling of supernovae. <b>2014</b> , 440, 387-404	79
2185	The colour distribution of galaxies at redshift five. <b>2014</b> , 440, 3714-3725	51
2184	M31 satellite masses compared to IDM subhaloes. <b>2014</b> , 440, 3511-3519	69
2183	COMPARING SIMULATED EMISSION FROM MOLECULAR CLOUDS USING EXPERIMENTAL DESIGN. <b>2014</b> , 783, 93	9
2182	EXTENDED HCN AND HCO+EMISSION IN THE STARBURST GALAXY M82. <b>2014</b> , 797, 134	16
2181	THE STAR FORMATION HISTORIES OF LOCAL GROUP DWARF GALAXIES. II. SEARCHING FOR SIGNATURES OF REIONIZATION. <b>2014</b> , 789, 148	108
2180	SMA OBSERVATIONS ON FAINT SUBMILLIMETER GALAXIES WITHS8502014, 789, 12	28
2179	COMPARING M31 AND MILKY WAY SATELLITES: THE EXTENDED STAR FORMATION HISTORIES OF ANDROMEDA II AND ANDROMEDA XVI. <b>2014</b> , 789, 24	27
2178	SUBARCSECOND IMAGING OF THE NGC 6334 I(N) PROTOCLUSTER: TWO DOZEN COMPACT SOURCES AND A MASSIVE DISK CANDIDATE. <b>2014</b> , 788, 187	41

2177	A MOLECULAR LINE SCAN IN THE HUBBLE DEEP FIELD NORTH. <b>2014</b> , 782, 78	54
2176	The SAMI Pilot Survey: the kinematic morphologydensity relation in Abell 85, Abell 168 and Abell 2399. <b>2014</b> , 443, 485-503	56
2175	A theory for the excitation of CO in star-forming galaxies. <b>2014</b> , 442, 1411-1428	72
2174	Exposing Sgr tidal debris behind the Galactic disc with M giants selected in WISE 2MASS. <b>2014</b> , 446, 3110-311	7 24
2173	Probing the interstellar medium of NGC 1569 with Herschel?. <b>2014</b> , 445, 1003-1022	4
2172	Two physical regimes for the giant H ii regions and giant molecular clouds in the Antennae galaxies. <b>2014</b> , 445, 1412-1423	15
2171	Early-time polarized optical light curve of GRB 131030A. <b>2014</b> , 445, L114-L118	10
2170	The discrepancy between dynamical and stellar masses in massive compact galaxies traces non-homology. <b>2014</b> , 440, 1634-1648	14
2169	A TALE OF TWO FEEDBACKS: STAR FORMATION IN THE HOST GALAXIES OF RADIO AGNs. <b>2014</b> , 784, 137	30
2168	THE STAR FORMATION HISTORIES OF LOCAL GROUP DWARF GALAXIES. I.HUBBLE SPACE TELESCOPE/WIDE FIELD PLANETARY CAMERA 2 OBSERVATIONS. <b>2014</b> , 789, 147	286
2167	ALMA OBSERVATIONS OF A MISALIGNED BINARY PROTOPLANETARY DISK SYSTEM IN ORION. <b>2014</b> , 796, 120	37
2166	HerschelOBSERVATIONS OF DUST AROUND THE HIGH-MASS X-RAY BINARY GX 301-2. <b>2014</b> , 797, 114	7
2165	THE GREEN BANK TELESCOPE MAPS THE DENSE, STAR-FORMING GAS IN THE NEARBY STARBURST GALAXY M82. <b>2014</b> , 780, L13	30
2164	WARM DUST AROUND COOL STARS: FIELD M DWARFS WITHWISE12 OR 22 th EXCESS EMISSION. <b>2014</b> , 794, 146	27
2163	STATISTICAL SEARCHES FOR MICROLENSING EVENTS IN LARGE, NON-UNIFORMLY SAMPLED TIME-DOMAIN SURVEYS: A TEST USING PALOMAR TRANSIENT FACTORY DATA. <b>2014</b> , 781, 35	10
2162	INFERRING THE GRAVITATIONAL POTENTIAL OF THE MILKY WAY WITH A FEW PRECISELY MEASURED STARS. <b>2014</b> , 794, 4	37
2161	THE FIRST TWO YEARS OF ELECTROMAGNETIC FOLLOW-UP WITH ADVANCED LIGO AND VIRGO. <b>2014</b> , 795, 105	141
2160	DARK MATTER HALOS IN GALAXIES AND GLOBULAR CLUSTER POPULATIONS. <b>2014</b> , 787, L5	78

2159	The massfinetallicityfitar formation rate relation at \$boldsymbol {z gtrsim 2}\$ with 3D Hubble Space Telescope. <b>2014</b> , 440, 2300-2312		74
2158	DISTRIBUTED LOW-MASS STAR FORMATION IN THE IRDC G34.43+00.24. <b>2014</b> , 791, 108		26
2157	SPECTROSCOPY OF THE INNER COMPANION OF THE PULSAR PSR J0337+1715. <b>2014</b> , 783, L23		19
2156	RESOLVED IMAGES OF THE PROTOPLANETARY DISK AROUND HD 100546 WITH ALMA. <b>2014</b> , 788, L34		63
2155	A STUDY OF DUST AND GAS AT MARS FROM COMET C/2013 A1 (SIDING SPRING). <b>2014</b> , 792, L16		21
2154	THE PANCHROMATIC HUBBLE ANDROMEDA TREASURY. VI. THE RELIABILITY OF FAR-ULTRAVIOLET FLUX AS A STAR FORMATION TRACER ON SUBKILOPARSEC SCALES. <b>2014</b> , 788, 12		7
2153	A 1.05M?COMPANION TO PSR J22220137: THE COOLEST KNOWN WHITE DWARF?. <b>2014</b> , 789, 119		17
2152	Comprehensive data reduction package for the Immersion GRating INfrared Spectrograph: IGRINS. <b>2014</b> , 53, 1647-1656		5
2151	Spectroscopic analysis in the virtual observatory environment with SPLAT-VO. <b>2014</b> , 7-8, 108-120		15
2150	Orion revisited. <i>Astronomy and Astrophysics</i> , <b>2014</b> , 564, A29	5.1	46
2150 2149	Orion revisited. <i>Astronomy and Astrophysics</i> , <b>2014</b> , 564, A29  AHerschelview of IC 1396 A: Unveiling the different sequences of star formation. <i>Astronomy and Astrophysics</i> , <b>2014</b> , 562, A131	5.1	46 12
2149	AHerschelview of IC 1396 A: Unveiling the different sequences of star formation. <i>Astronomy and</i>		
2149	AHerschelview of IC 1396 A: Unveiling the different sequences of star formation. <i>Astronomy and Astrophysics</i> , <b>2014</b> , 562, A131	5.1	12
2149 2148	AHerschelview of IC 1396 A: Unveiling the different sequences of star formation. <i>Astronomy and Astrophysics</i> , <b>2014</b> , 562, A131  Water in low-mass star-forming regions withHerschel. <i>Astronomy and Astrophysics</i> , <b>2014</b> , 572, A81  Optical polarization map of the Polaris Flare with RoboPol. <b>2015</b> , 452, 715-726	5.1	12
2149 2148 2147	AHerschelview of IC 1396 A: Unveiling the different sequences of star formation. <i>Astronomy and Astrophysics</i> , <b>2014</b> , 562, A131  Water in low-mass star-forming regions withHerschel. <i>Astronomy and Astrophysics</i> , <b>2014</b> , 572, A81  Optical polarization map of the Polaris Flare with RoboPol. <b>2015</b> , 452, 715-726	5.1	12 21 19
2149 2148 2147 2146	AHerschelview of IC 1396 A: Unveiling the different sequences of star formation. <i>Astronomy and Astrophysics</i> , <b>2014</b> , 562, A131  Water in low-mass star-forming regions withHerschel. <i>Astronomy and Astrophysics</i> , <b>2014</b> , 572, A81  Optical polarization map of the Polaris Flare with RoboPol. <b>2015</b> , 452, 715-726  Galaxy morphology and star formation in the Illustris Simulation atz'='0. <b>2015</b> , 454, 1886-1908	5.1	12 21 19 116
2149 2148 2147 2146 2145	AHerschelview of IC 1396 A: Unveiling the different sequences of star formation. <i>Astronomy and Astrophysics</i> , <b>2014</b> , 562, A131  Water in low-mass star-forming regions withHerschel. <i>Astronomy and Astrophysics</i> , <b>2014</b> , 572, A81  Optical polarization map of the Polaris Flare with RoboPol. <b>2015</b> , 452, 715-726  Galaxy morphology and star formation in the Illustris Simulation atz'='0. <b>2015</b> , 454, 1886-1908  The dependence of the AV prior for SN'ia on host mass and disc inclination. <b>2015</b> , 451, 2390-2398  SLUG Btochastically lighting up galaxies IIII. A suite of tools for simulated photometry,	5.1	12 21 19 116

2141	The SAMI Galaxy Survey: unveiling the nature of kinematically offset active galactic nuclei. <b>2015</b> , 451, 2780-2792	15
2140	Wavelength self-calibration and sky subtraction for Fabry <b>P</b> fot interferometers: applications to OSIRIS. <b>2015</b> , 454, 1387-1392	2
2139	Filament identification through mathematical morphology. <b>2015</b> , 452, 3435-3450	89
2138	IDENTIFICATION OF A CLASS OF LOW-MASS ASYMPTOTIC GIANT BRANCH STARS STRUGGLING TO BECOME CARBON STARS IN THE MAGELLANIC CLOUDS. <b>2015</b> , 810, 116	27
2137	X-RAY OUTBURSTS OF ESO 243-49 HLX-1: COMPARISON WITH GALACTIC LOW-MASS X-RAY BINARY TRANSIENTS. <b>2015</b> , 811, 23	13
2136	CONSTRUCTING A FLEXIBLE LIKELIHOOD FUNCTION FOR SPECTROSCOPIC INFERENCE. <b>2015</b> , 812, 128	73
2135	EIGHT ULTRA-FAINT GALAXY CANDIDATES DISCOVERED IN YEAR TWO OF THE DARK ENERGY SURVEY. <b>2015</b> , 813, 109	329
2134	EXCITATION MECHANISMS FOR HCN(10) AND HCO+(10) IN GALAXIES FROM THE GREAT OBSERVATORIES ALL-SKY LIRG SURVEY. <b>2015</b> , 814, 39	55
2133	THE EARLY ALMA VIEW OF THE FU Ori OUTBURST SYSTEM. <b>2015</b> , 812, 134	24
2132	WEAK TURBULENCE IN THE HD 163296 PROTOPLANETARY DISK REVEALED BY ALMA CO OBSERVATIONS. <b>2015</b> , 813, 99	172
2131	KINEMATICS AND CHEMISTRY OF RECENTLY DISCOVERED RETICULUM 2 AND HOROLOGIUM 1 DWARF GALAXIES. <b>2015</b> , 811, 62	104
2130	HUBBLE SPACE TELESCOPEPROPER MOTION (HSTPROMO) CATALOGS OF GALACTIC GLOBULAR CLUSTERS. III. DYNAMICAL DISTANCES AND MASS-TO-LIGHT RATIOs. <b>2015</b> , 812, 149	62
2129	KEPLERMONITORING OF AN L DWARF. II. CLOUDS WITH MULTI-YEAR LIFETIMES. <b>2015</b> , 813, 104	18
2128	ELEMENTAL DEPLETIONS IN THE MAGELLANIC CLOUDS AND THE EVOLUTION OF DEPLETIONS WITH METALLICITY. <b>2015</b> , 811, 78	26
2127	QUASAR CLASSIFICATION USING COLOR AND VARIABILITY. <b>2015</b> , 811, 95	46
2126	THE PANCHROMATIC HUBBLE ANDROMEDA TREASURY. VIII. A WIDE-AREA, HIGH-RESOLUTION MAP OF DUST EXTINCTION IN M31. <b>2015</b> , 814, 3	56
2125	MINING PLANET SEARCH DATA FOR BINARY STARS: THE DRACONIS SYSTEM. 2015, 815, 62	6
2124	NEAR-INFRARED VARIABILITY IN THE ORION NEBULA CLUSTER. <b>2015</b> , 150, 132	26

#### (2015-2015)

	2123	pairs. Astronomy and Astrophysics, <b>2015</b> , 576, A53	29
2	2122	PANCHROMATIC HUBBLE ANDROMEDA TREASURY. XIV. THE PERIODAGE RELATIONSHIP OF CEPHEID VARIABLES IN M31 STAR CLUSTERS. <b>2015</b> , 813, 31	13
2	2121	YSOVAR: MID-INFRARED VARIABILITY AMONG YSOs IN THE STAR FORMATION REGION GGD12-15. <b>2015</b> , 150, 145	16
2	2120	RAM PRESSURE STRIPPING OF THE LARGE MAGELLANIC CLOUDS DISK AS A PROBE OF THE MILKY WAYS CIRCUMGALACTIC MEDIUM. <b>2015</b> , 815, 77	93
2	2119	THE 2014 ALMA LONG BASELINE CAMPAIGN: OBSERVATIONS OF THE STRONGLY LENSED SUBMILLIMETER GALAXY HATLAS J090311.6+003906 AT $z=3.042$ . <b>2015</b> , 808, L4	70
2	2118	Learning from FITS: Limitations in use in modern astronomical research. <b>2015</b> , 12, 133-145	16
2	2117	The First Billion Years project: the escape fraction of ionizing photons in the epoch of reionization. <b>2015</b> , 451, 2544-2563	145
2	2116	Tracing quasar narrow-line regions across redshift: a library of high-S/N optical spectra. <b>2015</b> , 448, 3354-3362	5
2	2115	A reinterpretation of the TriangulumAndromeda stellar clouds: a population of halo stars kicked out of the Galactic disc. <b>2015</b> , 452, 676-685	73
2	2114	Decreased specific star formation rates in AGN host galaxies. <b>2015</b> , 452, 1841-1860	55
2			
	2113	New OB star candidates in the Carina Arm around Westerlund 2 from VPHAS+. <b>2015</b> , 450, 3855-3873	15
2		New OB star candidates in the Carina Arm around Westerlund 2 from VPHAS+. <b>2015</b> , 450, 3855-3873  High-order harmonics in light curves of Keplerplanets. <b>2015</b> , 453, L98-L102	20
2	2112	High-order harmonics in light curves of Keplerplanets. <b>2015</b> , 453, L98-L102	20
2	2111	High-order harmonics in light curves of Keplerplanets. <b>2015</b> , 453, L98-L102  CHEMISTRY OF THE MOST METAL-POOR STARS IN THE BULGE AND THEZ? 10 UNIVERSE. <b>2015</b> , 809, 110  Comparative internal kinematics of the H ii regions in interacting and isolated galaxies: implications	20
	2111	High-order harmonics in light curves of Keplerplanets. 2015, 453, L98-L102  CHEMISTRY OF THE MOST METAL-POOR STARS IN THE BULGE AND THEZ? 10 UNIVERSE. 2015, 809, 110  Comparative internal kinematics of the H ii regions in interacting and isolated galaxies: implications for massive star formation modes. 2015, 451, 1307-1330	20 38 14
2	2112 2111 2110 2109	High-order harmonics in light curves of Keplerplanets. 2015, 453, L98-L102  CHEMISTRY OF THE MOST METAL-POOR STARS IN THE BULGE AND THEZ? 10 UNIVERSE. 2015, 809, 110  Comparative internal kinematics of the H ii regions in interacting and isolated galaxies: implications for massive star formation modes. 2015, 451, 1307-1330  The neutral hydrogen cosmological mass density atz = 5. 2015, 452, 217-234  Far-infrared signatures and inner hole sizes of protoplanetary discs undergoing inside-out dust	20 38 14

2105	Galaxy Zoo: the dependence of the star formation tellar mass relation on spiral disc morphology. <b>2015</b> , 449, 820-827		51
2104	Calibration of the Swift-UVOT ultraviolet and visible grisms. <b>2015</b> , 449, 2514-2538		26
2103	Unifying X-ray scaling relations from galaxies to clusters. <b>2015</b> , 449, 3806-3826		87
2102	Galaxy interactions in compact groups III. Abundance and kinematic anomalies in HCG 91c. <b>2015</b> , 450, 2593-2614		22
2101	Two bright $z'>6$ quasars from VST ATLAS and a new method of optical plus mid-infrared colour selection. <b>2015</b> , 451, L16-L20		56
2100	Optical and X-ray profiles in the REXCESS sample of galaxy clusters*. <b>2015</b> , 448, 2644-2664		4
2099	A radio and X-ray study of the merging cluster A2319. <b>2015</b> , 448, 2495-2503		14
2098	YSOVAR: MID-INFRARED VARIABILITY OF YOUNG STELLAR OBJECTS AND THEIR DISKS IN THE CLUSTER IRAS 20050+2720. <b>2015</b> , 150, 118		16
2097	PANCHROMATIC HUBBLE ANDROMEDA TREASURY. XII. MAPPING STELLAR METALLICITY DISTRIBUTIONS IN M31. <b>2015</b> , 150, 189		21
2096	THE FIRST MILLIMETER DETECTION OF A NON-ACCRETING ULTRACOOL DWARF. <b>2015</b> , 815, 64		24
2095	Catalogues of isolated galaxies, isolated pairs, and isolated triplets in the local Universe. <i>Astronomy and Astrophysics</i> , <b>2015</b> , 578, A110	5.1	51
2094	DE082349 is a juvenile binary brown dwarf at 20.7 pc. <i>Astronomy and Astrophysics</i> , <b>2015</b> , 579, A61	5.1	9
2093	Accretion dynamics of EX Lupi in quiescence. Astronomy and Astrophysics, 2015, 580, A82	5.1	22
2092	XMM-Newtonand optical observations of the eclipsing polar CSS081231:071126+440405. <i>Astronomy and Astrophysics</i> , <b>2015</b> , 583, A130	5.1	7
2091	Measuring star formation with resolved observations: the test case of M 33. <i>Astronomy and Astrophysics</i> , <b>2015</b> , 578, A8	5.1	28
2090	High-mass star-forming cloud G0.38+0.04 in the Galactic center dust ridge contains H2CO and SiO masers. <i>Astronomy and Astrophysics</i> , <b>2015</b> , 584, L7	5.1	18
2089	High spectral resolution monitoring of Nova V339 Delphini with TIGRE. <i>Astronomy and Astrophysics</i> , <b>2015</b> , 581, A134	5.1	8
2088	TheHerschel/PACS view of the Cep OB2 region: Global protoplanetary disk evolution and clumpy star formation. <i>Astronomy and Astrophysics</i> , <b>2015</b> , 573, A19	5.1	12

#### (2015-2015)

2087	Evidence for two spatially separated UV continuum emitting regions in the Cloverleaf broad absorption line quasar. <i>Astronomy and Astrophysics</i> , <b>2015</b> , 582, A109	5.1	11	
2086	Cosmography of OB stars in the solar neighbourhood. <i>Astronomy and Astrophysics</i> , <b>2015</b> , 584, A26	5.1	37	
2085	The dust disk and companion of the nearby AGB star L2 Puppis. <i>Astronomy and Astrophysics</i> , <b>2015</b> , 578, A77	5.1	44	
2084	The dense gas mass fraction in the W51 cloud and its protoclusters. <i>Astronomy and Astrophysics</i> , <b>2015</b> , 573, A106	5.1	36	
2083	StrEngrenuvbyphotometry of the peculiar globular cluster NGC 2419. <i>Astronomy and Astrophysics</i> , <b>2015</b> , 581, A72	5.1	12	
2082	ASteCA: Automated Stellar Cluster Analysis. Astronomy and Astrophysics, 2015, 576, A6	5.1	51	
2081	Astrometric planet search around southern ultracool dwarfs. <i>Astronomy and Astrophysics</i> , <b>2015</b> , 577, A15	5.1	11	
2080	HOROLOGIUM II: A SECOND ULTRA-FAINT MILKY WAY SATELLITE IN THE HOROLOGIUM CONSTELLATION. <b>2015</b> , 808, L39		109	
2079	THE ROTATION PERIOD AND MAGNETIC FIELD OF THE T DWARF 2MASSI J1047539+212423 MEASURED FROM PERIODIC RADIO BURSTS. <b>2015</b> , 808, 189		27	
2078	V899 MON: AN OUTBURSTING PROTOSTAR WITH A PECULIAR LIGHT CURVE, AND ITS TRANSITION PHASES. <b>2015</b> , 815, 4		18	
2077	Metal-enriched, subkiloparsec gas clumps in the circumgalactic medium of a faint $z'=2.5$ galaxy?. <b>2015</b> , 446, 18-37		89	
2076	Star formation quenching in simulated group and cluster galaxies: when, how, and why?. <b>2015</b> , 447, 969	-992	88	
2075	Taking the band function too far: a tale of two 岳. <b>2015</b> , 451, 1511-1521		28	
2074	Deep radio imaging of 47 Tuc identifies the peculiar X-ray source X9 as a new black hole candidate. <b>2015</b> , 453, 3919-3932		72	
2073	Spiral galaxies as progenitors of pseudo-bulge hosting S0s. <b>2015</b> , 450, 873-882		11	
2072	BAT AGN spectroscopic survey <b>[</b> ]. X-ray emission and high-ionization optical emission lines. <b>2015</b> , 454, 3622-3634		46	
2071	Galaxy Zoo: evidence for diverse star formation histories through the green valley. <b>2015</b> , 450, 435-453		91	
2070	New members of the TW Hydrae Association and two accreting M-dwarfs in ScorpiusCentaurus. <b>2015</b> , 453, 2221-2232		12	

2069	The brown dwarf atmosphere monitoring (BAM) project [II. Multi-epoch monitoring of extremely cool brown dwarfs. <b>2015</b> , 448, 3775-3783	13
2068	BIG BANG NUCLEOSYNTHESIS AND THE HELIUM ISOTOPE RATIO. <b>2015</b> , 812, L12	15
2067	THE 2014 ALMA LONG BASELINE CAMPAIGN: FIRST RESULTS FROM HIGH ANGULAR RESOLUTION OBSERVATIONS TOWARD THE HL TAU REGION. <b>2015</b> , 808, L3	698
2066	Herschel-ATLAS: the surprising diversity of dust-selected galaxies in the local submillimetre Universe. <b>2015</b> , 452, 397-430	43
2065	PROPERTIES OF THE NEARBY BROWN DWARF WISEP J180026.60+013453.1. <b>2015</b> , 150, 179	4
2064	The formation of a quadruple star system with wide separation. <b>2015</b> , 518, 213-5	74
2063	Client interfaces to the Virtual Observatory Registry. <b>2015</b> , 10, 88-98	2
2062	NO TIME FOR DEAD TIME: TIMING ANALYSIS OF BRIGHT BLACK HOLE BINARIES WITHNUSTAR. <b>2015</b> , 800, 109	58
2061	TIDAL STREAM MORPHOLOGY AS AN INDICATOR OF DARK MATTER HALO GEOMETRY: THE CASE OF PALOMAR 5. <b>2015</b> , 799, 28	50
2060	IN-SYNC. II. VIRIAL STARS FROM SUBVIRIAL CORESTHE VELOCITY DISPERSION OF EMBEDDED PRE-MAIN-SEQUENCE STARS IN NGC 1333. <b>2015</b> , 799, 136	70
2059	MAIN-SEQUENCE STARS MASQUERADING AS YOUNG STELLAR OBJECTS IN THE CENTRAL MOLECULAR ZONE. <b>2015</b> , 799, 53	31
2058	TWO LOCAL VOLUME DWARF GALAXIES DISCOVERED IN 21 cm EMISSION: PISCES A AND B. <b>2015</b> , 798, L21	30
2057	AN ALMA SURVEY OF SUBMILLIMETER GALAXIES IN THE EXTENDED CHANDRA DEEP FIELD SOUTH: NEAR-INFRARED MORPHOLOGIES AND STELLAR SIZES. <b>2015</b> , 799, 194	86
2056	THE SURVEY OF LINES IN M31 (SLIM): INVESTIGATING THE ORIGINS OF [C II] EMISSION. <b>2015</b> , 798, 24	27
2055	HDFITS: Porting the FITS data model to HDF5. <b>2015</b> , 12, 212-220	12
2054	ASDF: A new data format for astronomy. <b>2015</b> , 12, 240-251	25
2053	Far-ultraviolet morphology of star-forming filaments in cool core brightest cluster galaxies. <b>2015</b> , 451, 3768-3800	59
2052	The Virtual Astronomical Observatory: Re-engineering access to astronomical data. <b>2015</b> , 11, 190-209	8

2051	Reprint of: Client interfaces to the Virtual Observatory Registry. <b>2015</b> , 11, 91-101	1
2050	The SAMI Galaxy Survey: cubism and covariance, putting round pegs into square holes. <b>2015</b> , 446, 1551-1566	79
2049	The SAMI Galaxy Survey: Early Data Release. <b>2015</b> , 446, 1567-1583	108
2048	New low-mass members of the Octans stellar association and an updated 30個0´Myr lithium age. <b>2015</b> , 447, 1267-1281	40
2047	Missing stellar mass in SED fitting: spatially unresolved photometry can underestimate galaxy masses. <b>2015</b> , 452, 235-245	36
2046	A DISK-BASED DYNAMICAL MASS ESTIMATE FOR THE YOUNG BINARY AK SCO. <b>2015</b> , 806, 154	58
2045	Triggering optical AGN: the need for cold gas, and the indirect roles of galaxy environment and interactions. <b>2015</b> , 447, 110-116	34
2044	SoFiA: a flexible source finder for 3D spectral line data. <b>2015</b> , 448, 1922-1929	101
2043	The LOFAR Transients Pipeline. <b>2015</b> , 11, 25-48	47
2042	THE SINS/zC-SINF SURVEY OFz~ 2 GALAXY KINEMATICS: REST-FRAME MORPHOLOGY, STRUCTURE, AND COLORS FROM NEAR-INFRAREDHUBBLE SPACE TELESCOPEIMAGING. <b>2015</b> , 802, 101	44
2041	HUBBLE SPACE TELESCOPEPROPER MOTION (HSTPROMO) CATALOGS OF GALACTIC GLOBULAR CLUSTERS. II. KINEMATIC PROFILES AND MAPS. <b>2015</b> , 803, 29	110
2040	CONSTRAINING THE RADIO-LOUD FRACTION OF QUASARS ATz> 5.5. <b>2015</b> , 804, 118	63
2039	BEASTS OF THE SOUTHERN WILD: DISCOVERY OF NINE ULTRA FAINT SATELLITES IN THE VICINITY OF THE MAGELLANIC CLOUDS. <b>2015</b> , 805, 130	358
2038	THE HIGH-MASS STELLAR INITIAL MASS FUNCTION IN M31 CLUSTERS. <b>2015</b> , 806, 198	41
2037	THE FORMATION OF FILAMENTARY BUNDLES IN TURBULENT MOLECULAR CLOUDS. 2015, 807, 67	44
2036	THE SIZES OF CANDIDATE GALAXIESz~ 9🖽0: CONFIRMATION OF THE BRIGHT CANDELS SAMPLE AND RELATION WITH LUMINOSITY AND MASS. <b>2015</b> , 808, 6	47
2035	THE AGES, METALLICITIES, AND ELEMENT ABUNDANCE RATIOS OF MASSIVE QUENCHED GALAXIES AT \$zsimeq 1.6\$. <b>2015</b> , 808, 161	70
2034	EVIDENCE FOR ENHANCED PERSISTENT EMISSION DURING SUB-EDDINGTON THERMONUCLEAR BURSTS. <b>2015</b> , 801, 60	45

2033	THE STAR FORMATION HISTORIES OF LOCAL GROUP DWARF GALAXIES. III. CHARACTERIZING QUENCHING IN LOW-MASS GALAXIES. <b>2015</b> , 804, 136	61
2032	THE NEEDLE IN THE 100 deg2HAYSTACK: UNCOVERING AFTERGLOWS OFFERMIGRBs WITH THE PALOMAR TRANSIENT FACTORY. <b>2015</b> , 806, 52	39
2031	SimPEG: An open source framework for simulation and gradient based parameter estimation in geophysical applications. <b>2015</b> , 85, 142-154	107
2030	Toyz: A framework for scientific analysis of large datasets and astronomical images. <b>2015</b> , 13, 50-57	5
2029	End-to-end simulation of high-contrast imaging systems: methods and results for the PICTURE mission family. <b>2015</b> ,	2
2028	SAMP, the Simple Application Messaging Protocol: Letting applications talk to each other. <b>2015</b> , 11, 81-90	14
2027	REVEALING TEPHEIS SECRET COMPANION AND INTRIGUING PAST. 2015, 804, 144	212
2026	Mass ratio of the 2´pc binary brown dwarf LUH´16 and limits on planetary companions from astrometry. <b>2015</b> , 453, L103-L107	14
2025	ASSESSING MOLECULAR OUTFLOWS AND TURBULENCE IN THE PROTOSTELLAR CLUSTER SERPENS SOUTH. <b>2015</b> , 803, 22	32
2024	A RADIO-POLARIZATION AND ROTATION MEASURE STUDY OF THE GUM NEBULA AND ITS ENVIRONMENT. <b>2015</b> , 804, 22	32
2023	ORAC-DR: A generic data reduction pipeline infrastructure. <b>2015</b> , 9, 40-48	21
2022	SunPy <b>B</b> ython for solar physics. <b>2015</b> , 8, 014009	61
2021	EVOLUTION IN THE BLACK HOLE <b>C</b> ALAXY SCALING RELATIONS AND THE DUTY CYCLE OF NUCLEAR ACTIVITY IN STAR-FORMING GALAXIES. <b>2015</b> , 802, 14	40
2020	NUSTARANDSUZAKUX-RAY SPECTROSCOPY OF NGC 4151: EVIDENCE FOR REFLECTION FROM THE INNER ACCRETION DISK. <b>2015</b> , 806, 149	47
2019	BAND-9 ALMA OBSERVATIONS OF THE $[{rm{N}},{rm{II}}]$ 122th LINE AND FIR CONTINUUM IN TWO HIGH-zGALAXIES. <b>2015</b> , 806, 260	23
2018	ASYMMETRIC ACCRETION FLOWS WITHIN A COMMON ENVELOPE. <b>2015</b> , 803, 41	77
2017	Are rotating planes of satellite galaxies ubiquitous?. <b>2015</b> , 453, 3840-3848	27
2016	The first stars: formation under X-ray feedback. <b>2015</b> , 453, 4137-4148	17

2015	THE PANCHROMATICHUBBLEANDROMEDA TREASURY. XI. THE SPATIALLY RESOLVED RECENT STAR FORMATION HISTORY OF M31. <b>2015</b> , 805, 183		69
2014	THE ELEVENTH AND TWELFTH DATA RELEASES OF THE SLOAN DIGITAL SKY SURVEY: FINAL DATA FROM SDSS-III. <b>2015</b> , 219, 12		1504
2013	THE ARCONS PIPELINE: DATA REDUCTION FOR MKID ARRAYS. <b>2015</b> , 219, 14		13
2012	Chimenea and other tools: Automated imaging of multi-epoch radio-synthesis data with CASA. <b>2015</b> , 13, 38-49		8
2011	Gaia's potential for the discovery of circumbinary planets. <b>2015</b> , 447, 287-297		49
2010	HSTEMISSION LINE GALAXIES ATz~ 2: COMPARING PHYSICAL PROPERTIES OF LYMAN ALPHA AND OPTICAL EMISSION LINE SELECTED GALAXIES. <b>2016</b> , 817, 79		41
2009	SIMULATINGASTRO-HOBSERVATIONS OF SLOSHING GAS MOTIONS IN THE CORES OF GALAXY CLUSTERS. <b>2016</b> , 821, 6		12
2008	AHUBBLE SPACE TELESCOPESTUDY OF THE ENIGMATIC MILKY WAY HALO GLOBULAR CLUSTER CRATER. <b>2016</b> , 822, 32		27
2007	ERRATUM: MILKY WAY RED DWARFS IN THE BORG SURVEY; GALACTIC SCALE-HEIGHT AND THE DISTRIBUTION OF DWARFS STARS IN WFC3 IMAGING[[2014, ApJ, 788, 77). <b>2016</b> , 825, 82		
2006	HSTIMAGING OF THE LOCAL VOLUME DWARF GALAXIES PISCES A AND B: PROTOTYPES FOR LOCAL GROUP DWARFS. <b>2016</b> , 827, 89		15
2005	ZFIRE: A KECK/MOSFIRE SPECTROSCOPIC SURVEY OF GALAXIES IN RICH ENVIRONMENTS ATz~ 2. <b>2016</b> , 828, 21		42
2004	AN ECCENTRIC BINARY MILLISECOND PULSAR WITH A HELIUM WHITE DWARF COMPANION IN THE GALACTIC FIELD. <b>2016</b> , 830, 36		19
2003	THE CANDIDATE CLUSTER AND PROTOCLUSTER CATALOG (CCPC). II. SPECTROSCOPICALLY IDENTIFIED STRUCTURES SPANNING 2 . <b>2016</b> , 833, 15		15
2002	HIGH-VELOCITY BIPOLAR MOLECULAR EMISSION FROM AN AGN TORUS. <b>2016</b> , 829, L7		66
2001	HUBBLE SPACE TELESCOPEPROPER MOTION (HSTPROMO) CATALOGS OF GALACTIC GLOBULAR CLUSTERS. IV. KINEMATIC PROFILES AND AVERAGE MASSES OF BLUE STRAGGLER STARS. <b>2016</b> , 827, 12		24
2000	OBSCURED AGNs IN BULGELESS HOSTS DISCOVERED BYWISE: THE CASE STUDY OF SDSS J1224+5555. <b>2016</b> , 827, 58		6
1999	Herschel-Planckdust optical depth and column density maps. <i>Astronomy and Astrophysics</i> , <b>2016</b> , 587, A106	5.1	28
1998	Stellar classification from single-band imaging using machine learning. <i>Astronomy and Astrophysics</i> , <b>2016</b> , 591, A54	5.1	13

1997	On the relation of optical obscuration and X-ray absorption in Seyfert galaxies. <i>Astronomy and Astrophysics</i> , <b>2016</b> , 586, A28	5.1	50
1996	gPhoton: THEGALEXPHOTON DATA ARCHIVE. <b>2016</b> , 833, 292		29
1995	The Lyman alpha reference sample. Astronomy and Astrophysics, 2016, 587, A78	5.1	28
1994	HI4PI: a full-sky H i survey based on EBHIS and GASS. Astronomy and Astrophysics, <b>2016</b> , 594, A116	5.1	392
1993	SPECTROSCOPY OF LUMINOUS COMPACT BLUE GALAXIES IN DISTANT CLUSTERS. II. PHYSICAL PROPERTIES OF dE PROGENITOR CANDIDATES. <b>2016</b> , 817, 87		5
1992	Precise radial velocities of giant stars. Astronomy and Astrophysics, <b>2016</b> , 595, A55	5.1	15
1991	A RICH GLOBULAR CLUSTER SYSTEM IN DRAGONFLY 17: ARE ULTRA-DIFFUSE GALAXIES PURE STELLAR HALOS?. <b>2016</b> , 822, L31		76
1990	Multi-wavelength landscape of the young galaxy cluster RXJ 1257.2+4738 atz= 0.866. <i>Astronomy and Astrophysics</i> , <b>2016</b> , 592, A108	5.1	3
1989	Identifying galaxy candidates in WSRT H i imaging of ultra-compact high velocity clouds. <i>Astronomy and Astrophysics</i> , <b>2016</b> , 596, A117	5.1	10
1988	THE PHOENIX STREAM: A COLD STREAM IN THE SOUTHERN HEMISPHERE. <b>2016</b> , 820, 58		38
1987	CLUSTER-LENSING: A PYTHON PACKAGE FOR GALAXY CLUSTERS AND MISCENTERING. <b>2016</b> , 152, 228		5
1986	The imprint of satellite accretion on the chemical and dynamical properties of disc galaxies. <i>Astronomy and Astrophysics</i> , <b>2016</b> , 586, A112	5.1	16
1985	SUPPLEMENT: LOING THE DISTANCE: MAPPING HOST GALAXIES OF LIGO AND VIRGO SOURCES IN THREE DIMENSIONS USING LOCAL COSMOGRAPHY AND TARGETED FOLLOW-UP[[2016, ApJL, 829, L15). <b>2016</b> , 226, 10		33
1984	The red dwarf pair GJ65 AB: inflated, spinning twins of Proxima. <i>Astronomy and Astrophysics</i> , <b>2016</b> , 593, A127	5.1	21
1983	SpIES: THE SPITZER IRAC EQUATORIAL SURVEY. <b>2016</b> , 225, 1		33
1982	The close circumstellar environment of Betelgeuse. Astronomy and Astrophysics, 2016, 585, A28	5.1	32
1981	Constraining the physical structure of the inner few 100 AU scales of deeply embedded low-mass protostars. <i>Astronomy and Astrophysics</i> , <b>2016</b> , 590, A33	5.1	29
1980	The effect of local and large-scale environments on nuclear activity and star formation. <i>Astronomy and Astrophysics</i> , <b>2016</b> , 592, A30	5.1	19

1979	Seeding the Galactic Centre gas stream: gravitational instabilities set the initial conditions for the formation of protocluster clouds. <b>2016</b> , 463, L122-L126		41	
1978	The Effelsberg-Bonn H i Survey: Milky Way gas. Astronomy and Astrophysics, <b>2016</b> , 585, A41	5.1	95	
1977	Dense gas in the Galactic central molecular zone is warm and heated by turbulence. <i>Astronomy and Astrophysics</i> , <b>2016</b> , 586, A50	5.1	128	
1976	An X-Shooter composite of bright 1 . <i>Astronomy and Astrophysics</i> , <b>2016</b> , 585, A87	5.1	85	
1975	Shape of the oxygen abundance profiles in CALIFA face-on spiral galaxies. <i>Astronomy and Astrophysics</i> , <b>2016</b> , 587, A70	5.1	103	
1974	Convolution kernels for multi-wavelength imaging. Astronomy and Astrophysics, 2016, 596, A63	5.1	9	
1973	The Lockman Hole project: LOFAR observations and spectral index properties of low-frequency radio sources. <b>2016</b> , 463, 2997-3020		49	
1972	The LyHuminosity function atz= 5.78.6 and the steep drop of the faint end: implications for reionization. <b>2016</b> , 463, 1678-1691		67	
1971	In-focus wavefront sensing using non-redundant mask-induced pupil diversity. <b>2016</b> , 24, 15506-21		4	
1970	K2ROTATION PERIODS FOR LOW-MASS HYADS AND THE IMPLICATIONS FOR GYROCHRONOLOGY. <b>2016</b> , 822, 47		85	
1969	Under pressure: quenching star formation in low-mass satellite galaxies via stripping. <b>2016</b> , 463, 1916-1	928	68	
1968	The physical and chemical structure of Sagittarius B2. Astronomy and Astrophysics, 2016, 588, A143	5.1	73	
1967	X-RAY PROPERTIES OF THE YOUNGEST RADIO SOURCES AND THEIR ENVIRONMENTS. <b>2016</b> , 823, 57		29	
1966	Cometary Science with the James Webb Space Telescope. <b>2016</b> , 128, 018009		15	
1965	STARK BROADENING OF HIGH-ORDER RADIO RECOMBINATION LINES TOWARD THE ORION NEBULA. <b>2016</b> , 828, 40		3	
1964	Three-dimensional distribution of hydrogen fluoride gas toward NGC 6334 I and I(N). <i>Astronomy and Astrophysics</i> , <b>2016</b> , 593, A37	5.1	7	
1963	Testing the dark matter subhalo hypothesis of the gamma-ray source 3FGL J2212.5+0703. <b>2016</b> , 94,		8	
1962	Gas absorption and dust extinction towards the Orion Nebula Cluster. <i>Astronomy and Astrophysics</i> , <b>2016</b> , 593, A7	5.1	9	

1961	A UNIFORM CATALOG OF MOLECULAR CLOUDS IN THE MILKY WAY. <b>2016</b> , 822, 52	97
1960	Calibration development strategies for the Daniel K. Inouye Solar Telescope (DKIST) data center. <b>2016</b> ,	
1959	THE MASSIVE PROTOSTELLAR CLUSTER NGC 6334I AT 220 au RESOLUTION: DISCOVERY OF FURTHER MULTIPLICITY, DIVERSITY, AND A HOT MULTI-CORE. <b>2016</b> , 832, 187	37
1958	CHAOS. III. GAS-PHASE ABUNDANCES IN NGC 5457. <b>2016</b> , 830, 4	77
1957	An M-dwarf star in the transition disk of Herbig HD 142527. Astronomy and Astrophysics, <b>2016</b> , 590, A90 $_{5.1}$	61
1956	ALMA observations of the nearby AGB star L2 Puppis. <i>Astronomy and Astrophysics</i> , <b>2016</b> , 596, A92 5.1	45
1955	CONNECTING CO INTENSITY MAPPING TO MOLECULAR GAS AND STAR FORMATION IN THE EPOCH OF GALAXY ASSEMBLY. <b>2016</b> , 817, 169	65
1954	NEW HALO STARS OF THE GALACTIC GLOBULAR CLUSTERS M3 AND M13 IN THE LAMOST DR1 CATALOG. <b>2016</b> , 829, 123	12
1953	A SYSTEMATIC STUDY OF MID-INFRARED EMISSION FROM CORE-COLLAPSE SUPERNOVAE WITH SPIRITS. <b>2016</b> , 833, 231	31
1952	Towards universal hybrid star formation rate estimators. <i>Astronomy and Astrophysics</i> , <b>2016</b> , 591, A6 $_{5.1}$	60
1951	THE ORION FINGERS: NEAR-IR SPECTRAL IMAGING OF AN EXPLOSIVE OUTFLOW. <b>2016</b> , 151, 173	15
1950	SPITZER OBSERVATIONS OF LONG-TERM INFRARED VARIABILITY AMONG YOUNG STELLAR OBJECTS IN CHAMAELEON I. <b>2016</b> , 833, 104	15
1949	Azimuthal asymmetries in the debris disk around HD 61005. Astronomy and Astrophysics, 2016, 591, A108 <sub>3.1</sub>	56
1948	CHEMICAL DIVERSITY IN THE ULTRA-FAINT DWARF GALAXY TUCANA II. <b>2016</b> , 832, L3	34
1947	OBSERVATIONAL CONSTRAINTS ON FIRST-STAR NUCLEOSYNTHESIS. I. EVIDENCE FOR MULTIPLE PROGENITORS OF CEMP-NO STARS. <b>2016</b> , 833, 20	103
1946	SUBMILLIMETER POLARIZATION OBSERVATION OF THE PROTOPLANETARY DISK AROUND HD 142527. <b>2016</b> , 831, L12	70
1945	gadfly: A pandas-based Framework for Analyzing GADGET Simulation Data. <b>2016</b> , 128, 114503	
1944	VISION (Vienna survey in Orion. <i>Astronomy and Astrophysics</i> , <b>2016</b> , 587, A153 5.1	45

# (2016-2016)

194	11HE FRAGMENTATION AND STABILITY OF HIERARCHICAL STRUCTURE IN SERPENS SOUTH. <b>2016</b> , 833, 204		24
194	FAINT SUBMILLIMETER GALAXIES IDENTIFIED THROUGH THEIR OPTICAL/NEAR-INFRARED COLORS. I. SPATIAL CLUSTERING AND HALO MASSES. <b>2016</b> , 831, 91		32
194	Close stellar conjunctions oftentauri A and B until 2050. Astronomy and Astrophysics, <b>2016</b> , 594, A107	5.1	34
194	Shadows cast on the transition disk of HD 135344B. <i>Astronomy and Astrophysics</i> , <b>2016</b> , 595, A113	5.1	110
193	SURFACE ALBEDO AND SPECTRAL VARIABILITY OF CERES. <b>2016</b> , 817, L22		36
193	ESTIMATING DISTANCES FROM PARALLAXES. II. PERFORMANCE OF BAYESIAN DISTANCE ESTIMATORS ON AGAIA-LIKE CATALOGUE. <b>2016</b> , 832, 137		112
193	Calibrated and completeness-corrected optical stellar density maps of the northern Galactic plane. <b>2016</b> , 457, 642-665		4
193	AST: A library for modelling and manipulating coordinate systems. <b>2016</b> , 15, 33-49		6
193	DISCOVERY OF A STELLAR OVERDENSITY IN ERIDANUS <b>P</b> HOENIX IN THE DARK ENERGY SURVEY. <b>2016</b> , 817, 135		29
193	CHANDRAX-RAY ANDHUBBLE SPACE TELESCOPEIMAGING OF OPTICALLY SELECTED  KILOPARSEC-SCALE BINARY ACTIVE GALACTIC NUCLEI. II. HOST GALAXY MORPHOLOGY AND AGN ACTIVITY. <b>2016</b> , 823, 50		18
193	Simulated stellar kinematics studies of high-redshift galaxies with the HARMONI Integral Field Spectrograph. <b>2016</b> , 458, 2405-2422		6
193	The cluster-scale environment of PKS 2155B04. <b>2016</b> , 455, 618-625		9
193	Chaotic dispersal of tidal debris. <b>2016</b> , 455, 1079-1098		40
193	30 A GLOBAL CORRECTION TO PPMXL PROPER MOTIONS. <b>2016</b> , 151, 99		16
192	THE POPULATION OF COMPACT RADIO SOURCES IN THE ORION NEBULA CLUSTER. <b>2016</b> , 822, 93		25
192	THE OUTER SOLAR SYSTEM ORIGINS SURVEY. I. DESIGN AND FIRST-QUARTER DISCOVERIES. <b>2016</b> , 152, 70		84
192	ULTRA-DEEP K S -BAND IMAGING OF THE HUBBLE FRONTIER FIELDS. <b>2016</b> , 226, 6		28
192	THE JCMT GOULD BELT SURVEY: EVIDENCE FOR DUST GRAIN EVOLUTION IN PERSEUS  STAR-FORMING CLUMPS. <b>2016</b> , 826, 95		34

1925	Enabling science with Gaia observations of naked-eye stars. <b>2016</b> ,	7
1924	RoboPol: the optical polarization of gamma-ray-loud and gamma-ray-quiet blazars. <b>2016</b> , 463, 3365-3380	56
1923	MEASURING PROTOPLANETARY DISK GAS SURFACE DENSITY PROFILES WITH ALMA. <b>2016</b> , 830, 32	20
1922	A CENSUS OF LARGE-SCALE (10 PC), VELOCITY-COHERENT, DENSE FILAMENTS IN THE NORTHERN GALACTIC PLANE: AUTOMATED IDENTIFICATION USING MINIMUM SPANNING TREE. <b>2016</b> , 226, 9	42
1921	THE SPECTACULAR RADIO-NEAR-IR-X-RAY JET OF 3C 111: THE X-RAY EMISSION MECHANISM AND JET KINEMATICS. <b>2016</b> , 826, 109	16
1920	WATER MASERS IN THE ANDROMEDA GALAXY. II. WHERE DO MASERS ARISE?. <b>2016</b> , 826, 136	3
1919	FORBIDDEN IRON LINES AND DUST DESTRUCTION IN SUPERNOVA REMNANT SHOCKS: THE CASE OF N49 IN THE LARGE MAGELLANIC CLOUD. <b>2016</b> , 826, 150	21
1918	THE MILKY WAY PROJECT AND ATLASGAL: THE DISTRIBUTION AND PHYSICAL PROPERTIES OF COLD CLUMPS NEAR INFRARED BUBBLES. <b>2016</b> , 825, 142	21
1917	Mocking the weak lensing universe: The LensTools Python computing package. <b>2016</b> , 17, 73-79	31
1916	RESOLVED MILLIMETER-WAVELENGTH OBSERVATIONS OF DEBRIS DISKS AROUND SOLAR-TYPE STARS. <b>2016</b> , 816, 27	32
1915	THE FIRST HIGH-PHASE OBSERVATIONS OF A KBO: NEW HORIZONS IMAGING OF (15810) 1994 JR 1 FROM THE KUIPER BELT. <b>2016</b> , 828, L15	14
1914	G11.92 <b>D</b> .61 MM1: a Keplerian disc around a massive young proto-O star. <b>2016</b> , 462, 4386-4401	64
1913	DEBRIS DISKS IN THE SCORPIUS LENTAURUS OB ASSOCIATION RESOLVED BY ALMA. 2016, 828, 25	59
1912	ON THE FERMI -GBM EVENT 0.4 s AFTER GW150914. <b>2016</b> , 827, L38	58
1911	THE PAN-STARRS1 DISTANT $z > 5.6$ QUASAR SURVEY: MORE THAN 100 QUASARS WITHIN THE FIRST GYR OF THE UNIVERSE. <b>2016</b> , 227, 11	193
1910	The prevalence of star formation as a function of Galactocentric radius. <b>2016</b> , 462, 3123-3129	23
1909	Soapy: an adaptive optics simulation written purely in Python for rapid concept development. 2016,	8
1908	A synoptic map of halo substructures from the Pan-STARRS1 3 Laurvey. <b>2016</b> , 463, 1759-1768	81

1907	THE CLOSE COMPANION MASS-RATIO DISTRIBUTION OF INTERMEDIATE-MASS STARS. <b>2016</b> , 152, 40	24
1906	Data processing and visualisation in the Rosetta Science Ground Segment. <b>2016</b> , 126, 475-487	5
1905	Rapid Bayesian position reconstruction for gravitational-wave transients. <b>2016</b> , 93,	175
1904	A CONSTRAINT ON QUASAR CLUSTERING ATz= 5 FROM A BINARY QUASAR. <b>2016</b> , 151, 61	17
1903	SUPPLEMENT: LOCALIZATION AND BROADBAND FOLLOW-UP OF THE GRAVITATIONAL-WAVE TRANSIENT GW150914[[2016, ApJL, 826, L13). <b>2016</b> , 225, 8	38
1902	The Gaia-ESO Survey: revisiting the Li-rich giant problem. <b>2016</b> , 461, 3336-3352	52
1901	PROTOSTARS AT LOW EXTINCTION IN ORION A. <b>2016</b> , 825, 91	9
1900	KIM 3: AN ULTRA-FAINT STAR CLUSTER IN THE CONSTELLATION OF CENTAURUS. <b>2016</b> , 820, 119	32
1899	SHIELD: NEUTRAL GAS KINEMATICS AND DYNAMICS. <b>2016</b> , 832, 89	20
1898	Investigating interoperability of the LSST data management software stack with Astropy. 2016,	3
1897	SEASONAL EVOLUTION ON THE NUCLEUS OF COMET C/2013 A1 (SIDING SPRING). <b>2016</b> , 817, L23	5
1896	Faint dwarf galaxies in Hickson Compact Group 90. <b>2016</b> , 463, 1284-1290	8
1895	VETTING GALACTIC LEAVITT LAW CALIBRATORS USING RADIAL VELOCITIES: ON THE VARIABILITY, BINARITY, AND POSSIBLE PARALLAX ERROR OF 19 LONG-PERIOD CEPHEIDS. <b>2016</b> , 226, 18	16
1894	FAR-INFRARED LINE SPECTRA OF ACTIVE GALAXIES FROM THE HERSCHEL /PACS SPECTROMETER: THE COMPLETE DATABASE. <b>2016</b> , 226, 19	41
1893	LOFAR 150-MHz observations of the Bolles field: catalogue and source counts. <b>2016</b> , 460, 2385-2412	119
1892	The average submillimetre properties of Lyman $\oplus$ lobs at $z = 3$ . <b>2016</b> , 460, 4075-4085	12
1891	Using 21 cm absorption surveys to measure the average H i spin temperature in distant galaxies. <b>2016</b> , 462, 1341-1350	12
1890	LOFAR/H-ATLAS: a deep low-frequency survey of theHerschel-ATLAS North Galactic Pole field. <b>2016</b> , 462, 1910-1936	79

1889	MUSE searches for galaxies near very metal-poor gas clouds at $z \sim 3$ : new constraints for cold accretion models. <b>2016</b> , 462, 1978-1988	49
1888	SHOCKFIND - an algorithm to identify magnetohydrodynamic shock waves in turbulent clouds. <b>2016</b> , 463, 1026-1039	11
1887	The dustier early-type galaxies deviate from late-type galaxies[scaling relations. 2016, 461, 2856-2866	13
1886	Ray-tracing critical-angle transmission gratings for the X-ray Surveyor and Explorer-size missions. <b>2016</b> ,	3
1885	EXPLORING DAMPED LyBYSTEM HOST GALAXIES USING GAMMA-RAY BURSTS. 2016, 832, 175	6
1884	WISEP J060738.65+242953.4: A NEARBY POLE-ON L8 BROWN DWARF WITH RADIO EMISSION. <b>2016</b> , 152, 123	7
1883	THE SECOND KONUS- WIND CATALOG OF SHORT GAMMA-RAY BURSTS. <b>2016</b> , 224, 10	38
1882	Project PANOPTES: a citizen-scientist exoplanet transit survey using commercial digital cameras. <b>2016</b> ,	
1881	HydroUnits: supporting dimensional analysis in hydrologic computing systems using sensor-based standards. <b>2016</b> , 18, 168-184	1
	COMPLETE ELEMENT ADUNDANCES OF NINE CTARS IN THE ADOCTOR CALAVOLDETICI HAINA H	
1880	COMPLETE ELEMENT ABUNDANCES OF NINE STARS IN THEr-PROCESS GALAXY RETICULUM II. <b>2016</b> , 830, 93	103
1880 1879		103
1879	2016, 830, 93  PORTRAIT OF A DARK HORSE: A PHOTOMETRIC AND SPECTROSCOPIC STUDY OF THE	Ĭ
1879	2016, 830, 93  PORTRAIT OF A DARK HORSE: A PHOTOMETRIC AND SPECTROSCOPIC STUDY OF THE ULTRA-FAINT MILKY WAY SATELLITE PEGASUS III. 2016, 833, 16	29
1879 1878 1877	PORTRAIT OF A DARK HORSE: A PHOTOMETRIC AND SPECTROSCOPIC STUDY OF THE ULTRA-FAINT MILKY WAY SATELLITE PEGASUS III. 2016, 833, 16  HOST GALAXY IDENTIFICATION FOR SUPERNOVA SURVEYS. 2016, 152, 154  THE LOCATION, CLUSTERING, AND PROPAGATION OF MASSIVE STAR FORMATION IN GIANT	29
1879 1878 1877	PORTRAIT OF A DARK HORSE: A PHOTOMETRIC AND SPECTROSCOPIC STUDY OF THE ULTRA-FAINT MILKY WAY SATELLITE PEGASUS III. 2016, 833, 16  HOST GALAXY IDENTIFICATION FOR SUPERNOVA SURVEYS. 2016, 152, 154  THE LOCATION, CLUSTERING, AND PROPAGATION OF MASSIVE STAR FORMATION IN GIANT MOLECULAR CLOUDS. 2016, 832, 43	29 36 11
1879 1878 1877	PORTRAIT OF A DARK HORSE: A PHOTOMETRIC AND SPECTROSCOPIC STUDY OF THE ULTRA-FAINT MILKY WAY SATELLITE PEGASUS III. 2016, 833, 16  HOST GALAXY IDENTIFICATION FOR SUPERNOVA SURVEYS. 2016, 152, 154  THE LOCATION, CLUSTERING, AND PROPAGATION OF MASSIVE STAR FORMATION IN GIANT MOLECULAR CLOUDS. 2016, 832, 43  The Australian Space Eye: studying the history of galaxy formation with a CubeSat. 2016,  SimCADO: an instrument data simulator package for MICADO at the E-ELT. 2016,	29 36 11
1879 1878 1877 1876	PORTRAIT OF A DARK HORSE: A PHOTOMETRIC AND SPECTROSCOPIC STUDY OF THE ULTRA-FAINT MILKY WAY SATELLITE PEGASUS III. 2016, 833, 16  HOST GALAXY IDENTIFICATION FOR SUPERNOVA SURVEYS. 2016, 152, 154  THE LOCATION, CLUSTERING, AND PROPAGATION OF MASSIVE STAR FORMATION IN GIANT MOLECULAR CLOUDS. 2016, 832, 43  The Australian Space Eye: studying the history of galaxy formation with a CubeSat. 2016,  SimCADO: an instrument data simulator package for MICADO at the E-ELT. 2016,	29 36 11 7

1871	The mass of planet GJ 676A b from ground-based astrometry. <i>Astronomy and Astrophysics</i> , <b>2016</b> , 595, A77	18	
1870	First on-sky results with ARGOS at LBT. <b>2016</b> ,	6	
1869	Toward gas exhaustion in the W51 high-mass protoclusters. Astronomy and Astrophysics, <b>2016</b> , 595, A27 $_{5.1}$	40	
1868	Cygrid: A fast Cython-powered convolution-based gridding module for Python. <i>Astronomy and Astrophysics</i> , <b>2016</b> , 591, A12	12	
1867	MAPPING THE GAS TURBULENCE IN THE COMA CLUSTER: PREDICTIONS FORASTRO-H. <b>2016</b> , 817, 110	16	
1866	MULTIWAVELENGTH STUDY OF QUIESCENT STATES OF Mrk 421 WITH UNPRECEDENTED HARD X-RAY COVERAGE PROVIDED BYNUSTARIN 2013. <b>2016</b> , 819, 156	63	
1865	The Geneva Reduction and Analysis Pipeline for High-contrast Imaging of planetary Companions. <b>2016</b> , 455, 2178-2186	30	
1864	Herschelfar-infrared photometry of theSwiftBurst Alert Telescope active galactic nuclei sample of the local universe III. SPIRE observations. <b>2016</b> , 456, 3335-3353	24	
1863	Phase-resolved spectroscopy of Type B quasi-periodic oscillations in GX 339-4. <b>2016</b> , 460, 2796-2810	33	
1862	Massive relic galaxies prefer dense environments. <b>2016</b> , 461, 156-163	14	
1861	An empirical determination of the dust mass absorption coefficient, <b>I</b> , using the Herschel Reference Survey. <b>2016</b> , 459, 1646-1658	33	
1860	On the connection between the metal-enriched intergalactic medium and galaxies: an O vigalaxy cross-correlation study atz2016, 460, 590-616	14	
1859	The winds from HL Tau. <b>2016</b> , 460, 627-633	14	
1858	RINGED SUBSTRUCTURE AND A GAP AT 1 au IN THE NEAREST PROTOPLANETARY DISK. <b>2016</b> , 820, L40	364	
1857	REVISITING THE MICROLENSING EVENT OGLE 2012-BLG-0026: A SOLAR MASS STAR WITH TWO COLD GIANT PLANETS. <b>2016</b> , 824, 83	59	
1856	EVOLUTION OF THERMALLY PULSING ASYMPTOTIC GIANT BRANCH STARS. V. CONSTRAINING THE MASS LOSS AND LIFETIMES OF INTERMEDIATE-MASS, LOW-METALLICITY AGB STARS*. <b>2016</b> , 822, 73	50	
1855	Towards the statistical detection of the warmflot intergalactic medium in intercluster filaments of the cosmic web. <b>2016</b> , 455, 2662-2697	25	
1854	Radio galaxies in ZFOURGE/NMBS: no difference in the properties of massive galaxies with and without radio-AGN out to $z=2.25$ . <b>2016</b> , 455, 2731-2744	19	

1853	NGC 6778: strengthening the link between extreme abundance discrepancy factors and central star binarity in planetary nebulae. <b>2016</b> , 455, 3263-3272	48
1852	The distribution of atomic hydrogen in eagle galaxies: morphologies, profiles, and H i holes. <b>2016</b> , 456, 1115-1136	95
1851	The origin of compact galaxies with anomalously high black hole masses. <b>2016</b> , 460, 1147-1161	28
1850	Radio Galaxy Zoo: discovery of a poor cluster through a giant wide-angle tail radio galaxy. <b>2016</b> , 460, 2376-2384	17
1849	The first stars: formation under cosmic ray feedback. <b>2016</b> , 460, 2432-2444	6
1848	Changing physical conditions in star-forming galaxies between redshifts 0´. <b>2016</b> , 460, 3002-3013	16
1847	The CALYMHA survey: Lytescape fraction and its dependence on galaxy properties atz= 2.23. <b>2016</b> , 458, 449-467	60
1846	Submillimeter array observations of NGC 2264-C: molecular outflows and driving sources. <b>2016</b> , 458, 1742-1767	12
1845	Resolving the planetesimal belt of HR 8799 with ALMA. <b>2016</b> , 460, L10-L14	74
1844	A new method to break the mass-sheet degeneracy using aperture moments. <b>2016</b> , 460, 2505-2525	1
1843	The GALAH survey: relative throughputs of the 2dF fibre positioner and the HERMES spectrograph from stellar targets. <b>2016</b> , 459, 1069-1081	8
1842	SPENDING TOO MUCH TIME AT THE GALACTIC BAR: CHAOTIC FANNING OF THE OPHIUCHUS STREAM. <b>2016</b> , 824, 104	27
1841	AN EXTERNAL SHOCK ORIGIN OF GRB 141028A. <b>2016</b> , 822, 63	18
1840	An enhanced merger fraction within the galaxy population of the SSA22 protocluster at $z=3.1$ . <b>2016</b> , 455, 2363-2370	21
1839	Dynamical formation and scattering of hierarchical triples: cross-sections, Kozaillidov oscillations, and collisions. <b>2016</b> , 456, 4219-4246	47
1838	CHIMERA: a wide-field, multi-colour, high-speed photometer at the prime focus of the Hale telescope. <b>2016</b> , 457, 3036-3049	37
1837	Insights into quasar UV spectra using unsupervised clustering analysis. <b>2016</b> , 459, 1659-1681	2
1836	Possible Population III remnants at redshift 3.5. <b>2016</b> , 457, L44-L48	16

1835	A DISK-BASED DYNAMICAL CONSTRAINT ON THE MASS OF THE YOUNG BINARY DQ TAU. <b>2016</b> , 818, 156	39
1834	The Palomar kernel-phase experiment: testing kernel phase interferometry for ground-based astronomical observations. <b>2016</b> , 455, 1647-1653	8
1833	THE SCUBA-2 COSMOLOGY LEGACY SURVEY: MULTIWAVELENGTH COUNTERPARTS TO 103SUBMILLIMETER GALAXIES IN THE UKIDSS-UDS FIELD. <b>2016</b> , 820, 82	44
1832	CosmoBolognaLib: C++ libraries for cosmological calculations. <b>2016</b> , 14, 35-42	30
1831	ADVANCED DATA VISUALIZATION IN ASTROPHYSICS: THE X3D PATHWAY. <b>2016</b> , 818, 115	17
1830	KIC 9246715: THE DOUBLE RED GIANT ECLIPSING BINARY WITH ODD OSCILLATIONS. <b>2016</b> , 818, 108	26
1829	CHIMPS: the13CO/C18O (J´=´3´->´2) Heterodyne Inner Milky Way Plane Survey. <b>2016</b> , 456, 2885-2899	54
1828	MOTION VERIFIED RED STARS (MoVeRS): A CATALOG OF PROPER MOTION SELECTED LOW-MASS STARS FROMWISE, SDSS, AND 2MASS. <b>2016</b> , 151, 41	10
1827	A method for selecting M dwarfs with an increased likelihood of unresolved ultracool companionship. <b>2016</b> , 457, 2192-2208	8
1826	THE CLOSE STELLAR COMPANIONS TO INTERMEDIATE-MASS BLACK HOLES. <b>2016</b> , 819, 70	34
1825	Deep Chandra observations of Pictor A. <b>2016</b> , 455, 3526-3545	43
1824	LAMOST 1: A DISRUPTED SATELLITE IN THE CONSTELLATION DRACO. <b>2016</b> , 816, L2	О
1823	Parallax of the L4.5 dwarf 2M1821+14 from high-precision astrometry with OSIRIS at GTC. <b>2016</b> , 455, 357-369	12
1822	An Open Catalog for Supernova Data. <b>2017</b> , 835, 64	<b>2</b> 60
1821	The Host Galaxy and Redshift of the Repeating Fast Radio Burst FRB 121102. <b>2017</b> , 834, L7	398
1820	EXPLODING SATELLITESTHE TIDAL DEBRIS OF THE ULTRA-FAINT DWARF GALAXY HERCULES. <b>2017</b> , 834, 112	22
1819	The Late-Type Extension to MoVeRS (LaTE-MoVeRS): Proper Motion Verified Low-mass Stars and Brown Dwarfs from SDSS, 2MASS, andWISE. <b>2017</b> , 153, 92	12
1818	LACEWING: A New Moving Group Analysis Code. <b>2017</b> , 153, 95	50

1817	A New Approach to the Internal Calibration of Reverberation-Mapping Spectra. 2017, 129, 024007		16
1816	GaLactic and Extragalactic All-sky Murchison Widefield Array (GLEAM) survey []. A low-frequency extragalactic catalogue. <b>2017</b> , 464, 1146-1167		275
1815	Trojan Asteroids in theKeplerCampaign 6 Field. <b>2017</b> , 153, 116		19
1814	Type Ibn Supernovae Show Photometric Homogeneity and Spectral Diversity at Maximum Light. <b>2017</b> , 836, 158		49
1813	Neutral ISM, Ly∄and Lyman-continuum in the Nearby Starburst Haro 11. <b>2017</b> , 837, 29		17
1812	The Joker:A Custom Monte Carlo Sampler for Binary-star and Exoplanet Radial Velocity Data. <b>2017</b> , 837, 20		78
1811	Proximal orbit around Ecentauri. Astronomy and Astrophysics, 2017, 598, L7	5.1	65
1810	Adapting astronomical source detection software to help detect animals in thermal images obtained by unmanned aerial systems. <b>2017</b> , 38, 2623-2638		47
1809	A Matched Filter Technique for Slow Radio Transient Detection and First Demonstration with the Murchison Widefield Array. <b>2017</b> , 153, 98		5
1808	The Grism Lens-Amplified Survey from Space (GLASS). XI. Detection of C iv in Multiple Images of thez= 6.11 LyEmitter behind RXC J2248.74431. <b>2017</b> , 839, 17		39
1807	Detectability of compact binary merger macronovae. <b>2017</b> , 34, 104001		102
1806	Discovery and Physical Characterization of a Large Scattered Disk Object at 92 au. <b>2017</b> , 839, L15		24
1805	Tycho-GaiaAstrometric Solution Parallaxes and Proper Motions for Five Galactic Globular Clusters. <b>2017</b> , 839, 89		23
1804	Location ofFray emission and magnetic field strengths in OJ 287. <i>Astronomy and Astrophysics</i> , <b>2017</b> , 597, A80	5.1	43
1803	Introducing Nightlight: A New FITS Viewer. <b>2017</b> , 129, 058003		1
1802	ALMA Observations of the Interaction of a Radio Jet with Molecular Gas in Minkowski's Object. <b>2017</b> , 838, 146		15
1801	Wide-field12CO (\$J=2mbox{}1\$) and13CO (\$J=2mbox{}1\$) Observations toward the Aquila Rift and Serpens Molecular Cloud Complexes. I. Molecular Clouds and Their Physical Properties. <b>2017</b> , 837, 154		15
1800	Reverberation Mapping of Optical Emission Lines in Five Active Galaxies. <b>2017</b> , 840, 97		57

1799 The Discovery and Origin of a Very High-velocity Cloud Toward M33. <b>2017</b> , 840, 65	2
1798 TheFermiGalactic Center GeV Excess and Implications for Dark Matter. <b>2017</b> , 840, 43	157
1797 Removing Visual Bias in Filament Identification: A New Goodness-of-fit Measure. <b>2017</b> , 840, L17	3
1796 Descattering of Giant Pulses in PSR B1957+20. <b>2017</b> , 840, L15	15
1795 Young Stars with SALT. <b>2017</b> , 840, 87	16
1794 Bolometric Light Curves of Peculiar Type II-P Supernovae. <b>2017</b> , 129, 044202	14
1793 Initial Estimates on the Performance of the LSST on the Detection of Eclipsing Binaries. <b>2017</b> , 129, 06.	5003 4
The RAVE-on Catalog of Stellar Atmospheric Parameters and Chemical Abundances for Chemo-dynamic Studies in theGaiaEra. <b>2017</b> , 840, 59	56
1791 Nebular Continuum and Line Emission in Stellar Population Synthesis Models. <b>2017</b> , 840, 44	119
1790 ATLASGAL-selected massive clumps in the inner Galaxy. <i>Astronomy and Astrophysics</i> , <b>2017</b> , 599, A139	5.1 48
1789 Spherical Panoramas for Astrophysical Data Visualization. <b>2017</b> , 129, 058004	3
1788 Poking the Beehive from Space: K2 Rotation Periods for Praesepe. <b>2017</b> , 842, 83	63
1787 Thermal Feedback in the High-mass Star- and Cluster-forming Region W51. <b>2017</b> , 842, 92	28
1786 The Peculiar Multiwavelength Evolution Of V1535 Sco. <b>2017</b> , 842, 73	11
Black Hole Growth Is Mainly Linked to Host-galaxy Stellar Mass Rather Than Star Formation Rate. <b>2017</b> , 842, 72	55
0 Constant Destricts the constant 2017	
1784 Gamma-sky.net: Portal to the gamma-ray sky. <b>2017</b> ,	
1784 Gamma-sky.net: Portal to the gamma-ray sky. 2017,  1783 A New Spectral Feature on the Trailing Hemisphere of Europa at 3.78th. 2017, 153, 250	8

1781	Comoving Stars inGaiaDR1: An Abundance of Very Wide Separation Comoving Pairs. 2017, 153, 257	93
1780	An atlas of exotic variability in IGR J17091B624: a comparison with GRS 1915+105. <b>2017</b> , 468, 4748-4771	17
1779	Unveiling the early-stage anatomy of a protocluster hub with ALMA. <b>2017</b> , 464, L31-L35	35
1778	The SLUGGS survey: dark matter fractions at large radii and assembly epochs of early-type galaxies from globular cluster kinematics. <b>2017</b> , 468, 3949-3964	33
1777	An ALMA survey of submillimetre galaxies in the COSMOS field: The extent of the radio-emitting region revealed by 3 GHz imaging with the Very Large Array. <i>Astronomy and Astrophysics</i> , <b>2017</b> , 602, A54 <sup>5.1</sup>	21
1776	Improving and Assessing Planet Sensitivity of the GPI Exoplanet Survey with a Forward Model Matched Filter. <b>2017</b> , 842, 14	66
1775	The ALHAMBRA survey:B-band luminosity function of quiescent and star-forming galaxies at 0.2 ½ . <i>Astronomy and Astrophysics</i> , <b>2017</b> , 599, A62	12
1774	A Catalog ofGALEXUltraviolet Emission from Asymptotic Giant Branch Stars. 2017, 841, 33	26
1773	TSAnalyzer, a GNSS time series analysis software. <b>2017</b> , 21, 1389-1394	12
1772	An Application of Multi-band Forced Photometry to One Square Degree of SERVS: Accurate Photometric Redshifts and Implications for Future Science. <b>2017</b> , 230, 9	18
1771	A New Approach to Convective Core Overshooting: Probabilistic Constraints from Color Magnitude Diagrams of LMC Clusters. <b>2017</b> , 841, 69	10
1770	Aperture-free star formation rate of SDSS star-forming galaxies. <i>Astronomy and Astrophysics</i> , <b>2017</b> , 599, A71	28
1769	A Study of Quasar Selection in the Supernova Fields of the Dark Energy Survey. <b>2017</b> , 153, 107	17
1768	The Dense Molecular Gas and Nuclear Activity in the ULIRG IRAS 13120 <b>B</b> 453. <b>2017</b> , 835, 213	20
1767	High-mass Star Formation in the Outer Scutum@entaurus Arm. 2017, 841, 121	11
1766	A DEEP PROPER MOTION CATALOG WITHIN THE SLOAN DIGITAL SKY SURVEY FOOTPRINT. II. THE WHITE DWARF LUMINOSITY FUNCTION. <b>2017</b> , 153, 10	22
1765	VIP: Vortex Image Processing Package for High-contrast Direct Imaging. <b>2017</b> , 154, 7	77
1764	A Radio-to-mm Census of Star-forming Galaxies in Protocluster 4C23.56 atZ= 2.5: Gas Mass and Its Fraction Revealed with ALMA. <b>2017</b> , 842, 55	26

1763	The connection between supernova remnants and the Galactic magnetic field: An analysis of quasi-parallel and quasi-perpendicular cosmic-ray acceleration for the axisymmetric sample.  **Astronomy and Astrophysics, 2017, 597, A121**	5.1	10	
1762	galkin: A new compilation of Milky Way rotation curve data. <b>2017</b> , 6, 54-62		18	
1761	Geographic and Annual Influences on Optical Follow-up of Gravitational Wave Events. 2017, 838, 46		2	
1760	The 2014 X-Ray Minimum of arinae as Seen by Swift. <b>2017</b> , 838, 45		23	
1759	Four Sub-Saturns with Dissimilar Densities: Windows into Planetary Cores and Envelopes. <b>2017</b> , 153, 142		74	
1758	Orion revisited. <i>Astronomy and Astrophysics</i> , <b>2017</b> , 598, A124	5.1	10	
1757	The Molecular Gas Environment in the 20 km s\( \textstyle \textsty		26	
1756	Collisions of Terrestrial Worlds: The Occurrence of Extreme Mid-infrared Excesses around Low-mass Field Stars. <b>2017</b> , 153, 165		21	
1755	Common Envelope Wind Tunnel: Coefficients of Drag and Accretion in a Simplified Context for Studying Flows around Objects Embedded within Stellar Envelopes. <b>2017</b> , 838, 56		58	
1754	Was 49b: An Overmassive AGN in a Merging Dwarf Galaxy?. <b>2017</b> , 836, 183		12	
1753	Radio Observations of the Tidal Disruption Event XMMSL1 J0740 <b>B</b> 5. <b>2017</b> , 837, 153		37	
1752	Extragalactic Peaked-spectrum Radio Sources at Low Frequencies. 2017, 836, 174		67	
1751	First Results from the KMOS Lens-Amplified Spectroscopic Survey (KLASS): Kinematics of Lensed Galaxies at Cosmic Noon. <b>2017</b> , 838, 14		33	
1750	Farthest Neighbor: The Distant Milky Way Satellite Eridanus II. <b>2017</b> , 838, 8		93	
1749	K2Ultracool Dwarfs Survey. I. Photometry of an L Dwarf Superflare. <b>2017</b> , 838, 22		15	
1748	SPATIALLY RESOLVED SPECTROSCOPY OF EUROPAB LARGE-SCALE COMPOSITIONAL UNITS AT 3個品 WITH KECK NIRSPEC. <b>2017</b> , 153, 13		16	
1747	Organized chaos: scatter in the relation between stellar mass and halo mass in small galaxies. <b>2017</b> , 464, 3108-3120		77	
1746	The Repeating Fast Radio Burst FRB 121102 as Seen on Milliarcsecond Angular Scales. <b>2017</b> , 834, L8		238	

1745	Circumstellar dust, PAHs and stellar populations in early-type galaxies: insights fromGALEXandWISE. <b>2017</b> , 464, 3920-3936	9
1744	Herschel-ATLAS: revealing dust build-up and decline across gas, dust and stellar mass selected samples II. Scaling relations. <b>2017</b> , 464, 4680-4705	36
1743	Galaxy Zoo: morphological classifications for 120 000 galaxies in HST legacy imaging. <b>2017</b> , 464, 4176-4203	38
1742	Architecture of the Andromeda galaxy: a quantitative analysis of clustering in the inner stellar halo. <b>2017</b> , 464, 4858-4865	2
1741	ON CORRELATED-NOISE ANALYSES APPLIED TO EXOPLANET LIGHT CURVES. <b>2017</b> , 153, 3	85
1740	Insights from Synthetic Star-forming Regions. I. Reliable Mock Observations from SPH Simulations. <b>2017</b> , 233, 1	9
1739	Virgo Redux: The Masses and Stellar Content of Nuclei in Early-type Galaxies from Multiband Photometry and Spectroscopy. <b>2017</b> , 849, 55	32
1738	The JCMT Transient Survey: Detection of Submillimeter Variability in a Class I Protostar EC 53 in Serpens Main. <b>2017</b> , 849, 69	31
1737	Integral Field Spectroscopy of Balmer-dominated Shocks in the Magellanic Cloud Supernova Remnant N103B. <b>2017</b> , 847, 122	14
1736	Detection and Implications of Laser-Induced Raman Scattering at Astronomical Observatories. <b>2017</b> , 7,	2
1735	Toward Space-like Photometric Precision from the Ground with Beam-shaping Diffusers. <b>2017</b> , 848, 9	60
1734	A Physical Model-based Correction for Charge Traps in theHubble Space Telescope® Wide Field Camera 3 Near-IR Detector and Its Applications to Transiting Exoplanets and Brown Dwarfs. <b>2017</b> , 153, 243	67
1733	No Difference in Orbital Parameters of RV-detected Giant Planets between 0.1 and 5 au in Single versus Multi-stellar Systems. <b>2017</b> , 153, 242	32
1732	Exploring the Efficacy and Limitations of Shock-cooling Models: New Analysis of Type II Supernovae Observed by theKeplerMission. <b>2017</b> , 848, 8	17
1731	Emulating Simulations of Cosmic Dawn for 21 cm Power Spectrum Constraints on Cosmology, Reionization, and X-Ray Heating. <b>2017</b> , 848, 23	52
1730	Chromospheric Activity of HAT-P-11: An Unusually Active Planet-hosting K Star. <b>2017</b> , 848, 58	36
1729	The Influence of Host Galaxies in Type Ia Supernova Cosmology. <b>2017</b> , 848, 56	20
1728	Galaxy Zoo: Major Galaxy Mergers Are Not a Significant Quenching Pathway. <b>2017</b> , 845, 145	19

1727	The Emergence of a Lanthanide-rich Kilonova Following the Merger of Two Neutron Stars. <b>2017</b> , 848, L27	353
1726	The Rapid Reddening and Featureless Optical Spectra of the Optical Counterpart of GW170817, AT 2017gfo, during the First Four Days. <b>2017</b> , 848, L32	93
1725	The Environment of the Binary Neutron Star Merger GW170817. <b>2017</b> , 848, L28	89
1724	The Distance to NGC 4993: The Host Galaxy of the Gravitational-wave Event GW170817. <b>2017</b> , 848, L31	67
1723	H-ATLAS/GAMA: magnification bias tomography. Astrophysical constraints above ~1 arcmin. <b>2017</b> , 2017, 024-024	13
1722	Early UV emission from disc-originated matter (DOM) in Type Ia supernovae in the double-degenerate scenario. <b>2017</b> , 470, 2510-2516	19
1721	Ultraviolet spectra of extreme nearby star-forming regions Dapproaching a local reference sample for JWST. <b>2017</b> , 472, 2608-2632	86
1720	Galaxy Zoo and sparcfire: constraints on spiral arm formation mechanisms from spiral arm number and pitch angles. <b>2017</b> , 472, 2263-2279	29
1719	Stellar inventory of the solar neighbourhood using Gaia DR1. <b>2017</b> , 470, 1360-1387	80
1718	A large HBurvey of star formation in relaxed and merging galaxy cluster environments atz~ 0.15 <b>D</b> .3. <b>2017</b> , 465, 2916-2935	22
1717	Expansion of Kes 73, A Shell Supernova Remnant Containing a Magnetar. <b>2017</b> , 846, 13	16
1716	Connecting X-ray absorption and 21 cm neutral hydrogen absorption in obscured radio AGN. <b>2017</b> , 471, 2952-2973	13
1715	Beyond the Kepler/K2 bright limit: variability in the seven brightest members of the Pleiades. <b>2017</b> , 471, 2882-2901	44
1714	GaiaReveals a Metal-rich, in situ Component of the Local Stellar Halo. <b>2017</b> , 845, 101	99
1713	The PyCASSO database: spatially resolved stellar population properties for CALIFA galaxies. <b>2017</b> , 471, 3727-3752	33
1712	Activity and Kinematics of White Dwarf-M Dwarf Binaries from the SUPERBLINK Proper Motion Survey. <b>2017</b> , 154, 118	13
1711	The Green Bank Ammonia Survey: Dense Cores under Pressure in Orion A. <b>2017</b> , 846, 144	51
1710	The SAGA Survey. I. Satellite Galaxy Populations around Eight Milky Way Analogs. <b>2017</b> , 847, 4	109

1709	Measuring Filament Orientation: A New Quantitative, Local Approach. <b>2017</b> , 232, 6	2
1708	Mid-infrared Variability of Changing-look AGNs. 2017, 846, L7	62
1707	Gaps and length asymmetry in the stellar stream Palomar 5 as effects of Galactic bar rotation. <b>2017</b> , 1, 633-639	54
1706	Accreting Double White Dwarf Binaries: Implications forLISA. <b>2017</b> , 846, 95	43
1705	On the Age of the TRAPPIST-1 System. <b>2017</b> , 845, 110	64
1704	High-mass Starless Clumps in the Inner Galactic Plane: The Sample and Dust Properties. <b>2017</b> , 231, 11	21
1703	Improving the full spectrum fitting method: accurate convolution with Gauss⊞ermite functions. <b>2017</b> , 466, 798-811	515
1702	PHIBSS: exploring the dependence of the COH2 conversion factor on total mass surface density at z. <b>2017</b> , 467, 4886-4901	15
1701	First Demonstration of ECHO: an External Calibrator for Hydrogen Observatories. 2017, 129, 035002	14
1700	Monitoring Telluric Absorption with CAMAL. <b>2017</b> , 129, 085002	8
1699	Not so lumpy after all: modelling the depletion of dark matter subhaloes by Milky Way-like galaxies´. <b>2017</b> , 471, 1709-1727	173
1698	The chemistry of episodic accretion in embedded objects. <i>Astronomy and Astrophysics</i> , <b>2017</b> , 604, A15 $_{5.1}$	20
1697	H i and cosmological constraints from intensity mapping, optical and CMB surveys. <b>2017</b> , 470, 4251-4260	36
1696	Corral framework: Trustworthy and fully functional data intensive parallel astronomical pipelines. <b>2017</b> , 20, 140-154	3
1695	Arm and interarm abundance gradients in CALIFA spiral galaxies. <i>Astronomy and Astrophysics</i> , <b>2017</b> , 603, A113	21
1694	Prediction of a Red Nova Outburst in KIC 9832227. <b>2017</b> , 840, 1	22
1693	Discovery of a dual active galactic nucleus with ~8 kpc separation. <b>2017</b> , 470, L49-L53	27
1692	K2Ultracool Dwarfs Survey. II. The White Light Flare Rate of Young Brown Dwarfs. <b>2017</b> , 845, 33	31

1691	VLA Radio Observations of theHSTFrontier Fields Cluster Abell 2744: The Discovery of New Radio Relics. <b>2017</b> , 845, 81	29
1690	Discerning dark energy models with high redshift standard candles. <b>2017</b> , 472, 1413-1420	3
1689	Prospects for the detection of high-energy (E > 25 GeV) Fermi pulsars with the Cherenkov Telescope Array. <b>2017</b> , 471, 431-446	3
1688	A millimeter Continuum SizeIluminosity Relationship for Protoplanetary Disks. <b>2017</b> , 845, 44	113
1687	The metallicity and star formation activity of long gamma-ray burst hosts for z´. <b>2017</b> , 469, 4921-4932	9
1686	The Circumgalactic Medium. <b>2017</b> , 55, 389-432	389
1685	1I/2017 U1 (Dumuamua) is Hot: Imaging, Spectroscopy, and Search of Meteor Activity. <b>2017</b> , 851, L5	67
1684	THE PANCHROMATIC HUBBLE ANDROMEDA TREASURY. XVII. EXAMINING OBSCURED STAR FORMATION WITH SYNTHETIC ULTRAVIOLET FLUX MAPS IN M31. <b>2017</b> , 834, 70	8
1683	UNTANGLING THE NEAR-IR SPECTRAL FEATURES IN THE PROTOPLANETARY ENVIRONMENT OF KH 15D. <b>2017</b> , 834, 119	7
1682	HST/COS OBSERVATIONS OF IONIZED GAS ACCRETION AT THE DISKHALO INTERFACE OF M33. <b>2017</b> , 834, 179	26
1681	Lessons from the Onset of a Common Envelope Episode: the Remarkable M31 2015 Luminous Red Nova Outburst. <b>2017</b> , 835, 282	56
1680	A Mote in Andromeda's Disk: A Misidentified Periodic AGN behind M31. <b>2017</b> , 850, 86	13
1679	Discovery of Diffuse Dwarf Galaxy Candidates around M101. <b>2017</b> , 850, 109	43
1678	Giant Ly∄ebulae in the Illustris Simulation. <b>2017</b> , 835, 207	12
1677	A Spatially Resolved Study of Cold Dust, Molecular Gas, H ii Regions, and Stars in thez= 2.12 Submillimeter Galaxy ALESS67.1. <b>2017</b> , 846, 108	52
1676	Linking the X3D Pathway to Integral Field Spectrographs: YSNR 1E 0102.2-7219 in the SMC as a Case Study. <b>2017</b> , 129, 058012	9
1675	LSSGalPy: Interactive Visualization of the Large-scale Environment Around Galaxies. <b>2017</b> , 129, 058005	3
1674	Evidence That the Directly Imaged Planet HD 131399 Ab Is a Background Star. <b>2017</b> , 154, 218	41

1673	A Multiwavelength Study of Nearby Millisecond Pulsar PSR J1400🛮 431: Improved Astrometry and an Optical Detection of Its Cool White Dwarf Companion. <b>2017</b> , 847, 25	12
1672	The Green Bank Ammonia Survey: Observations of Hierarchical Dense Gas Structures in Cepheus-L1251. <b>2017</b> , 850, 3	13
1671	Insights from Synthetic Star-forming Regions. II. Verifying Dust Surface Density, Dust Temperature, and Gas Mass Measurements With Modified Blackbody Fitting. <b>2017</b> , 849, 1	5
1670	AGN Populations in Large-volume X-Ray Surveys: Photometric Redshifts and Population Types Found in the Stripe 82X Survey. <b>2017</b> , 850, 66	33
1669	Revealing Black Holes with Gaia. <b>2017</b> , 850, L13	32
1668	A Multi-telescope Campaign on FRB 121102: Implications for the FRB Population. <b>2017</b> , 850, 76	125
1667	Resynchronization of the Asynchronous Polar CD Ind. <b>2017</b> , 129, 044204	9
1666	The local nanohertz gravitational-wave landscape from supermassive black hole binaries. <b>2017</b> , 1, 886-892	69
1665	pyLIMA: An Open-source Package for Microlensing Modeling. I. Presentation of the Software and Analysis of Single-lens Models. <b>2017</b> , 154, 203	39
1664	Morphology Dependence of Stellar Age in Quenched Galaxies at Redshift ~1.2:Massive Compact Galaxies Are Older than More Extended Ones. <b>2017</b> , 838, 94	30
1663	Project AMIGA: A Minimal Covering Factor for Optically Thick Circumgalactic Gas around the Andromeda Galaxy. <b>2017</b> , 846, 141	10
1662	The Survey of Lines in M31 (SLIM): The Drivers of the [C ii]/TIR Variation. 2017, 842, 128	10
1661	(Almost) Dark Galaxies in the ALFALFA Survey: Isolated H i-bearing Ultra-diffuse Galaxies. <b>2017</b> , 842, 133	110
1660	An artificial neural network to discover hypervelocity stars: candidates in Gaia DR1/TGAS. <b>2017</b> , 470, 1388-1403	19
1659	Mining Hubble Space Telescope images. <b>2017</b> ,	3
1658	ALMA Observations of Asymmetric Molecular Gas Emission from a Protoplanetary Disk in the Orion Nebula. <b>2017</b> , 153, 233	3
1657	Kinematics of the ionized and molecular gas in nearby luminous infrared interacting galaxies. <b>2017</b> , 465, 3461-3474	4
1656	Identifying tools for comparing simulations and observations of spectral-line data cubes. <b>2017</b> , 471, 1506-153	017

1655	Disentangling the Circumnuclear Environs of Centaurus A. III. An Inner Molecular Ring, Nuclear Shocks, and the CO to Warm H2Interface. <b>2017</b> , 843, 136	22
1654	A Three-dimensional View of Turbulence: Constraints on Turbulent Motions in the HD 163296 Protoplanetary Disk Using DCO+. <b>2017</b> , 843, 150	156
1653	Star Formation atz= 2.481 in the Lensed Galaxy SDSS J1110+6459. II. What is Missed at the Normal Resolution of theHubble Space Telescope?. <b>2017</b> , 843, 79	20
1652	The JCMT Transient Survey: Data Reduction and Calibration Methods. <b>2017</b> , 843, 55	20
1651	ATLASGAL-selected massive clumps in the inner Galaxy. <i>Astronomy and Astrophysics</i> , <b>2017</b> , 603, A33 5.1	40
1650	The Green Bank Ammonia Survey: First Results of NH3Mapping of the Gould Belt. <b>2017</b> , 843, 63	92
1649	Are merging black holes born from stellar collapse or previous mergers?. <b>2017</b> , 95,	154
1648	Galaxy Zoo: the interplay of quenching mechanisms in the group environment?. <b>2017</b> , 469, 3670-3687	30
1647	Observational Evidence for High Neutronization in Supernova Remnants: Implications for Type Ia Supernova Progenitors. <b>2017</b> , 843, 35	26
1646	The MUSCLES Treasury Survey. IV. Scaling Relations for Ultraviolet, Ca ii K, and Energetic Particle Fluxes from M Dwarfs. <b>2017</b> , 843, 31	60
1645	z~ 2: An Epoch of Disk Assembly. <b>2017</b> , 843, 46	57
1644	Massive black hole binary mergers in dynamical galactic environments. <b>2017</b> , 464, 3131-3157	80
1643	Galaxy Zoo: quantitative visual morphological classifications for 48 000 galaxies from CANDELS. <b>2017</b> , 464, 4420-4447	51
1642	Galaxy gas as obscurer []. GRBs x-ray galaxies and find an \$N_{{rm H}}^{3}propto M_{star }\$ relation. <b>2017</b> , 464, 4545-4566	24
1641	Mid-infrared spectra of comet nuclei. <b>2017</b> , 284, 344-358	14
1640	The SAMI Galaxy Survey: spatially resolving the environmental quenching of star formation in GAMA galaxies. <b>2017</b> , 464, 121-142	54
1639	Making a case for open research: Implications for reproducibility and transparency. <b>2017</b> , 54, 583-586	5
1638	A study of the effects of faint dust comae on the spectra of asteroids. <b>2017</b> , 468, 1556-1566	4

1637	Infrared Morphology of Regions of Ionized Hydrogen. <b>2017</b> , 61, 1015-1030	6
1636	The statistical challenge of constraining the low-mass IMF in Local Group dwarf galaxies. <b>2017</b> , 468, 319-332	18
1635	A distributed learning architecture for big imaging problems in astrophysics. 2017,	
1634	Diverse stellar haloes in nearby Milky Way mass disc galaxies. <b>2017</b> , 466, 1491-1512	65
1633	On the possible triple central star system of PN SuWt 2: no mbage at the heart of the Wedding Ring. <b>2017</b> , 466, 2034-2038	10
1632	Herschelfar-infrared photometry of the Swift Burst Alert Telescope active galactic nuclei sample of the local universe III. Global star-forming properties and the lack of a connection to nuclear activity. <b>2017</b> , 466, 3161-3183	36
1631	XMMDewtonobservations of the peculiar cataclysmic variable Lanning 386: X-ray evidence for a magnetic primary. <b>2017</b> , 466, 2202-2211	5
1630	The Survey of Centaurus A's Baryonic Structures (SCABS) III. The extended globular cluster system of NGC 5128 and its nearby environment. <b>2017</b> , 469, 3444-3467	17
1629	Galaxy Zoo: finding offset discs and bars in SDSS galaxies?. <b>2017</b> , 469, 3363-3373	14
1628	UVI colour gradients of 0.4′. <b>2017</b> , 469, 4063-4082	22
1627	Modelling the luminosities and sizes of radio sources: radio luminosity function at $z = 6$ . <b>2017</b> , 469, 4083-4094	18
1626	Gaia 1 and 2. A pair of new Galactic star clusters. <b>2017</b> , 470, 2702-2709	52
1625	Stellar disc truncations and extended haloes in face-on spiral galaxies. <b>2017</b> , 470, 427-444	13
1624	A GMOS-N IFU study of the central H ii region in the blue compact dwarf galaxy NGC 4449: kinematics, nebular metallicity and star formation?. <b>2017</b> , 470, 4618-4637	14
1623	The First Billion Years project: constraining the dust attenuation law of star-forming galaxies at z ? 5. <b>2017</b> , 470, 3006-3026	52
1622	H0LiCOW III. Spectroscopic survey and galaxy-group identification of the strong gravitational lens system HE 0435I1223. <b>2017</b> , 470, 4838-4857	39
1621	Star-forming galaxies in intermediate-redshift clusters: stellar versus dynamical masses of luminous compact blue galaxies. <b>2017</b> , 470, 4382-4396	2
1620	Large-scale retrospective relative spectrophotometric self-calibration in space. <b>2017</b> , 467, 3677-3698	5

1619	H0LiCOW III. Quantifying the effect of mass along the line of sight to the gravitational lens HE 0435II223 through weighted galaxy counts?. <b>2017</b> , 467, 4220-4242	70
1618	Low-resolution near-infrared spectroscopic signatures of unresolved ultracool companions to M dwarfs. <b>2017</b> , 467, 5001-5021	2
1617	the-wizz: clustering redshift estimation for everyone. <b>2017</b> , 467, 3576-3589	33
1616	VLT/FORS2 comparative transmission spectroscopy II: Confirmation of a cloud deck and Rayleigh scattering in WASP-31b, but no potassium?. <b>2017</b> , 467, 4591-4605	61
1615	The Fan Region at 1.5 GHz []. Polarized synchrotron emission extending beyond the Perseus Arm. <b>2017</b> , 467, 4631-4646	16
1614	Cosmology with XMM galaxy clusters: the X-CLASS/GROND catalogue and photometric redshifts. <b>2017</b> , 468, 662-684	9
1613	A measurement of the z´=´0 UV background from H⊞luorescence. <b>2017</b> , 467, 4802-4816	34
1612	Search for exoplanets around pulsating stars of AE type in Kepler short-cadence data and the case of KIC 8197761. <b>2017</b> , 467, 4663-4673	35
1611	The mass distribution of Population III stars. <b>2017</b> , 468, 418-425	18
1610	Constraints on AGN feedback from its Sunyaev Zel'dovich imprint on the cosmic background radiation. <b>2017</b> , 468, 577-596	17
1609	The WAGGS project II. The WiFeS Atlas of Galactic Globular cluster Spectra. 2017, 468, 3828-3849	21
1608	Rayleigh scattering in the transmission spectrum of HAT-P-18b. <b>2017</b> , 468, 3907-3916	34
1607	The redshift evolution of major merger triggering of luminous AGNs: a slight enhancement at z $\sim$ 2. <b>2017</b> , 470, 755-770	27
1606	MARXS: A Modular Software to Ray-trace X-Ray Instrumentation. <b>2017</b> , 154, 243	8
1605	Spectroscopic binaries in the Solar Twin Planet Search program: from substellarhass to M dwarf companions. <b>2017</b> , 472, 3425-3436	9
1604	The chemistry of protoplanetary fragments formed via gravitational instabilities. <b>2017</b> , 472, 189-204	43
1603	Simultaneous low- and high-mass star formation in a massive protocluster: ALMA observations of G11.92D.61?. <b>2017</b> , 468, 3694-3708	35
1602	The Northern arc of $\bar{\mu}$ Eridanië Debris Ring as seen by ALMA. <b>2017</b> , 469, 3200-3212	57

1601	Supermassive black holes in disc-dominated galaxies outgrow their bulges and co-evolve with their host galaxies. <b>2017</b> , 470, 1559-1569	22
1600	The MUSE view of the host galaxy of GRB 100316D. <b>2017</b> , 472, 4480-4496	26
1599	Towards a new classification of galaxies: principal component analysis of CALIFA circular velocity curves. <b>2017</b> , 469, 2539-2594	22
1598	Know the Planet, Know the Star: Precise Stellar Densities fromKeplerTransit Light Curves. <b>2017</b> , 154, 228	33
1597	Data Reduction and Image Reconstruction Techniques for Non-redundant Masking. <b>2017</b> , 233, 9	5
1596	MASSIVE STAR FORMATION IN THE LMC. I. N159 AND N160 COMPLEXES. <b>2017</b> , 834, 122	1
1595	The First Simultaneous X-Ray/Radio Detection of the First Be/BH System MWC 656. <b>2017</b> , 835, L33	20
1594	Insights from Synthetic Star-forming Regions. III. Calibration of Measurement and Techniques of Star Formation Rates. <b>2017</b> , 849, 2	9
1593	Molecular Gas Kinematics and Star Formation Properties of the Strongly-lensed Quasar Host Galaxy RXS J1131 231. <b>2017</b> , 836, 180	9
1592	Col-OSSOS: Colors of the Interstellar Planetesimal 1I/Dumuamua. 2017, 851, L38	75
1592 1591	Col-OSSOS: Colors of the Interstellar Planetesimal 11/Dumuamua. 2017, 851, L38  An Optically Faint Quasar Survey atz~ 5 in the CFHTLS Wide Field: Estimates of the Black Hole Masses and Eddington Ratios. 2017, 846, 57	75 6
1591	An Optically Faint Quasar Survey atz~ 5 in the CFHTLS Wide Field: Estimates of the Black Hole	
1591	An Optically Faint Quasar Survey atz~ 5 in the CFHTLS Wide Field: Estimates of the Black Hole Masses and Eddington Ratios. <b>2017</b> , 846, 57	6
1591 1590	An Optically Faint Quasar Survey atz~ 5 in the CFHTLS Wide Field: Estimates of the Black Hole Masses and Eddington Ratios. 2017, 846, 57  A New, Large-scale Map of Interstellar Reddening Derived from H i Emission. 2017, 846, 38  On Estimation of Contamination from Hydrogen Cyanide in Carbon Monoxide Line-intensity Mapping. 2017, 846, 60	6 56
1591 1590 1589	An Optically Faint Quasar Survey atz~ 5 in the CFHTLS Wide Field: Estimates of the Black Hole Masses and Eddington Ratios. 2017, 846, 57  A New, Large-scale Map of Interstellar Reddening Derived from H i Emission. 2017, 846, 38  On Estimation of Contamination from Hydrogen Cyanide in Carbon Monoxide Line-intensity Mapping. 2017, 846, 60	6 56 8
1591 1590 1589 1588	An Optically Faint Quasar Survey atz~ 5 in the CFHTLS Wide Field: Estimates of the Black Hole Masses and Eddington Ratios. 2017, 846, 57  A New, Large-scale Map of Interstellar Reddening Derived from H i Emission. 2017, 846, 38  On Estimation of Contamination from Hydrogen Cyanide in Carbon Monoxide Line-intensity Mapping. 2017, 846, 60  The Starspots of HAT-P-11: Evidence for a Solar-like Dynamo. 2017, 846, 99  A 1.4 deg2 blind survey for C II], C III] and C IV at z ~ 0.7 ll.5 ll. Nature, morphologies and	6 56 8 72
1591 1590 1589 1588	An Optically Faint Quasar Survey atz~ 5 in the CFHTLS Wide Field: Estimates of the Black Hole Masses and Eddington Ratios. 2017, 846, 57  A New, Large-scale Map of Interstellar Reddening Derived from H i Emission. 2017, 846, 38  On Estimation of Contamination from Hydrogen Cyanide in Carbon Monoxide Line-intensity Mapping. 2017, 846, 60  The Starspots of HAT-P-11: Evidence for a Solar-like Dynamo. 2017, 846, 99  A 1.4 deg2 blind survey for C II], C III] and C IV at z ~ 0.7 1.5 1. Nature, morphologies and equivalent widths. 2017, 471, 2558-2574	6 56 8 72

	A closer look at the Bharacteristic width of molecular cloud filaments. <b>2017</b> , 466, 2529-2541	48
1582	On the use of variability time-scales as an early classifier of radio transients and variables. <b>2017</b> , 471, 3788-3805	3
1581	MALT-45: A 7 mm survey of the southern Galaxy III. ATCA follow-up observations of 44 GHz class I methanol masers. <b>2017</b> , 471, 3915-3954	14
1580	Characterization of the ionosphere above the Murchison Radio Observatory using the Murchison Widefield Array. <b>2017</b> , 471, 3974-3987	29
1579	Siriusly, a newly identified intermediate-age Milky Way stellar cluster: a spectroscopic study of Gaia´1. <b>2017</b> , 471, 4087-4098	8
1578	On the Rotation Period and Shape of the Hyperbolic Asteroid 1I/Dumuamua (2017 U1) from Its Lightcurve. <b>2017</b> , 851, L31	41
1577	The Herschel ATLAS Data Release 2, Paper I. Submillimeter and Far-infrared Images of the South and North Galactic Poles: The Largest Herschel Survey of the Extragalactic Sky. <b>2017</b> , 233, 26	28
1576	Periodic eclipses of the young star PDS 110 discovered with WASP and KELT photometry. <b>2017</b> , 471, 740-749	33
1575	The Hydrangea simulations: galaxy formation in and around massive clusters. 2017, 470, 4186-4208	114
1574	Bolles-HiZELS: an optical to near-infrared survey of emission-line galaxies at z´=´0.44.7. <b>2017</b> , 471, 629-649	2.7
27 1	bobes Thereas. an optical to fical himarca survey of emission line galaxies at 2 = 0.44.7. 2017, 471, 625 645	31
1573	BAT AGN Spectroscopic Survey. I. Spectral Measurements, Derived Quantities, and AGN Demographics. <b>2017</b> , 850, 74	138
	BAT AGN Spectroscopic Survey. I. Spectral Measurements, Derived Quantities, and AGN	
1573	BAT AGN Spectroscopic Survey. I. Spectral Measurements, Derived Quantities, and AGN Demographics. <b>2017</b> , 850, 74  The fundamental stellar parameters of FGK stars in the SEEDS survey Norman, OK 73071, USA.	138
1573 1572 1571	BAT AGN Spectroscopic Survey. I. Spectral Measurements, Derived Quantities, and AGN Demographics. <b>2017</b> , 850, 74  The fundamental stellar parameters of FGK stars in the SEEDS survey Norman, OK 73071, USA. <b>2017</b> , 472, 1736-1752  ESO 452BC11: the lowest mass globular cluster with a potential chemical inhomogeneity. <b>2017</b> ,	138 5
1573 1572 1571	BAT AGN Spectroscopic Survey. I. Spectral Measurements, Derived Quantities, and AGN Demographics. 2017, 850, 74  The fundamental stellar parameters of FGK stars in the SEEDS survey Norman, OK 73071, USA. 2017, 472, 1736-1752  ESO 452BC11: the lowest mass globular cluster with a potential chemical inhomogeneity. 2017, 472, 2856-2868  The varying mass distribution of molecular clouds across M83. 2017, 468, 1769-1781	138 5 15
1573 1572 1571 1570	BAT AGN Spectroscopic Survey. I. Spectral Measurements, Derived Quantities, and AGN Demographics. 2017, 850, 74  The fundamental stellar parameters of FGK stars in the SEEDS survey Norman, OK 73071, USA. 2017, 472, 1736-1752  ESO 452BC11: the lowest mass globular cluster with a potential chemical inhomogeneity. 2017, 472, 2856-2868  The varying mass distribution of molecular clouds across M83. 2017, 468, 1769-1781  Initial Mass Function Variability (or Not) among Low-velocity Dispersion, Compact Stellar Systems.	138 5 15 50
1573 1572 1571 1570	BAT AGN Spectroscopic Survey. I. Spectral Measurements, Derived Quantities, and AGN Demographics. 2017, 850, 74  The fundamental stellar parameters of FGK stars in the SEEDS survey Norman, OK 73071, USA. 2017, 472, 1736-1752  ESO 452BC11: the lowest mass globular cluster with a potential chemical inhomogeneity. 2017, 472, 2856-2868  The varying mass distribution of molecular clouds across M83. 2017, 468, 1769-1781  Initial Mass Function Variability (or Not) among Low-velocity Dispersion, Compact Stellar Systems. 2017, 850, L14	138 5 15 50 18

1565	Trident: A Universal Tool for Generating Synthetic Absorption Spectra from Astrophysical Simulations. <b>2017</b> , 847, 59	42
1564	Accretion Disk Assembly During Common Envelope Evolution: Implications for Feedback and LIGO Binary Black Hole Formation. <b>2017</b> , 845, 173	34
1563	A Tale of Two Transients: GW 170104 and GRB 170105A. <b>2017</b> , 845, 152	24
1562	New Low-mass Eclipsing Binary Systems in Praesepe Discovered by K2. <b>2017</b> , 849, 11	71
1561	Three-phase Interstellar Medium in Galaxies Resolving Evolution with Star Formation and Supernova Feedback (TIGRESS): Algorithms, Fiducial Model, and Convergence. <b>2017</b> , 846, 133	84
1560	The FluxCompensator: Making Radiative Transfer Models of Hydrodynamical Simulations Directly Comparable to Real Observations. <b>2017</b> , 849, 3	8
1559	Detection of 36 GHz Class I Methanol Maser Emission toward NGC 4945. <b>2017</b> , 846, 156	15
1558	Buried AGNs in Advanced Mergers: Mid-infrared Color Selection as a Dual AGN Candidate Finder. <b>2017</b> , 848, 126	48
1557	The Small Magellanic Cloud Investigation of Dust and Gas Evolution (SMIDGE): The Dust Extinction Curve from Red Clump Stars. <b>2017</b> , 847, 102	13
1556	A 2500 deg2CMB Lensing Map from Combined South Pole Telescope andPlanckData. <b>2017</b> , 849, 124	33
1555	Mapping the LyEmission around az~ 6.6 QSO with MUSE: Extended Emission and a Companion at a Close Separation. <b>2017</b> , 848, 78	32
1554	Spectral Variability of Two Rapidly Rotating Brown Dwarfs: 2MASS J08354256-0819237 and 2MASS J18212815+1414010. <b>2017</b> , 849, 163	6
1553	The JCMT Transient Survey: Identifying Submillimeter Continuum Variability over Several Year Timescales Using Archival JCMT Gould Belt Survey Observations. <b>2017</b> , 849, 107	16
1552	ALMA Observations of a Quiescent Molecular Cloud in the Large Magellanic Cloud. <b>2017</b> , 850, 139	19
1551	An Infrared Census of DUST in Nearby Galaxies withSpitzer(DUSTiNGS). IV. Discovery of High-redshift AGB Analogs. <b>2017</b> , 851, 152	22
1550	FRB 121102 Is Coincident with a Star-forming Region in Its Host Galaxy. <b>2017</b> , 843, L8	98
1549	Testing the Recovery of Intrinsic Galaxy Sizes and Masses of z $\sim$ 2 Massive Galaxies Using Cosmological Simulations. <b>2017</b> , 844, L6	18
1548	The Little Cub: Discovery of an Extremely Metal-poor Star-forming Galaxy in the Local Universe. <b>2017</b> , 845, L22	17

1547	BAT AGN Spectroscopic Survey. V. X-Ray Properties of the Swift /BAT 70-month AGN Catalog. <b>2017</b> , 233, 17	190
1546	Variable Dynamics in the Inner Disk of HD 135344B Revealed with Multi-epoch Scattered Light Imaging. <b>2017</b> , 849, 143	37
1545	Eight new luminous z lb quasars discovered via SED model fitting of VISTA, WISE and Dark Energy Survey Year 1 observations. <b>2017</b> , 468, 4702-4718	66
1544	The Extended IRTF Spectral Library: Expanded Coverage in Metallicity, Temperature, and Surface Gravity. <b>2017</b> , 230, 23	44
1543	Dwarf galaxy mass estimators versus cosmological simulations. <b>2017</b> , 472, 4786-4796	19
1542	Can planet formation resolve the dust budget crisis in high-redshift galaxies?. <b>2017</b> , 472, 2289-2296	19
1541	The immitigable nature of assembly bias: the impact of halo definition on assembly bias. <b>2017</b> , 472, 1088-110	530
1540	Extremely late photometry of the nearby SN 2011fe. <b>2017</b> , 472, 2534-2542	22
1539	The Architecture of the GW Ori Young Triple-star System and Its Disk: Dynamical Masses, Mutual Inclinations, and Recurrent Eclipses. <b>2017</b> , 851, 132	15
1538	Witnessing galaxy assembly in an extended zB structure. <b>2017</b> , 471, 3686-3698	27
1537	Towards a consistent model for both the H i and stellar mass functions of galaxies. <b>2017</b> , 472, 1981-1990	6
1536	The gravitational wave background from massive black hole binaries in Illustris: spectral features and time to detection with pulsar timing arrays. <b>2017</b> , 471, 4508-4526	58
1535	Determination of Dark Matter Halo Mass from Dynamics of Satellite Galaxies. <b>2017</b> , 850, 116	17
1534	Dissecting the active galactic nucleus in Circinus II. Peculiar mid-IR morphology explained by a dusty hollow cone. <b>2017</b> , 472, 3854-3870	39
1533	The Araucaria Project: The Distance to the Fornax Dwarf Galaxy from Near-infrared Photometry of RR Lyrae Stars. <b>2017</b> , 154, 263	16
1532	Real-time colouring and filtering with graphics shaders. <b>2017</b> , 471, 3323-3346	4
1531	The ultracompact nature of the black hole candidate X-ray binary 47 Tuc X9. <b>2017</b> , 467, 2199-2216	54
1530	Parallel computation of magnetic field parameters from HMI active region patches. 2017,	1

1529	Multiwavelength Stellar Polarimetry of the Filamentary Cloud IC5146. I. Dust Properties. 2017, 849, 157	15
1528	The planetary nebula IC 4776 and its post-common-envelope binary central star. <b>2017</b> , 471, 3529-3546	15
1527	Wide binaries in Tycho-Gaia: search method and the distribution of orbital separations. <b>2017</b> , 472, 675-699	59
1526	The deep OB star population in Carina from the VST Photometric H岳urvey (VPHAS+). <b>2017</b> , 465, 1807-1830	18
1525	The structural and size evolution of star-forming galaxies over the last 11 Gyr. 2017, 465, 2717-2733	24
1524	Galaxy Zoo: star formation versus spiral arm number. <b>2017</b> , 468, 1850-1863	14
1523	Do individualSpitzeryoung stellar object candidates enclose multiple UKIDSS sources?. <i>Astronomy and Astrophysics</i> , <b>2017</b> , 598, A136	6
1522	Hydrogen in diffuse molecular clouds in the Milky Way. <i>Astronomy and Astrophysics</i> , <b>2017</b> , 600, A2 5.1	13
1521	Estimating extinction using unsupervised machine learning. <i>Astronomy and Astrophysics</i> , <b>2017</b> , 601, A137 <sub>5.1</sub>	11
1520	TOPCAT: Desktop Exploration of Tabular Data for Astronomy and Beyond. <b>2017</b> , 4, 18	7
1520 1519	TOPCAT: Desktop Exploration of Tabular Data for Astronomy and Beyond. <b>2017</b> , 4, 18  The Universality of the Rapid Neutron-capture Process Revealed by a Possible Disrupted Dwarf Galaxy Star. <b>2017</b> , 850, 179	7
1519	The Universality of the Rapid Neutron-capture Process Revealed by a Possible Disrupted Dwarf	
1519	The Universality of the Rapid Neutron-capture Process Revealed by a Possible Disrupted Dwarf Galaxy Star. <b>2017</b> , 850, 179	10
1519 1518	The Universality of the Rapid Neutron-capture Process Revealed by a Possible Disrupted Dwarf Galaxy Star. 2017, 850, 179  The Extended Baryonic Halo of NGC 3923. 2017, 5, 29  Multi-epoch observations with high spatial resolution of multiple T Tauri systems. Astronomy and Astrophysics, 2017, 603, A74  5.1	10
1519 1518 1517	The Universality of the Rapid Neutron-capture Process Revealed by a Possible Disrupted Dwarf Galaxy Star. 2017, 850, 179  The Extended Baryonic Halo of NGC 3923. 2017, 5, 29  Multi-epoch observations with high spatial resolution of multiple T Tauri systems. Astronomy and Astrophysics, 2017, 603, A74  5.1	10 2 9
1519 1518 1517 1516	The Universality of the Rapid Neutron-capture Process Revealed by a Possible Disrupted Dwarf Galaxy Star. 2017, 850, 179  The Extended Baryonic Halo of NGC 3923. 2017, 5, 29  Multi-epoch observations with high spatial resolution of multiple T Tauri systems. Astronomy and Astrophysics, 2017, 603, A74  Average Spectral Properties of Type Ia Supernova Host Galaxies. 2017, 850, 135  DeepChandraobservations of the stripped galaxy group falling into Abell 2142. Astronomy and	10 2 9
1519 1518 1517 1516 1515	The Universality of the Rapid Neutron-capture Process Revealed by a Possible Disrupted Dwarf Galaxy Star. 2017, 850, 179  The Extended Baryonic Halo of NGC 3923. 2017, 5, 29  Multi-epoch observations with high spatial resolution of multiple T Tauri systems. Astronomy and Astrophysics, 2017, 603, A74  Average Spectral Properties of Type Ia Supernova Host Galaxies. 2017, 850, 135  DeepChandraobservations of the stripped galaxy group falling into Abell 2142. Astronomy and Astrophysics, 2017, 605, A25  Very Low-mass Stars and Brown Dwarfs in Upper Scorpius UsingGaiaDR1: Mass Function, Disks, and	10 2 9 5 26

## (2017-2017)

1511	The spatially resolved star formation history of CALIFA galaxies. <i>Astronomy and Astrophysics</i> , <b>2017</b> , 608, A27	47	
1510	Two NIRCam Channels are Better than One: HowJWSTCan Do More Science with NIRCam Short-wavelength Dispersed Hartmann Sensor. <b>2017</b> , 129, 015001	14	
1509	Deep Subaru Hyper Suprime-Cam Observations of Milky Way Satellites Columba I and Triangulum II. <b>2017</b> , 154, 267	25	
1508	Evidence for azimuthal variations of the oxygen-abundance gradient tracing the spiral structure of the galaxy HCG 91c. <i>Astronomy and Astrophysics</i> , <b>2017</b> , 601, A61	33	
1507	Multi-Site Simultaneous Time-Resolved Photometry with a Low Cost Electro-Optics System. <b>2017</b> , 17,	3	
1506	Measurement of picometer-scale mirror dynamics. <b>2017</b> , 56, 6457-6465	5	
1505	ZFIRE: using H⊕quivalent widths to investigate the in situ initial mass function at z ~ 2. <b>2017</b> , 468, 3071-3108	15	
1504	The spin rates of O stars in WR + O binaries <b>II</b> . Motivation, methodology, and first results from SALT. <b>2017</b> , 464, 2066-2074	18	
1503	A modular set of synthetic spectral energy distributions for young stellar objects. <i>Astronomy and Astrophysics</i> , <b>2017</b> , 600, A11	44	
1502	Radiative age mapping of the remnant radio galaxy B2 0924+30: the LOFAR perspective. <i>Astronomy and Astrophysics</i> , <b>2017</b> , 600, A65	20	
1501	bRing: An observatory dedicated to monitoring the Pictoris b Hill sphere transit. <i>Astronomy and Astrophysics</i> , <b>2017</b> , 607, A45	14	
1500	Galaxy and Mass Assembly (GAMA): active galactic nuclei in pairs of galaxies. 2017, 465, 2671-2686	28	
1499	Temperature structure and kinematics of the IRDC G035.3900.33. <i>Astronomy and Astrophysics</i> , <b>2017</b> , 606, A133	19	
1498	Galactocentric variation of the gas-to-dust ratio and its relation with metallicity. <i>Astronomy and Astrophysics</i> , <b>2017</b> , 606, L12	34	
1497	Massive close pairs measure rapid galaxy assembly in mergers at high redshift. <b>2017</b> , 468, 207-216	47	
1496	Mass distribution in the core of MACS J1206. <i>Astronomy and Astrophysics</i> , <b>2017</b> , 607, A93 5.1	33	
1495	A broad perspective on multiple abundance populations in the globular cluster NGC 1851. <b>2017</b> , 465, 1123-1136	15	
1494	VDES J2325B229 az= 2.7 gravitationally lensed quasar discovered using morphology-independent supervised machine learning. <b>2017</b> , 465, 4325-4334	54	

1493 Modeling 237 Lyman-⊞pectra of the MUSE-Wide survey. <i>Astronomy and Astrophysics</i> , <b>2017</b> , 608, A13	<b>39</b> 5.1	36
1492 Polarized scattered light from self-luminous exoplanets. <i>Astronomy and Astrophysics</i> , <b>2017</b> , 607, A4	2 5.1	30
Observational calibration of the projection factor of Cepheids. <i>Astronomy and Astrophysics</i> , <b>2017</b> , 600, A127	5.1	24
A companion on the planet/brown dwarf mass boundary on a wide orbit discovered by gravitationa microlensing. <i>Astronomy and Astrophysics</i> , <b>2017</b> , 604, A103	l 5.1	10
LSDCat: Detection and cataloguing of emission-line sources in integral-field spectroscopy datacubes. <i>Astronomy and Astrophysics</i> , <b>2017</b> , 602, A111	5.1	35
[Fe XIV] and [Fe XI] reveal the forward shock in SNR 1E 0102.2-7219. Astronomy and Astrophysics, <b>2017</b> , 602, L4	5.1	15
1487 Detecting unresolved binary stars in Euclid VIS images. <i>Astronomy and Astrophysics</i> , <b>2017</b> , 606, A119	9 5.1	2
1486 The faint radio sky: VLBA observations of the COSMOS field. <i>Astronomy and Astrophysics</i> , <b>2017</b> , 607	', A13 <b>ट्र</b> ₁	29
The production and escape of Lyman-Continuum radiation from star-forming galaxies atz~ 2 and their redshift evolution. <b>2017</b> , 465, 3637-3655		58
1484 The convective surface of the red supergiant Antares. <i>Astronomy and Astrophysics</i> , <b>2017</b> , 605, A108	5.1	5
Spectroscopic and photometric oscillatory envelope variability during the S Doradus outburst of the luminous blue variable R71. <i>Astronomy and Astrophysics</i> , <b>2017</b> , 608, A124	5.1	12
1482 The origin of the enhanced metallicity of satellite galaxies. <b>2017</b> , 464, 508-529		27
1481 HELP: xid+, the probabilistic de-blender forHerschelSPIRE maps. <b>2017</b> , 464, 885-896		66
$_{1480}$ Non-parametric morphologies of mergers in the Illustris simulation. <b>2017</b> , 465, 1106-1122		9
Illuminating the past 8 billion years of cold gas towards two gravitationally lensed quasars. <b>2017</b> , 465, 4450-4467		21
A consistent measure of the merger histories of massive galaxies using close-pair statistics $\blacksquare$ . Major mergers at z´. <b>2017</b> , 470, 3507-3531		64
Searching for faint comoving companions to the Eentauri system in the VVV survey infrared images. <b>2017</b> , 472, 3952-3958		17
1476 X-ray observations of FO Aqr during the 2016 low state. <b>2017</b> , 469, 956-967		10

1475	TRUST. Astronomy and Astrophysics, <b>2017</b> , 603, A114	5.1	22
1474	StarHorse: a Bayesian tool for determining stellar masses, ages, distances, and extinctions for field stars. <b>2018</b> , 476, 2556-2583		94
1473	Improving time-delay cosmography with spatially resolved kinematics. 2018, 473, 210-226		40
1472	Stochastic Order Redshift Technique (SORT): a simple, efficient and robust method to improve cosmological redshift measurements. <b>2018</b> , 473, 366-379		1
1471	Simulating Radio Emission from Low-mass Stars. <b>2018</b> , 854, 7		12
1470	Kronos and Krios: Evidence for Accretion of a Massive, Rocky Planetary System in a Comoving Pair of Solar-type Stars. <b>2018</b> , 854, 138		54
1469	Wandering off the centre: a characterization of the random motion of intermediate-mass black holes in star clusters. <b>2018</b> , 475, 1574-1586		10
1468	Morphology and Kinematics of Filaments in the Serpens and Perseus Molecular Clouds. <b>2018</b> , 853, 169		29
1467	Atmospheric stellar parameters for large surveys using FASMA, a new spectral synthesis package. <b>2018</b> , 473, 5066-5097		13
1466	ChromaStarPy: A Stellar Atmosphere and Spectrum Modeling and Visualization Lab in Python. <b>2018</b> , 854, 82		2
1465	The LyReference Sample. VIII. Characterizing LyBcattering in Nearby Galaxies. 2018, 852, 9		8
1464	Search for Dark Matter Annihilation in Galaxy Groups. <b>2018</b> , 120, 101101		28
1463	Stellar Population Synthesis of Star-forming Clumps in Galaxy Pairs and Non-interacting Spiral Galaxies. <b>2018</b> , 234, 35		5
1462	On the Nature of Ultra-faint Dwarf Galaxy Candidates. I. DES1, Eridanus III, and Tucana V. <b>2018</b> , 852, 68		29
1461	Gaia17biu/SN 2017egm in NGC 3191: The Closest Hydrogen-poor Superluminous Supernova to Date Is in a Normal, Massive, Metal-rich Spiral Galaxy. <b>2018</b> , 853, 57		46
1460	Spectroscopic Observations of the Outflowing Wind in the Lensed Quasar SDSS J1001+5027. <b>2018</b> , 854, 69		5
1459	Continuum Reverberation Mapping of the Accretion Disks in Two Seyfert 1 Galaxies. <b>2018</b> , 854, 107		32
1458	Precise Time Delays from Strongly Gravitationally Lensed Type Ia Supernovae with Chromatically Microlensed Images. <b>2018</b> , 855, 22		43

1457	Precision Orbit of Delphini and Prospects for Astrometric Detection of Exoplanets. 2018, 855, 1	9
1456	The Next Generation Transit Survey (NGTS). 2018, 475, 4476-4493	127
1455	The Next Generation Fornax Survey (NGFS). II. The Central Dwarf Galaxy Population. 2018, 855, 142	47
1454	Modelling the gas kinematics of an atypical Ly Emitting compact dwarf galaxy. 2018, 474, 12-19	2
1453	Detecting outliers and learning complex structures with large spectroscopic surveys (a) case study with APOGEE stars. <b>2018</b> , 476, 2117-2136	22
1452	First Results from theHerscheland ALMA Spectroscopic Surveys of the SMC: The Relationship between [C ii]-bright Gas and CO-bright Gas at Low Metallicity. <b>2018</b> , 853, 111	18
1451	The fraction of AGNs in major merger galaxies and its luminosity dependence. <b>2018</b> , 476, 2308-2317	21
1450	SALT HRS discovery of a long-period double-degenerate binary in the planetary nebula NGC 1360. <b>2018</b> , 473, 2275-2287	15
1449	A Survey of CH3CN and HC3N in Protoplanetary Disks. <b>2018</b> , 857, 69	61
1448	Hyperactivity and Dust Composition of Comet 103P/Hartley 2 During the EPOXI Encounter. <b>2018</b> , 155, 199	6
1447	From Actinides to Zinc: Using the Full Abundance Pattern of the Brightest Star in Reticulum II to Distinguish between Differentr-process Sites. <b>2018</b> , 856, 138	39
1446	Spotting stellar activity cycles in Gaia astrometry. <b>2018</b> , 476, 5408-5416	11
1445	The Mass and Absorption Columns of Galactic Gaseous Halos. <b>2018</b> , 856, 5	24
1444	Slicing COSMOS with SC4K: the evolution of typical Ly lemitters and the Ly lescape fraction from z´~´2 to 6. <b>2018</b> , 476, 4725-4752	58
1443	Identification of the central compact object in the young supernova remnant 1E 0102.2🛭 219. <b>2018</b> , 2, 465-471	14
1442	Detecting Weak Spectral Lines in Interferometric Data through Matched Filtering. 2018, 155, 182	42
1441	Dark Energy Survey Year 1 Results: The Photometric Data Set for Cosmology. <b>2018</b> , 235, 33	150
1440	Two-fluid dusty shocks: simple benchmarking problems and applications to protoplanetary discs. <b>2018</b> , 476, 3185-3194	5

## (2018-2018)

1439	Mapping the Tidal Destruction of the Hercules Dwarf: A Wide-field DECam Imaging Search for RR Lyrae Stars. <b>2018</b> , 852, 44	28
1438	Turbulence in the TW Hya Disk. <b>2018</b> , 856, 117	109
1437	Phase Curves of WASP-33b and HD 149026b and a New Correlation between Phase Curve Offset and Irradiation Temperature. <b>2018</b> , 155, 83	79
1436	The need for speed: escape velocity and dynamical mass measurements of the Andromeda galaxy. <b>2018</b> , 475, 4043-4054	29
1435	Linking black hole growth with host galaxies: the accretion tellar mass relation and its cosmic evolution. <b>2018</b> , 475, 1887-1911	43
1434	A stellar census in globular clusters with MUSE: The contribution of rotation to cluster dynamics studied with 200 000 stars. <b>2018</b> , 473, 5591-5616	117
1433	Investigating the Binarity of S0-2: Implications for Its Origins and Robustness as a Probe of the Laws of Gravity around a Supermassive Black Hole. <b>2018</b> , 854, 12	36
1432	Discovery of 36 eclipsing EL CVn binaries found by the Palomar Transient Factory. <b>2018</b> , 475, 2560-2590	19
1431	Gravitational instability of filamentary molecular clouds, including ambipolar diffusion; non-isothermal filament. <b>2018</b> , 475, 2632-2641	5
1430	LOFAR/H-ATLAS: the low-frequency radio luminosityEtar formation rate relation. 2018, 475, 3010-3028	52
1429	Zodiacal Exoplanets in Time (ZEIT). VI. A Three-planet System in the Hyades Cluster Including an Earth-sized Planet. <b>2018</b> , 155, 4	67
1428	2MASS J11151597+1937266: A Young, Dusty, Isolated, Planetary-mass Object with a Potential Wide Stellar Companion. <b>2018</b> , 853, 75	3
1427	The Dusty Galactic Center as Seen by SCUBA-2. <b>2018</b> , 234, 22	22
1426	A Testable Conspiracy: Simulating Baryonic Effects on Self-interacting Dark Matter Halos. <b>2018</b> , 853, 109	48
1425	Characterising and identifying galaxy protoclusters. <b>2018</b> , 474, 4612-4628	20
1424	Planck Sunyaev⊠el⊞ovich cluster mass calibration using Hyper Suprime-Cam weak lensing. <b>2018</b> , 70,	29
1423	The GALEX /S 4 G Surface Brightness and Color Profiles Catalog. I. Surface Photometry and Color Gradients of Galaxies. <b>2018</b> , 234, 18	15
1422	Distributed Cosmic Ray Detection Using Cloud Computing. <b>2018</b> , 414-429	1

1421	The kinematics of the Scorpius-Centaurus OB association from Gaia DR1. 2018, 476, 381-398	77
1420	CO and Dust Properties in the TW Hya Disk from High-resolution ALMA Observations. <b>2018</b> , 852, 122	92
1419	DESCQA: An Automated Validation Framework for Synthetic Sky Catalogs. <b>2018</b> , 234, 36	13
1418	Mapping low-frequency carbon radio recombination lines towards Cassiopeia A at 340, 148, 54, and 43 MHz. <b>2018</b> , 475, 2496-2511	11
1417	KVN observations reveal multiple Fray emission regions in 3C 84?. <b>2018</b> , 475, 368-378	23
1416	Detection of a westward hotspot offset in the atmosphere of hot gas giant CoRoT-2b. <b>2018</b> , 2, 220-227	59
1415	Meeting the Cool Neighbors. XII. An Optically Anchored Analysis of the Near-infrared Spectra of L Dwarfs. <b>2018</b> , 155, 34	24
1414	Pipeline for the Detection of Serendipitous Stellar Occultations by Kuiper Belt Objects with the Colibri Fast-photometry Array. <b>2018</b> , 130, 014502	8
1413	The GALFA-H i Survey Data Release 2. <b>2018</b> , 234, 2	44
1412	APO Time-resolved Color Photometry of Highly Elongated Interstellar Object 1I/Dumuamua. <b>2018</b> , 852, L2	70
1411	On the Mass and Luminosity Functions of Tidal Disruption Flares: Rate Suppression due to Black Hole Event Horizons. <b>2018</b> , 852, 72	58
1410	PaSD-qc: quality control for single cell whole-genome sequencing data using power spectral density estimation. <b>2018</b> , 46, e20	11
1409	Characterization and photometric performance of the Hyper Suprime-Cam Software Pipeline. <b>2018</b> , 70,	63
1408	High-mass Star Formation through Filamentary Collapse and Clump-fed Accretion in G22. <b>2018</b> , 852, 12	36
1407	Hierarchical Fragmentation in the Perseus Molecular Cloud: From the Cloud Scale to Protostellar Objects. <b>2018</b> , 853, 5	31
1406	Spatially Resolved Stellar Kinematics from LEGA-C: Increased Rotational Support in z $\sim$ 0.8 Quiscent Galaxies. <b>2018</b> , 858, 60	34
1405	Superresolution Interferometric Imaging with Sparse Modeling Using Total Squared Variation: Application to Imaging the Black Hole Shadow. <b>2018</b> , 858, 56	25
1404	Star-forming Galaxies as AGN Imposters? A Theoretical Investigation of the Mid-infrared Colors of AGNs and Extreme Starbursts. <b>2018</b> , 858, 38	21

1403	Interplanetary Scintillation with the Murchison Widefield Array I: a sub-arcsecond survey over 900 deg2 at 79 and 158 MHz. <b>2018</b> , 473, 2965-2983	13
1402	Ionized gas kinematics in bipolar H ii regions. <b>2018</b> , 478, 3530-3543	7
1401	The dipole anisotropy of AllWISE galaxies. <b>2018</b> , 477, 1772-1781	10
1400	Single sources in the low-frequency gravitational wave sky: properties and time to detection by pulsar timing arrays. <b>2018</b> , 477, 964-976	30
1399	On the Nature of Ultra-faint Dwarf Galaxy Candidates. II. The Case of Cetus II. <b>2018</b> , 857, 70	14
1398	Illuminating Low Surface Brightness Galaxies with the Hyper Suprime-Cam Survey. 2018, 857, 104	94
1397	ALMA observations of the narrow HR 4796A debris ring. 2018, 475, 4924-4938	26
1396	Investigating the diversity of supernovae type lax: a MUSE and NOT spectroscopic study of their environments. <b>2018</b> , 473, 1359-1387	31
1395	Integrating human and machine intelligence in galaxy morphology classification tasks. <b>2018</b> , 476, 5516-5534	32
1394	Global Properties of M31日Stellar Halo from the SPLASH Survey. III. Measuring the Stellar Velocity Dispersion Profile. <b>2018</b> , 852, 128	19
1393	Near-infrared Stellar Populations in the Metal-poor, Dwarf Irregular Galaxies Sextans A and Leo A. <b>2018</b> , 854, 117	13
1392	An L+T Spectral Binary with Possible AB Doradus Kinematics. <b>2018</b> , 854, 101	4
1391	The Extraordinary Outburst in the Massive Protostellar System NGC 6334I-MM1: Emergence of Strong 6.7 GHz Methanol Masers. <b>2018</b> , 854, 170	43
1390	One Percent Determination of the Primordial Deuterium Abundance. <b>2018</b> , 855, 102	196
1389	Possible Photometric Signatures of Moderately Advanced Civilizations: The Clarke Exobelt. <b>2018</b> , 855, 110	13
1388	Advanced Diagnostics for the Study of Linearly Polarized Emission. II. Application to Diffuse Interstellar Radio Synchrotron Emission. <b>2018</b> , 855, 29	13
1387	iPTF Archival Search for Fast Optical Transients. <b>2018</b> , 854, L13	14
1386	Cosmic evolution and metal aversion in superluminous supernova host galaxies. <b>2018</b> , 473, 1258-1285	88

1385	Kinematics, turbulence, and star formation of $z \sim 1$ strongly lensed galaxies seen with MUSE. <b>2018</b> , 477, 18-44	27
1384	Awakening the BALROG: BAyesian Location Reconstruction Of GRBs. 2018, 476, 1427-1444	15
1383	The California-KeplerSurvey. IV. Metal-rich Stars Host a Greater Diversity of Planets. <b>2018</b> , 155, 89	168
1382	Distributed Star Formation throughout the Galactic Center Cloud Sgr B2. <b>2018</b> , 853, 171	55
1381	Quasar microlensing models with constraints on the Quasar light curves. <b>2018</b> , 473, 616-620	
1380	Stellar Multiplicity Meets Stellar Evolution and Metallicity: The APOGEE View. 2018, 854, 147	64
1379	The Sloan Digital Sky Survey Reverberation Mapping Project: The C iv Blueshift, Its Variability, and Its Dependence Upon Quasar Properties. <b>2018</b> , 854, 128	25
1378	Rapid Evolution of the Gaseous Exoplanetary Debris around the White Dwarf Star HE 13492305. <b>2018</b> , 854, 40	35
1377	A Gaussian Mixture Model for Nulling Pulsars. <b>2018</b> , 855, 14	5
1376	The Optical/Near-infrared Extinction Law in Highly Reddened Regions. 2018, 855, 13	20
1375	Filamentary Fragmentation and Accretion in High-mass Star-forming Molecular Clouds. 2018, 855, 9	53
1374	Massive Outflows Associated with ATLASGAL Clumps. <b>2018</b> , 235, 3	25
1373	The Atacama Cosmology Telescope: The Two-season ACTPol Sunyaev Zelflovich Effect Selected Cluster Catalog. <b>2018</b> , 235, 20	93
1372	The NuSTAR Extragalactic Surveys: Source Catalog and the Compton-thick Fraction in the UDS Field. <b>2018</b> , 235, 17	15
1371	HFF-DeepSpace Photometric Catalogs of the 12 Hubble Frontier Fields, Clusters, and Parallels: Photometry, Photometric Redshifts, and Stellar Masses. <b>2018</b> , 235, 14	38
1370	A UV-to-NIR Study of Molecular Gas in the Dust Cavity around RY Lupi. <b>2018</b> , 855, 98	12
1369	2004 EW 95 : A Phyllosilicate-bearing Carbonaceous Asteroid in the Kuiper Belt. <b>2018</b> , 855, L26	8
1368	Fundamental Properties of Co-moving Stars Observed byGaia. <b>2018</b> , 155, 149	10

## (2018-2018)

1367	The First Hours of the GW170817 Kilonova and the Importance of Early Optical and Ultraviolet Observations for Constraining Emission Models. <b>2018</b> , 855, L23	57
1366	On the Gas Content and Efficiency of AGN Feedback in Low-redshift Quasars. <b>2018</b> , 854, 158	46
1365	A VLT/MUSE galaxy survey towards QSO Q1410: looking for a WHIM traced by BLAs in inter-cluster filaments?. <b>2018</b> , 477, 2991-3013	4
1364	Microlensing makes lensed quasar time delays significantly time variable. <b>2018</b> , 473, 80-90	50
1363	Mapping extragalactic dark matter annihilation with galaxy surveys: A systematic study of stacked group searches. <b>2018</b> , 97,	22
1362	The VLA Nascent Disk And Multiplicity Survey of Perseus Protostars (VANDAM). III. Extended Radio Emission from Protostars in Perseus. <b>2018</b> , 852, 18	14
1361	The EDGECALIFA survey: the influence of galactic rotation on the molecular depletion time across the Hubble sequence. <b>2018</b> , 475, 1791-1808	36
1360	Planet Four: Terrains Discovery of araneiforms outside of the South Polar layered deposits. <b>2018</b> , 308, 148-187	14
1359	The New Horizons and Hubble Space Telescope search for rings, dust, and debris in the Pluto-Charon system. <b>2018</b> , 301, 155-172	9
1358	Transit visibility zones of the Solar system planets. <b>2018</b> , 473, 345-354	26
1357	Ships Passing in the Night: Spectroscopic Analysis of Two Ultra-faint Satellites in the Constellation Carina. <b>2018</b> , 857, 145	38
1356	Reassessing Exoplanet Light Curves with a Thermal Model. <b>2018</b> , 156, 28	9
1355	The Pan-STARRS1 Proper-motion Survey for Young Brown Dwarfs in Nearby Star-forming Regions. I. Taurus Discoveries and a Reddening-free Classification Method for Ultracool Dwarfs. <b>2018</b> , 858, 41	22
1354	The Gould's Belt Distances Survey (GOBELINS). IV. Distance, Depth, and Kinematics of the Taurus Star-forming Region. <b>2018</b> , 859, 33	61
1353	Chemodynamical Clustering Applied to APOGEE Data: Rediscovering Globular Clusters. 2018, 860, 70	9
1352	Assessing the Impact of Astrochemistry on Molecular Cloud Turbulence Statistics. 2018, 860, 157	7
1351	Optically Thick H i Does Not Dominate Dark Gas in the Local ISM. <b>2018</b> , 862, 131	25
1350	Actions Are Weak Stellar Age Indicators in the Milky Way Disk. <b>2018</b> , 867, 31	8

1349	Mapping Lyman Continuum Escape in Tololo 1247🛭 32. <b>2018</b> , 867, 2		9
1348	Superluminous Supernovae in LSST: Rates, Detection Metrics, and Light-curve Modeling. <b>2018</b> , 869, 166		26
1347	The low-frequency radio eclipses of the black widow pulsar J1810+1744. <b>2018</b> , 476, 1968-1981		30
1346	3D shape of Orion A from Gaia DR2. <i>Astronomy and Astrophysics</i> , <b>2018</b> , 619, A106	;.1	73
1345	ZFOURGE: Using Composite Spectral Energy Distributions to Characterize Galaxy Populations at 1 2018, 863, 131		18
1344	Constraints on accretion disk size in the massive type 1 quasar PG 2308+098 from optical continuum reverberation lags. <b>2018</b> , 70,		8
1343	Prediction of astrometric microlensing events from Gaia DR2 proper motions. <i>Astronomy and Astrophysics</i> , <b>2018</b> , 620, A175	5.1	9
1342	Refraction in exoplanet atmospheres. <i>Astronomy and Astrophysics</i> , <b>2018</b> , 609, A90	j.1	3
1341	Probing the Southern Fermi Bubble in Ultraviolet Absorption Using Distant AGNs. 2018, 860, 98		18
1340	The Disk Substructures at High Angular Resolution Project (DSHARP). V. Interpreting ALMA Maps of Protoplanetary Disks in Terms of a Dust Model. <b>2018</b> , 869, L45		115
1339	Bound Outflows, Unbound Ejecta, and the Shaping of Bipolar Remnants during Stellar Coalescence. <b>2018</b> , 868, 136		45
1338	Shocked POststarburst Galaxy Survey. III. The Ultraviolet Properties of SPOGs. <b>2018</b> , 863, 28		3
1337	A Model for Clumpy Self-enrichment in Globular Clusters. <b>2018</b> , 863, 99		13
1336	Stellar Population Diagnostics of the Massive Star Binary Fraction. <b>2018</b> , 867, 125		13
1335	The Distribution and Excitation of CH3CN in a Solar Nebula Analog. <b>2018</b> , 859, 131		42
1334	The Next Generation Fornax Survey (NGFS). IV. Mass and Age Bimodality of Nuclear Clusters in the Fornax Core Region. <b>2018</b> , 860, 4		26
1333	Searching for the Lowest-metallicity Galaxies in the Local Universe. <b>2018</b> , 863, 134		18
1332	Scaling Relations Associated with Millimeter Continuum Sizes in Protoplanetary Disks. <b>2018</b> , 865, 157		70

1331	Wide-field Optical Spectroscopy of Abell 133: A Search for Filaments Reported in X-Ray Observations. <b>2018</b> , 867, 25		16
1330	Rotating Stars from Kepler Observed with Gaia DR2. <b>2018</b> , 868, 151		20
1329	Shocked Interstellar Clouds and Dust Grain Destruction in the LMC Supernova Remnant N132D. <b>2018</b> , 237, 10		12
1328	COLOSSUS: A Python Toolkit for Cosmology, Large-scale Structure, and Dark Matter Halos. <b>2018</b> , 239, 35		141
1327	astroplan: An Open Source Observation Planning Package in Python. <b>2018</b> , 155, 128		27
1326	Stellar masses, metallicity gradients, and suppressed star formation revealed in a new sample of absorption selected galaxies. <i>Astronomy and Astrophysics</i> , <b>2018</b> , 618, A129	5.1	17
1325	Power spectrum multipoles on the curved sky: an application to the 6-degree Field Galaxy Survey. <b>2018</b> , 479, 5168-5183		24
1324	A detection of the environmental dependence of the sizes and stellar haloes of massive central galaxies. <b>2018</b> , 480, 521-537		16
1323	A case study of triggered star formation in Cygnus X. <b>2018</b> , 481, 1862-1872		2
1322	Testing strong line metallicity diagnostics at z´~ ´2. <b>2018</b> , 481, 3520-3533		12
1321	Kepler K2 observations of the transitional millisecond pulsar PSR J1023+0038. <b>2018</b> , 477, 1120-1132		22
1320	Constraining the Anomalous Microwave Emission Mechanism in the S140 Star-forming Region with Spectroscopic Observations between 4 and 8 GHz at the Green Bank Telescope. <b>2018</b> , 864, 97		1
1319	The Disk Substructures at High Angular Resolution Project (DSHARP). VII. The Planet <b>D</b> isk Interactions Interpretation. <b>2018</b> , 869, L47		194
1318	The XXL Survey. Astronomy and Astrophysics, 2018, 620, A13	5.1	11
1317	Discovery of three strongly lensed quasars in the Sloan Digital Sky Survey. 2018, 477, L70-L74		13
1316	An Isothermal Outflow in High-mass Star-forming Region G240.31+0.07. <b>2018</b> , 860, 106		4
1315	New Evidence for the Dusty Wind Model: Polar Dust and a Hot Core in the Type-1 Seyfert ESO 323-G77. <b>2018</b> , 862, 17		30
1314	A Dense Companion to the Short-period Millisecond Pulsar Binary PSR J0636+5128. <b>2018</b> , 864, 15		16

1313	MOSFiT: Modular Open Source Fitter for Transients. <b>2018</b> , 236, 6	73
1312	ALMACAL III. A combined ALMA and MUSE survey for neutral, molecular, and ionized gas in an H i-absorption-selected system. <b>2018</b> , 475, 492-507	21
1311	The detection of intergalactic H $\stackrel{\text{\tiny Le}}{=}$ mission from the Slug Nebula at z ~ 2.3. <b>2018</b> , 480, 2094-2108	12
1310	The origin of the Blue tiltlbf globular cluster populations in the E-MOSAICS simulations. <b>2018</b> , 480, 3279-3301	28
1309	IDM predictions for the satellite population of M33. <b>2018</b> , 480, 1883-1897	10
1308	The utility of Ly æmission lines as a probe of interactions between high redshift galaxies and their environments. <b>2018</b> , 480, 1938-1949	2
1307	Constraining the nature of DG Tau AB thermal and non-thermal radio emission. 2018, 481, 5532-5542	4
1306	Dusty galaxies in the Epoch of Reionization: simulations. <b>2018</b> , 477, 552-565	58
1305	GPI Spectra of HR 8799 c, d, and e from 1.5 to 2.4 th with KLIP Forward Modeling. 2018, 155, 226	36
1304	Binary Companions of Evolved Stars in APOGEE DR14: Search Method and Catalog of ~5000 Companions. <b>2018</b> , 156, 18	1182
1304		1182 8
1303	Companions. 2018, 156, 18  An Ice Giant Exoplanet Interpretation of the Anomaly in Microlensing Event OGLE-2011-BLG-0173.	
1303	An Ice Giant Exoplanet Interpretation of the Anomaly in Microlensing Event OGLE-2011-BLG-0173.  2018, 156, 104  Models of Tidally Induced Gas Filaments in the Magellanic Stream. 2018, 857, 101	8
1303	Companions. 2018, 156, 18  An Ice Giant Exoplanet Interpretation of the Anomaly in Microlensing Event OGLE-2011-BLG-0173. 2018, 156, 104  Models of Tidally Induced Gas Filaments in the Magellanic Stream. 2018, 857, 101	8
1303 1302 1301	An Ice Giant Exoplanet Interpretation of the Anomaly in Microlensing Event OGLE-2011-BLG-0173.  2018, 156, 104  Models of Tidally Induced Gas Filaments in the Magellanic Stream. 2018, 857, 101  Herschel PACS Observations of 410 Myr Old Classical T Tauri Stars in Orion OB1. 2018, 859, 1  CLUMP-3D: Three-dimensional Shape and Structure of 20 CLASH Galaxy Clusters from Combined	8 25 9
1303 1302 1301 1300	An Ice Giant Exoplanet Interpretation of the Anomaly in Microlensing Event OGLE-2011-BLG-0173.  2018, 156, 104  Models of Tidally Induced Gas Filaments in the Magellanic Stream. 2018, 857, 101  Herschel PACS Observations of 4110 Myr Old Classical T Tauri Stars in Orion OB1. 2018, 859, 1  CLUMP-3D: Three-dimensional Shape and Structure of 20 CLASH Galaxy Clusters from Combined Weak and Strong Lensing. 2018, 860, 126  X-Ray Variability from the Ultraluminous Black Hole Candidate X-Ray Binary in the Globular Cluster	8 25 9
1303 1302 1301 1300	An Ice Giant Exoplanet Interpretation of the Anomaly in Microlensing Event OGLE-2011-BLG-0173.  2018, 156, 104  Models of Tidally Induced Gas Filaments in the Magellanic Stream. 2018, 857, 101  Herschel PACS Observations of 4filo Myr Old Classical T Tauri Stars in Orion OB1. 2018, 859, 1  CLUMP-3D: Three-dimensional Shape and Structure of 20 CLASH Galaxy Clusters from Combined Weak and Strong Lensing. 2018, 860, 126  X-Ray Variability from the Ultraluminous Black Hole Candidate X-Ray Binary in the Globular Cluster RZ 2109. 2018, 862, 108	8 25 9 19

1295	Donl Blink: Constraining the Circumstellar Environment of the Interacting Type Ia Supernova 2015cp. <b>2018</b> , 868, 21		6	
1294	The 2016 Outburst of PSR J1119-6127: Cooling and a Spin-down-dominated Glitch. <b>2018</b> , 869, 180		13	
1293	Searching for Short-timescale Variability in the Ultraviolet with the GALEX gPhoton Archive. I. Artifacts and Spurious Periodicities. <b>2018</b> , 238, 25		4	
1292	A Synthetic Sample of Short-cadence Solar-like Oscillators for TESS. <b>2018</b> , 239, 34		10	
1291	A Universal Break in the Planet-to-star Mass-ratio Function of Kepler MKG Stars. <b>2018</b> , 856, L28		24	
1290	1D Kinematics from Stars and Ionized Gas at z $\sim$ 0.8 from the LEGA-C Spectroscopic Survey of Massive Galaxies. <b>2018</b> , 868, L36		12	
1289	Constraining physical conditions for the PDR of Trumpler 14 in the Carina Nebula. <i>Astronomy and Astrophysics</i> , <b>2018</b> , 618, A53	.1	14	
1288	Redshifted broad absorption line quasars found via machine-learned spectral similarity. <b>2018</b> , 480, 3889-3	897	6	
1287	Clear and Cloudy Exoplanet Forecasts for JWST: Maps, Retrieved Composition, and Constraints on Formation with MIRI and NIRCam. <b>2018</b> , 156, 40		19	
1286	Scientific Domain Knowledge Improves Exoplanet Transit Classification with Deep Learning. <b>2018</b> , 869, L7		37	
1285	Optical High-resolution Spectroscopy of 14 Young Eich Stars. <b>2018</b> , 860, 49		10	
1284	Hunting for Radio Emission from the Intermittent Pulsar J1107-5907 at Low Frequencies. <b>2018</b> , 869, 134		7	
1283	The convective photosphere of the red supergiant CE Tauri. <i>Astronomy and Astrophysics</i> , <b>2018</b> , 614, A12 <sub>5</sub>	.1	11	
1282	OH absorption in the first quadrant of the Milky Way as seen by THOR. <i>Astronomy and Astrophysics</i> , <b>2018</b> , 618, A159	.1	12	
1281	Evolution of the anti-truncated stellar profiles of S0 galaxies since $z = 0.6$ in the SHARDS survey. Astronomy and Astrophysics, <b>2018</b> , 615, A26	.1	3	
1280	The HP2 Survey. Astronomy and Astrophysics, <b>2018</b> , 620, A24	.1	6	
1279	The VMC survey. Astronomy and Astrophysics, 2018, 613, L8	.1	14	
1278	The less significant role of large-scale environment than optical AGN in nearby, isolated elliptical galaxies. <i>Astronomy and Astrophysics</i> , <b>2018</b> , 620, A117	.1	3	

1277	Primordial deuterium abundance at z abs = 2:504 towards Q1009+2956. <b>2018</b> , 1038, 012012		10
1276	ALMA Observations toward the Starburst Dwarf Galaxy NGC 5253. I. Molecular Cloud Properties and Scaling Relations. <b>2018</b> , 864, 120		14
1275	VIS3COS. Astronomy and Astrophysics, <b>2018</b> , 620, A186	5.1	19
1274	The evolution of X-ray bursts in the <b>B</b> ursting PulsarlGRO J1744\(\bar{\Omega}\)8. <b>2018</b> , 481, 2273-2298		6
1273	3D mapping of young stars in the solar neighbourhood with Gaia DR2. <i>Astronomy and Astrophysics</i> , <b>2018</b> , 620, A172	5.1	62
1272	Multiple star systems in the Orion nebula. Astronomy and Astrophysics, 2018, 620, A116	5.1	10
1271	Vaex: big data exploration in the era of Gaia. Astronomy and Astrophysics, 2018, 618, A13	5.1	24
1270	Photometric Study of Comet C/2014 S2 (PANSTARRS) After the Perihelion. <b>2018</b> , 122, 53-71		2
1269	Gaia DR2 study of Herbig Ae/Be stars. Astronomy and Astrophysics, 2018, 620, A128	5.1	74
1268	MOPSS. I. Flat Optical Spectra for the Hot Jupiters WASP-4 b and WASP-52b. <b>2018</b> , 156, 122		12
1267	The MAVERIC Survey: A Transitional Millisecond Pulsar Candidate in Terzan 5. <b>2018</b> , 864, 28		14
1266	The VLA Nascent Disk and Multiplicity Survey of Perseus Protostars (VANDAM). IV. Free <b>f</b> free Emission from Protostars: Links to Infrared Properties, Outflow Tracers, and Protostellar Disk Masses. <b>2018</b> , 238, 19		75
1265	Connecting young star clusters to CO molecular gas in NGC 7793 with ALMAIIEGUS. 2018, 481, 1016-10	27	41
1264	High-time-resolution Photometry of AR Scorpii: Confirmation of the White Dwarf Spin-down. <b>2018</b> , 156, 150		14
1263	Untangling Cosmic Magnetic Fields: Faraday Tomography at Metre Wavelengths with LOFAR. <b>2018</b> , 6, 126		9
1262	The MUSE Hubble Ultra Deep Field Survey. Astronomy and Astrophysics, 2018, 619, A27	5.1	38
1261	The XXL Survey. Astronomy and Astrophysics, <b>2018</b> , 620, A19	5.1	6
1260	The Far-Infrared Radio Correlation at low radio frequency with LOFAR/H-ATLAS. <b>2018</b> , 480, 5625-5644		20

1259	The dependence of mass and environment on the secular processes of AGNs in terms of morphology, colour, and specific star-formation rate. <i>Astronomy and Astrophysics</i> , <b>2018</b> , 620, A113	5.1	11
1258	The galaxy clustering crisis in abundance matching. <b>2018</b> , 477, 359-383		34
1257	SPHERE view of Wolf-Rayet 104. Astronomy and Astrophysics, 2018, 618, A108	5.1	8
1256	The kinematics of cluster galaxies via velocity dispersion profiles. <b>2018</b> , 481, 1507-1521		10
1255	The close circumstellar environment of Betelgeuse. Astronomy and Astrophysics, 2018, 609, A67	5.1	35
1254	Formation of S0s via disc accretion around high-redshift compact ellipticals. <b>2018</b> , 477, 2030-2041		17
1253	A low Lyman Continuum escape fraction of . <b>2018</b> , 478, 791-799		42
1252	Raman-scattered laser guide-star photons to monitor the scatter of astronomical telescope mirrors. <i>Astronomy and Astrophysics</i> , <b>2018</b> , 618, L7	5.1	1
1251	The excitation mechanisms and evolutionary stages of UWISH2 planetary nebula candidates. <b>2018</b> , 480, 1563-1579		1
1250	Dac-Man: Data Change Management for Scientific Datasets on HPC systems. 2018,		3
1249	An ALMA study of the Orion Integral Filament. Astronomy and Astrophysics, 2018, 610, A77	5.1	108
1248	A Virgo Environmental Survey Tracing Ionised Gas Emission (VESTIGE). <i>Astronomy and Astrophysics</i> , <b>2018</b> , 614, A57	5.1	43
1247	The Power of Low Frequencies: Faraday Tomography in the Sub-GHz Regime. <b>2018</b> , 6, 112		5
1246	Small- and large-scale galactic conformity in SDSS DR7. <b>2018</b> , 480, 2031-2045		15
1245	V902 Monocerotis: A likely disc-accreting intermediate polar. <i>Astronomy and Astrophysics</i> , <b>2018</b> , 617, A52	5.1	5
1244	Mapping the core of the Tarantula Nebula with VLT-MUSE. Astronomy and Astrophysics, 2018, 614, A147	5.1	19
1243	A Morphological Classification Model to Identify Unresolved PanSTARRS1 Sources: Application in the ZTF Real-time Pipeline. <b>2018</b> , 130, 128001		50
1242	New Rotation Period Measurements for M Dwarfs in the Southern Hemisphere: An Abundance of Slowly Rotating, Fully Convective Stars. <b>2018</b> , 156, 217		44

1241	On-the-fly Mapping of New Pulsars. <b>2018</b> , 156, 190		2
1240	Molecular Gas and Star Formation Properties in Early Stage Mergers: SMA CO(2-1) Observations of the LIRGs NGC 3110 and NGC 232. <b>2018</b> , 866, 77		9
1239	The NuSTAR Extragalactic Surveys: Unveiling Rare, Buried AGNs and Detecting the Contributors to the Peak of the Cosmic X-Ray Background. <b>2018</b> , 867, 162		4
1238	A Collection of New Dwarf Galaxies in NGC 51288 Western Halo. <b>2018</b> , 867, L15		13
1237	The host galaxy of the short GRB 111117A at z = 2.211. Astronomy and Astrophysics, <b>2018</b> , 616, A48	5.1	15
1236	Refining the origins of the gamma-ray binary 1FGL J1018.6B856. <i>Astronomy and Astrophysics</i> , <b>2018</b> , 619, A26	5.1	3
1235	The Dual Role of Starbursts and Active Galactic Nuclei in Driving Extreme Molecular Outflows. <b>2018</b> , 859, 35		15
1234	Binary Pulsar Distances and Velocities from Gaia Data Release 2. <b>2018</b> , 864, 26		29
1233	Bolles III is a Disrupting Dwarf Galaxy Associated with the Styx Stellar Stream. 2018, 865, 7		18
1232	The Spatially Resolved Dust-to-metals Ratio in M101. <b>2018</b> , 865, 117		25
1231	A Study of Two Diffuse Dwarf Galaxies in the Field. <b>2018</b> , 866, 112		22
1230	Unveiling the environment and faint features of the isolated galaxy CIG 96 with deep optical and HI observations. <i>Astronomy and Astrophysics</i> , <b>2018</b> , 619, A163	5.1	5
1229	Follow-up Imaging of Disk Candidates from the Disk Detective Citizen Science Project: New Discoveries and False Positives in WISE Circumstellar Disk Surveys. <b>2018</b> , 868, 43		9
1228	The Spectroscopic Hertzsprung <b>R</b> ussell Diagram of Hot Massive Stars in the Small Magellanic Cloud. <b>2018</b> , 868, 57		12
1227	The First Year of S-CUBED: The Swift Small Magellanic Cloud Survey. <b>2018</b> , 868, 47		14
1226	A Revised Exoplanet Yield from the Transiting Exoplanet Survey Satellite (TESS). <b>2018</b> , 239, 2		176
1225	The Dark Energy Survey: Data Release 1. <b>2018</b> , 239, 18		313
1224	Identifying Tidal Disruption Events via Prior Photometric Selection of Their Preferred Hosts. <b>2018</b> , 868, 99		9

1223	The 21-SPONGE H i Absorption Line Survey. I. The Temperature of Galactic H i. <b>2018</b> , 238, 14		42
	On the Interpretation of Far-infrared Spectral Energy Distributions. I. The 850 fb Molecular Mass Estimator. <b>2018</b> , 867, 102		20
	The Dust-selected Molecular Clouds in the Northeast Region of the Small Magellanic Cloud. <b>2018</b> , 867, 117		1
1220	The Information Content in Cold Stellar Streams. <b>2018</b> , 867, 101		43
	A Transitional Disk around an Intermediate-mass Star in the Sparse Population of the Orion OB1 Association. <b>2018</b> , 867, 116		5
1218	Snakes on a SpaceshipAn Overview of Python in Heliophysics. <b>2018</b> , 123, 10,384		11
1217	The Spectral Type of the Ionizing Stars and the Infrared Fluxes of HII Regions. 2018, 62, 764-773		2
1216	A Large Moving Group within the Lower Centaurus Crux Association. <b>2018</b> , 868, 32		23
1215	The PAU Survey: a forward modeling approach for narrow-band imaging. <b>2018</b> , 2018, 035-035		7
1214	Dense Molecular Filaments Feeding a Starburst: ALMA Maps of CO(312) in Henize 2110. 2018, 867, 165		3
1213	When nature tries to trick us. Astronomy and Astrophysics, 2018, 619, A84	5.1	7
	The Seahorse Nebula: New views of the filamentary infrared dark cloud G304.74+01.32 from SABOCA, Herschel, and WISE. <i>Astronomy and Astrophysics</i> , <b>2018</b> , 609, A123	5.1	4
イライイ	The California-Kepler Survey. VII. Precise Planet Radii Leveraging Gaia DR2 Reveal the Stellar Mass Dependence of the Planet Radius Gap. <b>2018</b> , 156, 264		243
1210	VERITAS Observations of the BL Lac Object TXS 0506+056. <b>2018</b> , 861, L20		19
	Inferring the star formation histories of massive quiescent galaxies with bagpipes: evidence for multiple quenching mechanisms. <b>2018</b> , 480, 4379-4401		111
1208	A Large Ground-based Observing Campaign of the Disintegrating Planet K2-22b. <b>2018</b> , 156, 227		7
1207	K2 Ultracool Dwarfs Survey. III. White Light Flares Are Ubiquitous in M6-L0 Dwarfs. <b>2018</b> , 858, 55		32
1206	An Ultra Metal-poor Star Near the Hydrogen-burning Limit. <b>2018</b> , 867, 98		20

1205	VLBA+GBT observations of the COSMOS field and radio source counts at 1.4 GHz. <i>Astronomy and Astrophysics</i> , <b>2018</b> , 616, A128	5.1	4
1204	A Galaxy-scale Fountain of Cold Molecular Gas Pumped by a Black Hole. <b>2018</b> , 865, 13		55
1203	The Extraordinary Outburst in the Massive Protostellar System NGC 6334I-MM1: Flaring of the Water Masers in a NorthBouth Bipolar Outflow Driven by MM1B. <b>2018</b> , 866, 87		29
1202	Y Dwarf Trigonometric Parallaxes from the Spitzer Space Telescope. <b>2018</b> , 867, 109		18
1201	A Search for the Host Galaxy of FRB 171020. <b>2018</b> , 867, L10		30
1200	Binary Companions of Evolved Stars in APOGEE DR14: Orbital Circularization. <b>2018</b> , 867, 5		19
1199	Mode Changing and Giant Pulses in the Millisecond Pulsar PSR B1957+20. <b>2018</b> , 867, L2		16
1198	Detection of 84 GHz Class I Methanol Maser Emission toward NGC 253. <b>2018</b> , 867, L4		4
1197	The Gaia DR2 view of the Gamma Velorum cluster: resolving the 6D structure. <i>Astronomy and Astrophysics</i> , <b>2018</b> , 616, L12	5.1	27
1196	Confirmation of double peaked Ly $\stackrel{\bullet}{\mathbb{R}}$ mission at z = 6.593. <i>Astronomy and Astrophysics</i> , <b>2018</b> , 619, A136	5.1	46
1195	SDSS-IV MaNGA: spatially resolved star formation histories and the connection to galaxy physical properties. <b>2018</b> , 480, 2544-2561		22
1194	Diffuser-assisted Photometric Follow-up Observations of the Neptune-sized Planets K2-28b and K2-100b. <b>2018</b> , 156, 266		13
1193	Back to Normallfor the Disintegrating Planet Candidate KIC 12557548 b. <b>2018</b> , 156, 281		4
1192	Extreme Asteroids in the Pan-STARRS 1 Survey. <b>2018</b> , 156, 282		4
1191	The HOSTS SurveyExozodiacal Dust Measurements for 30 Stars. <b>2018</b> , 155, 194		61
1190	Beryllium detection in the very fast nova ASASSN-16kt (V407 Lupi). <b>2018</b> , 478, 1601-1610		16
1189	The MAVERIC Survey: Still No Evidence for Accreting Intermediate-mass Black Holes in Globular Clusters. <b>2018</b> , 862, 16		55
1188	The SLUGGS Survey: The Inner Dark Matter Density Slope of the Massive Elliptical Galaxy NGC 1407. <b>2018</b> , 863, 130		14

1187	Cosmic happenstance: 24-µm selected, multicomponent Herschel sources are line-of-sight projections. <b>2018</b> , 480, 4124-4137		3
1186	New member candidates of Upper Scorpius from Gaia DR1. Astronomy and Astrophysics, 2018, 618, A12	5.1	11
1185	Radio synchrotron spectra of star-forming galaxies. Astronomy and Astrophysics, 2018, 611, A55	5.1	35
1184	Detection of He I 10830 A absorption on HD 189733 b with CARMENES high-resolution transmission spectroscopy. <i>Astronomy and Astrophysics</i> , <b>2018</b> , 620, A97	5.1	80
1183	Observational constraints on the physical nature of submillimetre source multiplicity: chance projections are common. <b>2018</b> , 476, 2278-2287		19
1182	Disentangling dark physics with cosmic microwave background experiments. <b>2018</b> , 98,		8
1181	Nowhere to Hide: Radio-faint AGN in GOODS-N field. Astronomy and Astrophysics, 2018, 619, A48	5.1	8
1180	TensorFit a tool to analyse spectral cubes in a tensor mode. <b>2018</b> , 25, 195-202		
1179	The Serpens filament at the onset of slightly supercritical collapse. <i>Astronomy and Astrophysics</i> , <b>2018</b> , 620, A62	5.1	10
1178	The Disk Substructures at High Angular Resolution Project (DSHARP). II. Characteristics of Annular Substructures. <b>2018</b> , 869, L42		217
1178 1177			217 8 <sub>7</sub>
	Substructures. 2018, 869, L42  The Disk Substructures at High Angular Resolution Project (DSHARP). III. Spiral Structures in the	5.1	, i
1177	Substructures. 2018, 869, L42  The Disk Substructures at High Angular Resolution Project (DSHARP). III. Spiral Structures in the Millimeter Continuum of the Elias 27, IM Lup, and WaOph 6 Disks. 2018, 869, L43  Multiwavelength approach to classifying transient events in the direction of M 31. Astronomy and	5.1	87
1177 1176	Substructures. 2018, 869, L42  The Disk Substructures at High Angular Resolution Project (DSHARP). III. Spiral Structures in the Millimeter Continuum of the Elias 27, IM Lup, and WaOph 6 Disks. 2018, 869, L43  Multiwavelength approach to classifying transient events in the direction of M 31. Astronomy and Astrophysics, 2018, 615, A152  The Massive and Distant Clusters of WISE Survey. IV. The Distribution of Active Galactic Nuclei in	5.1	87
1177 1176 1175	Substructures. 2018, 869, L42  The Disk Substructures at High Angular Resolution Project (DSHARP). III. Spiral Structures in the Millimeter Continuum of the Elias 27, IM Lup, and WaOph 6 Disks. 2018, 869, L43  Multiwavelength approach to classifying transient events in the direction of M 31. Astronomy and Astrophysics, 2018, 615, A152  The Massive and Distant Clusters of WISE Survey. IV. The Distribution of Active Galactic Nuclei in Galaxy Clusters at z ~ 1. 2018, 869, 131  Substellar and low-mass dwarf identification with near-infrared imaging space observatories.		8 <sub>7</sub> 2 10
1177 1176 1175	The Disk Substructures at High Angular Resolution Project (DSHARP). III. Spiral Structures in the Millimeter Continuum of the Elias 27, IM Lup, and WaOph 6 Disks. 2018, 869, L43  Multiwavelength approach to classifying transient events in the direction of M 31. Astronomy and Astrophysics, 2018, 615, A152  The Massive and Distant Clusters of WISE Survey. IV. The Distribution of Active Galactic Nuclei in Galaxy Clusters at z ~ 1. 2018, 869, 131  Substellar and low-mass dwarf identification with near-infrared imaging space observatories. Astronomy and Astrophysics, 2018, 620, A132		87 2 10
1177 1176 1175 1174 1173	The Disk Substructures at High Angular Resolution Project (DSHARP). III. Spiral Structures in the Millimeter Continuum of the Elias 27, IM Lup, and WaOph 6 Disks. 2018, 869, L43  Multiwavelength approach to classifying transient events in the direction of M 31. Astronomy and Astrophysics, 2018, 615, A152  The Massive and Distant Clusters of WISE Survey. IV. The Distribution of Active Galactic Nuclei in Galaxy Clusters at z ~ 1. 2018, 869, 131  Substellar and low-mass dwarf identification with near-infrared imaging space observatories. Astronomy and Astrophysics, 2018, 620, A132  Search for dark matter annihilation in the Milky Way halo. 2018, 98,  Gathering dust: A galaxy-wide study of dust emission from cloud complexes in NGC 300. Astronomy	5.1	87 2 10 5

1169	G11.92🛭.61 MM 1: A Fragmented Keplerian Disk Surrounding a Proto-O Star. <b>2018</b> , 869, L24		36
1168	Mining the Kilo-Degree Survey for solar system objects. <i>Astronomy and Astrophysics</i> , <b>2018</b> , 610, A21	5.1	13
1167	Magnification Bias of Distant Galaxies in the Hubble Frontier Fields: Testing Wave Versus Particle Dark Matter Predictions. <b>2018</b> , 862, 156		11
1166	Temperature constraints from inversions of synthetic solar optical, UV, and radio spectra. <i>Astronomy and Astrophysics</i> , <b>2018</b> , 620, A124	5.1	21
1165	Towards a Framework for Offering Remote Sensing Data in an Analysis-Ready Format. 2018,		1
1164	The shape of oxygen abundance profiles explored with MUSE: evidence for widespread deviations from single gradients. <i>Astronomy and Astrophysics</i> , <b>2018</b> , 609, A119	5.1	79
1163	The impact of Lyman-Fradiative transfer on large-scale clustering in the Illustris simulation. <i>Astronomy and Astrophysics</i> , <b>2018</b> , 614, A31	5.1	17
1162	DustPedia: Multiwavelength photometry and imagery of 875 nearby galaxies in 42 ultraviolet-microwave bands. <i>Astronomy and Astrophysics</i> , <b>2018</b> , 609, A37	5.1	52
1161	Environmental quenching of low-mass field galaxies. <b>2018</b> , 477, 4491-4498		26
1160	Kinetic Tomography. II. A Second Method for Mapping the Velocity Field of the Milky Way Interstellar Medium and a Comparison with Spiral Structure Models. <b>2018</b> , 156, 248		6
1159	A Redshift-independent Efficiency Model: Star Formation and Stellar Masses in Dark Matter Halos at z ? 4. <b>2018</b> , 868, 92		88
1158	LISA verification binaries with updated distances from Gaia Data Release 2. <b>2018</b> , 480, 302-309		75
1157	The causes of the red sequence, the blue cloud, the green valley, and the green mountain. <b>2018</b> , 481, 1183-1194		18
1156	A model-independent comparison of the variability of accreting neutron stars and black holes. <b>2018</b> , 481, 3761-3781		4
1155	Source selection for cluster weak lensing measurements in the Hyper Suprime-Cam survey. <b>2018</b> , 70,		23
1154	Dynamics and Formation of the Near-resonant K2-24 System: Insights from Transit-timing Variations and Radial Velocities. <b>2018</b> , 156, 89		21
1153	Improving Gaia Parallax Precision with a Data-driven Model of Stars. 2018, 156, 145		17
1152	nbodykit: An Open-source, Massively Parallel Toolkit for Large-scale Structure. <b>2018</b> , 156, 160		110

1151	Off the Beaten Path: Gaia Reveals GD-1 Stars outside of the Main Stream. <b>2018</b> , 863, L20	61
1150	The Main Belt Asteroid Shape Distribution from Gaia Data Release 2. <b>2018</b> , 156, 139	8
1149	Chandrasekhar and Sub-Chandrasekhar Models for the X-Ray Emission of Type Ia Supernova Remnants. I. Bulk Properties. <b>2018</b> , 865, 151	13
1148	The GeMS/GSAOI Galactic Globular Cluster Survey (G4CS). I. A Pilot Study of the Stellar Populations in NGC 2298 and NGC 3201. <b>2018</b> , 865, 160	9
1147	A search for a surviving companion in SN 1006. <b>2018</b> , 479, 192-199	16
1146	Resolution convergence in cosmological hydrodynamical simulations using adaptive mesh refinement. <b>2018</b> , 477, 983-1003	3
1145	Black Holes and Neutron Stars in Nearby Galaxies: Insights from NuSTAR. <b>2018</b> , 864, 150	10
1144	Constraining the inclination of the low-mass X-ray binary Cen´X-4. <b>2018</b> , 478, 4317-4322	3
1143	Imaging extended emission-line regions of obscured AGN with the Subaru Hyper Suprime-Cam Survey. <b>2018</b> , 480, 2302-2323	16
1142	The VANDELS survey: dust attenuation in star-forming galaxies at $z = 3-4$ . <b>2018</b> , 476, 3218-3232	27
1141	The nature of luminous Ly ${\mathbb{L}}$ emitters at z ~ 2 ${\mathbb{S}}$ : maximal dust-poor starbursts and highly ionizing AGN. <b>2018</b> , 477, 2817-2840	54
1140	Infrared colours and inferred masses of metal-poor giant stars in the Kepler field. <b>2018</b> , 478, 2812-2818	5
1139	The Planck Cold Clump G108.37-01.06: A Site of Complex Interplay between H ii Regions, Young Clusters, and Filaments. <b>2018</b> , 864, 154	10
1138	Circumstellar ammonia in oxygen-rich evolved stars. <i>Astronomy and Astrophysics</i> , <b>2018</b> , 612, A48 5.1	11
1137	The origin of the diverse morphologies and kinematics of Milky Way-mass galaxies in the FIRE-2 simulations. <b>2018</b> , 481, 4133-4157	62
1136	High redshift galaxies in the ALHAMBRA survey. <i>Astronomy and Astrophysics</i> , <b>2018</b> , 614, A129 5.1	8
1135	Polarized point sources in the LOFAR Two-meter Sky Survey: A preliminary catalog. <i>Astronomy and Astrophysics</i> , <b>2018</b> , 613, A58	26
1134	Interstellar magnetic cannon targeting the Galactic halo. Astronomy and Astrophysics, <b>2018</b> , 617, A101 $_{5.1}$	7

1133	Measuring Radial Orbit Migration in the Galactic Disk. <b>2018</b> , 865, 96	68
1132	Tracking Advanced Planetary Systems (TAPAS) with HARPS-N. <i>Astronomy and Astrophysics</i> , <b>2018</b> , 613, A47	. 10
1131	Aldebaran bl Temperate Past Uncovered in Planet Search Data. 2018, 865, L20	14
1130	Footpoints of the giant molecular loops in the Galactic center region. <i>Astronomy and Astrophysics</i> , <b>2018</b> , 613, A42	5
1129	The JWST Extragalactic Mock Catalog: Modeling Galaxy Populations from the UV through the Near-IR over 13 Billion Years of Cosmic History. <b>2018</b> , 236, 33	59
1128	Extended and broad Ly æmission around a BAL quasar at z´~´5. <b>2018</b> , 476, 2421-2431	17
1127	Predicting the hypervelocity star population in Gaia. <b>2018</b> , 476, 4697-4712	25
1126	Star formation history of the Galactic bulge from deep HST imaging of low reddening windows. <b>2018</b> , 477, 3507-3519	38
1125	Discovery of X-Rays from the Old and Faint Pulsar J1154B250. <b>2018</b> , 865, 116	5
1124	Spatially unresolved SED fitting can underestimate galaxy masses: a solution to the missing mass problem. <b>2018</b> , 476, 1532-1547	25
1123	Resolving the host galaxy of a distant blazar with LBT/LUCI 1 + ARGOS. 2018, 476, 1835-1839	3
1122	Absorption and emission features of 7Be ii in the outburst spectra of V838 Her (Nova Her 1991). <b>2018</b> , 481, 2261-2272	14
1121	Mr-Moose: an advanced SED-fitting tool for heterogeneous multi-wavelength data sets. <b>2018</b> , 477, 4981-50	000 3
1120	Evidence for a New Component of High-Energy Solar Gamma-Ray Production. <b>2018</b> , 121, 131103	11
1119	Reliable detection and characterization of low-frequency polarized sources in the LOFAR M51 field.  Astronomy and Astrophysics, <b>2018</b> , 617, A136	9
1118	The First Tidally Disrupted Ultra-faint Dwarf Galaxy?: A Spectroscopic Analysis of the Tucana III Stream. <b>2018</b> , 866, 22	43
1117	A NICER Discovery of a Low-frequency Quasi-periodic Oscillation in the Soft-intermediate State of MAXI J1535B71. <b>2018</b> , 865, L15	24

1115	Revolutionizing Our Understanding of AGN Feedback and its Importance to Galaxy Evolution in the Era of the Next Generation Very Large Array. <b>2018</b> , 859, 23		18
1114	Characteristics and Performance of the CALorimetric Electron Telescope (CALET) Calorimeter for Gamma-Ray Observations. <b>2018</b> , 238, 5		10
1113	Kinematics of the atomic ISM in M33 on 80 pc scales. <b>2018</b> , 479, 2505-2533		22
1112	Evolution of Quasar Stochastic Variability along Its Main Sequence. <b>2018</b> , 866, 74		11
1111	Host galaxies of SNe Ic-BL with and without long gamma-ray bursts. <i>Astronomy and Astrophysics</i> , <b>2018</b> , 617, A105	5.1	21
1110	COSMOGRAIL. Astronomy and Astrophysics, 2018, 616, A183	5.1	37
1109	Exploring the Origins of Earth Nitrogen: Astronomical Observations of Nitrogen-bearing Organics in Protostellar Environments. <b>2018</b> , 866, 156		5
1108	Periastron Observations of TeV Gamma-Ray Emission from a Binary System with a 50-year Period. <b>2018</b> , 867, L19		27
1107	Evidence for Ultra-diffuse Galaxy Hormation hrough Galaxy Interactions. 2018, 866, L11		32
	and the control of th		
1106	The Astropy Project: Building an Open-science Project and Status of the v2.0 Core Package. <b>2018</b> , 156, 123		2084
1106			2084
	Simultaneous Spectral Energy Distribution and Near-infrared Interferometry Modeling of HD	5.1	<u> </u>
1105	Simultaneous Spectral Energy Distribution and Near-infrared Interferometry Modeling of HD 142666. <b>2018</b> , 866, 23  Observational constraints on key-parameters of cosmic reionisation history. <i>Astronomy and</i>	5.1	11
1105	Simultaneous Spectral Energy Distribution and Near-infrared Interferometry Modeling of HD 142666. 2018, 866, 23  Observational constraints on key-parameters of cosmic reionisation history. Astronomy and Astrophysics, 2018, 616, A113	5.1	11 18
1105 1104 1103	Simultaneous Spectral Energy Distribution and Near-infrared Interferometry Modeling of HD 142666. 2018, 866, 23  Observational constraints on key-parameters of cosmic reionisation history. Astronomy and Astrophysics, 2018, 616, A113  Nebular Spectroscopy of the Blue BumplType Ia Supernova 2017cbv. 2018, 863, 24  Mapping the neutral atomic hydrogen gas outflow in the restarted radio galaxy 3C 236. Astronomy		11 18 32
1105 1104 1103 1102	Simultaneous Spectral Energy Distribution and Near-infrared Interferometry Modeling of HD 142666. 2018, 866, 23  Observational constraints on key-parameters of cosmic reionisation history. Astronomy and Astrophysics, 2018, 616, A113  Nebular Spectroscopy of the Blue BumplType Ia Supernova 2017cbv. 2018, 863, 24  Mapping the neutral atomic hydrogen gas outflow in the restarted radio galaxy 3C 236. Astronomy and Astrophysics, 2018, 617, A38  Disentangling multiple high-energy emission components in the Vela X pulsar wind nebula with the Fermi Large Area Telescope. Astronomy and Astrophysics, 2018, 617, A78  The Stripe 82 12 GHz Very Large Array Snapshot Survey; host galaxy properties and accretion	5.1	11 18 32 13
1105 1104 1103 1102	Simultaneous Spectral Energy Distribution and Near-infrared Interferometry Modeling of HD 142666. 2018, 866, 23  Observational constraints on key-parameters of cosmic reionisation history. Astronomy and Astrophysics, 2018, 616, A113  Nebular Spectroscopy of the Blue BumplType Ia Supernova 2017cbv. 2018, 863, 24  Mapping the neutral atomic hydrogen gas outflow in the restarted radio galaxy 3C 236. Astronomy and Astrophysics, 2018, 617, A38  Disentangling multiple high-energy emission components in the Vela X pulsar wind nebula with the Fermi Large Area Telescope. Astronomy and Astrophysics, 2018, 617, A78  The Stripe 82 12 GHz Very Large Array Snapshot Survey: host galaxy properties and accretion rates of radio galaxies. 2018, 480, 358-370	5.1	11 18 32 13

	date high-z protoclusters among the Planck compact sources, as revealed by HerschelßPIRE. 476, 3336-3359		20
	ng star formation and ISM properties using galaxy disk inclination. <i>Astronomy and Astrophysics</i> 3, 615, A7	5.1	10
1095 SAFA	RI: Searching Asteroids for Activity Revealing Indicators. <b>2018</b> , 130, 114502		9
	e UV compactness and morphologies of typical Lyman $ \oplus $ mitters from $z \sim 2$ to $z \sim 6$ . <b>2018</b> , 3479-5501		37
	ST Unbiased Galactic plane Imaging survey with the Nobeyama 45 m telescope (FUGIN). III. ble evidence for formation of NGC 6618 cluster in M 17 by cloudfiloud collision. <b>2018</b> , 70,		30
	aday Rotation Study of the Stellar Bubble and H ii Region Associated with the W4 Complex. 865, 65		9
1091 Revis	ed Radii of Kepler Stars and Planets Using Gaia Data Release 2. <b>2018</b> , 866, 99		162
A Gai 1090 618, A	a DR2 view of the open cluster population in the Milky Way. <i>Astronomy and Astrophysics</i> , <b>2018</b> , A93	5.1	338
	patialKinematic Structure of the Region of Massive Star Formation S255N on Various Scales. 62, 326-345		3
1088 The T	ROY project. <i>Astronomy and Astrophysics</i> , <b>2018</b> , 618, A42	5.1	16
1087 <b>Spati</b>	al organization of the somatosensory cortex revealed by osmFISH. <b>2018</b> , 15, 932-935		195
, .	e dynamically distinct stellar populations in the halo of M49. Astronomy and Astrophysics, <b>2018</b> ,	5.1	195
1086 Three 616, A	e dynamically distinct stellar populations in the halo of M49. Astronomy and Astrophysics, <b>2018</b> ,	5.1	
Three 616, A	dynamically distinct stellar populations in the halo of M49. <i>Astronomy and Astrophysics</i> , <b>2018</b> , A123  tic synchrotron distribution derived from 152 H ii region absorption features in the full		18
1086 Three 616, A 1085 Galac GLEA	dynamically distinct stellar populations in the halo of M49. <i>Astronomy and Astrophysics</i> , <b>2018</b> , A123  tic synchrotron distribution derived from 152 H ii region absorption features in the full M survey. <b>2018</b> , 479, 4041-4055		18
1086 Three 616, A 1085 Galac GLEA 1084 Gas a	e dynamically distinct stellar populations in the halo of M49. <i>Astronomy and Astrophysics</i> , <b>2018</b> , A123  tic synchrotron distribution derived from 152 H ii region absorption features in the full M survey. <b>2018</b> , 479, 4041-4055  and galaxies in filaments between clusters of galaxies. <i>Astronomy and Astrophysics</i> , <b>2018</b> , 609, A49	5.1 5.1	18 9 29
1086 Three 616, A  1085 Galac GLEA  1084 Gas a  1083 Integ	e dynamically distinct stellar populations in the halo of M49. <i>Astronomy and Astrophysics</i> , <b>2018</b> , A123  tic synchrotron distribution derived from 152 H ii region absorption features in the full M survey. <b>2018</b> , 479, 4041-4055  and galaxies in filaments between clusters of galaxies. <i>Astronomy and Astrophysics</i> , <b>2018</b> , 609, A49  arated-light analyses vs. colour-magnitude diagrams. <i>Astronomy and Astrophysics</i> , <b>2018</b> , 617, A18	5.1 5.1	18 9 29 16

1079 A search for transiting planets in the Pictoris system. Astronomy and Astrophysics, 2018, 615, A145	5.1	6
Measurement of Source Star Colors with the K2C9-CFHT Multi-color Microlensing Survey. <b>2018</b> , 130, 104401		12
Baryon content in a sample of 91 galaxy clusters selected by the South Pole Telescope at 0.2´. <b>2018</b> , 478, 3072-3099		50
1076 Resolving the kinematics of the discs around Galactic B[e] supergiants. <b>2018</b> , 480, 320-344		14
1075 How black holes stop their host galaxy from growing without AGN feedback. <b>2018</b> , 480, 5673-5688		1
1074 Computational astrophysics for the future. <b>2018</b> , 361, 979-980		12
1073 Parallaxes of Cool Objects with WISE: Filling in for Gaia. <b>2018</b> , 862, 173		8
1072 Gaia transients in galactic nuclei. <b>2018</b> , 481, 307-323		11
fcmaker: Automating the creation of ESO-compliant finding charts for Observing Blocks on p2. <b>2018</b> , 25, 81-88		2
1070 X-Ray Absorption in Young Core-collapse Supernova Remnants. <b>2018</b> , 864, 175		11
1069 The 30 Year Search for the Compact Object in SN 1987A. <b>2018</b> , 864, 174		20
1068 Possible Bright Starspots on TRAPPIST-1. <b>2018</b> , 857, 39		51
1067 Kepler-1656b: A Dense Sub-Saturn with an Extreme Eccentricity. <b>2018</b> , 156, 147		9
1066 realfast: Real-time, Commensal Fast Transient Surveys with the Very Large Array. <b>2018</b> , 236, 8		30
1065 JOVIAL: Notebook-based astronomical data analysis in the cloud. <b>2018</b> , 25, 110-117		4
1064 Obscured star formation in bright z ? 7 Lyman-break galaxies. <b>2018</b> , 481, 1631-1644		33
JINGLE, a JCMT legacy survey of dust and gas for galaxy evolution studies []. Survey overview and first results. <b>2018</b> , 481, 3497-3519		18
1062 Evolution of the degree of substructures in simulated galaxy clusters. <b>2018</b> , 478, 2086-2096		1

1061	The GALAH Survey: second data release. 2018, 478, 4513-4552	193
1060	K2-260 b: a hot Jupiter transiting an F star, and K2-261 b: a warm Saturn around a bright G star. <b>2018</b> , 481, 596-612	16
1059	Cosmology with the pairwise kinematic SZ effect: calibration and validation using hydrodynamical simulations. <b>2018</b> , 478, 5320-5335	10
1058	The evolution of young HII regions. <i>Astronomy and Astrophysics</i> , <b>2018</b> , 611, A99 5.1	15
1057	Resolving the ISM at the Peak of Cosmic Star Formation with ALMA: The Distribution of CO and Dust Continuum in $z \sim 2.5$ Submillimeter Galaxies. <b>2018</b> , 863, 56	56
1056	Nucleus of active asteroid 358P/Pan-STARRS (P/2012 T1). <i>Astronomy and Astrophysics</i> , <b>2018</b> , 616, A54 5.1	1
1055	Using the full power of the cosmic microwave background to probe axion dark matter. <b>2018</b> , 476, 3063-3085	49
1054	Comment on "An excess of massive stars in the local 30 Doradus starburst". <b>2018</b> , 361,	12
1053	Galactic Archeology with the AEGIS Survey: The Evolution of Carbon and Iron in the Galactic Halo. <b>2018</b> , 861, 146	34
1052	Results from EDGES High-band. II. Constraints on Parameters of Early Galaxies. <b>2018</b> , 863, 11	29
1051	SMHASH: anatomy of the Orphan Stream using RR Lyrae stars. <b>2018</b> , 479, 570-587	12
1050	Investigations of the Class I methanol masers in NGC 4945. <b>2018</b> , 480, 4578-4588	5
1049	Searching for Cool Dust. II. Infrared Imaging of The OH/IR Supergiants, NML Cyg, VX Sgr, S Per, and the Normal Red Supergiants RS Per and T Per. <b>2018</b> , 155, 212	11
1048	Optimal extinction measurements. <i>Astronomy and Astrophysics</i> , <b>2018</b> , 615, A174 5.1	2
1047	Cloud-scale Molecular Gas Properties in 15 Nearby Galaxies. <b>2018</b> , 860, 172	128
1046	Time evolution of intrinsic alignments of galaxies. <b>2018</b> , 2018, 030-030	19
1045	Flat Rotation Curves Found in Merging Dusty Starbursts atz= 2.3 through Tilted-ring Modeling. <b>2018</b> , 864, L11	6
1044	aflak: Pluggable Visual Programming Environment with Quick Feedback Loop Tuned for Multi-Spectral Astrophysical Observations. <b>2018</b> ,	

1043	Brightest galaxies as halo centre tracers in SDSS DR7. 2018, 473, 2830-2851	19
1042	LLAMA: normal star formation efficiencies of molecular gas in the centres of luminous Seyfert galaxies. <b>2018</b> , 473, 5658-5679	39
1041	The relationship between Class I and Class II methanol masers at high angular resolution. 2018, 477, 507-524	9
1040	On the kinematics of a runaway Be star population. <b>2018</b> , 477, 5261-5278	19
1039	The space density of post-period minimum Cataclysmic Variables. <b>2018</b> , 473, 3241-3250	7
1038	Neutral hydrogen (H i) gas content of galaxies at z 🛈 .32. <b>2018</b> , 473, 1879-1894	38
1037	Gas kinematics, morphology and angular momentum in the FIRE simulations. <b>2018</b> , 473, 1930-1955	94
1036	Galaxy Zoo: secular evolution of barred galaxies from structural decomposition of multiband images. <b>2018</b> , 473, 4731-4753	52
1035	LRG-BEASTS III: ground-based transmission spectrum of the gas giant orbiting the cool dwarf WASP-80. <b>2018</b> , 474, 876-885	20
1034	Forming spectroscopic massive protobinaries by disc fragmentation. <b>2018</b> , 473, 3615-3637	50
1033	Detectability of Galactic Faraday Rotation in multiwavelength CMB observations. <b>2018</b> , 473, 4795-4804	
1032	The impact of galaxy formation on satellite kinematics and redshift-space distortions. <b>2018</b> , 475, 2530-2544	17
1031	A simulation-based analytic model of radio galaxies. <b>2018</b> , 475, 2768-2786	56
1030	True versus apparent shapes of bow shocks. <b>2018</b> , 477, 2431-2454	5
1029	The stellar mass, star formation rate and dark matter halo properties of LAEs at $z \sim 2$ . <b>2018</b> , 70,	23
1028	Core Emergence in a Massive Infrared Dark Cloud: A Comparison between Mid-IR Extinction and 1.3 mm Emission. <b>2018</b> , 855, L25	8
1027	Radiative transfer modelling of W33A MM1: 3D structure and dynamics of a complex massive star-forming region. <b>2018</b> , 478, 2505-2525	28
1026	The CARMA-NRO Orion Survey. <b>2018</b> , 236, 25	44

1025	First gas-phase metallicity gradients of 0.1? z? 0.8 galaxies with MUSE. <b>2018</b> , 478, 4293-4316	35
1024	LOFAR-Bolles: properties of high- and low-excitation radio galaxies at 0.5´. <b>2018</b> , 475, 3429-3452	27
1023	The Clustering of High-redshift (2.9 匝.1) Quasars in SDSS Stripe 82. <b>2018</b> , 859, 20	22
1022	The impact of redshift on galaxy morphometric classification: case studies for SDSS, DES, LSST and HST with morfometryka. <b>2018</b> , 473, 2701-2713	5
1021	A survey of eight hot Jupiters in secondary eclipse using WIRCam at CFHT. <b>2018</b> , 474, 4264-4277	8
1020	The dependence of bar frequency on galaxy mass, colour, and gas content hand angular resolution In the local universe. <b>2018</b> , 474, 5372-5392	47
1019	Major merging history in CANDELS. I. Evolution of the incidence of massive galaxy galaxy pairs from $z=3$ to $z\sim0$ . <b>2018</b> , 475, 1549-1573	44
1018	HAT-P-11: Discovery of a Second Planet and a Clue to Understanding Exoplanet Obliquities. <b>2018</b> , 155, 255	41
1017	Radial measurements of IMF-sensitive absorption features in two massive ETGs. <b>2018</b> , 475, 1073-1092	23
1016	The infraredEadio correlation of spheroid- and disc-dominated star-forming galaxies to z´~´1.5 in the COSMOS field. <b>2018</b> , 475, 827-838	21
1015	The binary fraction of planetary nebula central stars - III. the promise of VPHAS+. <b>2018</b> , 475, 4504-4523	8
1014	Discovery and characterization of 3000+ main-sequence binaries from APOGEE spectra. <b>2018</b> , 476, 528-553	51
1013	Sumo Puff: Tidal debris or disturbed ultra-diffuse galaxy?. <b>2018</b> , 70,	14
1012	Remnant radio-loud AGN in the Herschel-ATLAS field. <b>2018</b> , 475, 4557-4578	32
1011	Automatic physical inference with information maximizing neural networks. 2018, 97,	32
1010	Spectroscopic characterization of the stellar content of ultra-diffuse galaxies. <b>2018</b> , 478, 2034-2045	44
1009	No Time for Dead Time: Use the Fourier Amplitude Differences to Normalize Dead-time-affected Periodograms. <b>2018</b> , 853, L21	8
1008	Dark Galaxy Candidates at Redshift ~3.5 Detected with MUSE. <b>2018</b> , 859, 53	29

## (2018-2018)

1007	Cloud Atlas: Rotational Modulations in the L/T Transition Brown Dwarf Companion HN Peg B. <b>2018</b> , 155, 132		22	
1006	Numerical Simulations of Multiphase Winds and Fountains from Star-forming Galactic Disks. I. Solar Neighborhood TIGRESS Model. <b>2018</b> , 853, 173		91	
1005	Detection of a Population of Carbon-enhanced Metal-poor Stars in the Sculptor Dwarf Spheroidal Galaxy. <b>2018</b> , 856, 142		16	
1004	The ALMA-PILS Survey: Formaldehyde deuteration in warm gas on small scales toward IRAS 16293\( \textbf{2}\)422 B. <i>Astronomy and Astrophysics</i> , <b>2018</b> , 610, A54	5.1	40	
1003	Direction-dependent Corrections in Polarimetric Radio Imaging. II. A-solver Methodology: A Low-order Solver for the A-term of the A-projection Algorithm. <b>2018</b> , 155, 3		7	
1002	The Faint End of thez= 5 Quasar Luminosity Function from the CFHTLS. <b>2018</b> , 155, 131		52	
1001	The First Data Release from SweetSpot: 74 Supernovae in 36 Nights on WIYN+WHIRC. <b>2018</b> , 155, 201		7	
1000	Chemical Abundances of New Member Stars in the Tucana II Dwarf Galaxy. 2018, 857, 74		28	
999	Advanced Diagnostics for the Study of Linearly Polarized Emission. I. Derivation. <b>2018</b> , 853, 9		13	
998	Herscheland ALMA Observations of Massive SZE-selected Clusters. <b>2018</b> , 853, 195		1	
997	The JCMT Transient Survey: Stochastic and Secular Variability of Protostars and Disks In the Submillimeter Region Observed over 18 Months. <b>2018</b> , 854, 31		24	
996	Where Are All of the Gas-bearing Local Dwarf Galaxies? Quantifying Possible Impacts of Reionization. <b>2018</b> , 857, 45		18	
995	An uncertainty principle for star formation III. A new method for characterizing the cloud-scale physics of star formation and feedback across cosmic history. <b>2018</b> , 479, 1866-1952		54	
994	Xi-cam: a versatile interface for data visualization and analysis. <b>2018</b> , 25, 1261-1270		59	
993	Laser-only Adaptive Optics Achieves Significant Image Quality Gains Compared to Seeing-limited Observations over the Entire Sky. <b>2018</b> , 155, 59		1	
992	YSOVAR: Mid-infrared Variability among YSOs in the Star Formation Region Serpens South. <b>2018</b> , 155, 99		13	
991	The Galaxy Cluster Merger Catalog: An Online Repository of Mock Observations from Simulated Galaxy Cluster Mergers. <b>2018</b> , 234, 4		13	
990	The Lives of Stars: Insights from the TGASRAVEIIAMOST Data Set. <b>2018</b> , 860, 91		5	

989	An Iwasawallaniguchi effect for Compton-thick active galactic nuclei. 2018, 477, 3775-3790	13
988	The Orion Fingers: H2Temperatures and Excitation in an Explosive Outflow. <b>2018</b> , 857, 7	3
987	Gas kinematics in FIRE simulated galaxies compared to spatially unresolved HI observations. <b>2018</b> , 477, 1536-1548	23
986	Systematic search for tidal features around nearby galaxies. <i>Astronomy and Astrophysics</i> , <b>2018</b> , 614, A143,.1	28
985	The stellar population and initial mass function of NGC 1399 with MUSE. 2018, 479, 2443-2456	27
984	Radio Galaxy Zoo: machine learning for radio source host galaxy cross-identification. <b>2018</b> , 478, 5547-5563	26
983	The Voigt and complex error function: Humlaka rational approximation generalized. 2018, 479, 3068-3075	9
982	AnHST/STIS Optical Transmission Spectrum of Warm Neptune GJ 436b. <b>2018</b> , 155, 66	25
981	MMT Spectroscopy of Supernova Remnant Candidates in M33. <b>2018</b> , 855, 140	18
980	Integral Field Spectroscopy of Supernova Remnant 1E0102🛭 219 Reveals Fast-moving Hydrogen and Sulfur-rich Ejecta. <b>2018</b> , 853, L32	10
979	Distribution of Serpens South protostars revealed with ALMA. <i>Astronomy and Astrophysics</i> , <b>2018</b> , 615, A9	26
978	The RINGS Survey. III. Medium-resolution HEabryPEot Kinematic Data Set. <b>2018</b> , 155, 123	1
977	BAT AGN Spectroscopic Survey. VIII. Type 1 AGN with Massive Absorbing Columns. <b>2018</b> , 856, 154	17
976	The Universe Is Reionizing atz~ 7: Bayesian Inference of the IGM Neutral Fraction Using LyEmission from Galaxies. <b>2018</b> , 856, 2	141
975	A Falling Corona Model for the Anomalous Behavior of the Broad Emission Lines in NGC 5548. <b>2018</b> , 857, 86	12
974	K2 precision lightcurve: Twelve days in the Pluto-Charon system. <b>2018</b> , 314, 265-273	4
973	A search for faint high-redshift radio galaxy candidates at 150 MHz. <b>2018</b> , 475, 5041-5058	13
972	What Do theHitomiObservations Tell Us About the Turbulent Velocities in the Perseus Cluster? Probing the Velocity Field with Mock Observations. <b>2018</b> , 853, 180	22

971	The Spectral and Environment Properties of z $\sim$ 2.0 $\[0.5\]$ Quasar Pairs. <b>2018</b> , 860, 41	8
970	The Volumetric Rate of Calcium-rich Transients in the Local Universe. <b>2018</b> , 858, 50	27
969	Spatial Distribution of the Milky Way Hot Gaseous Halo Constrained by Suzaku X-Ray Observations. <b>2018</b> , 862, 34	35
968	Atmospheric turbulence forecasting with a general circulation model for Cerro Paranal. 2018, 480, 1278-1299	16
967	Calibrating the HISA temperature: Measuring the temperature of the Riegel©rutcher cloud. <b>2018</b> , 479, 1465-1490	15
966	The gas-phase metallicities of star-forming galaxies in aperture-matched SDSS samples follow potential rather than mass or average surface density. <b>2018</b> , 479, 1807-1821	12
965	Northern Galactic molecular cloud clumps in Hi-GAL: dense gas map and environmental trends. <b>2018</b> , 480, 893-904	3
964	Expanding CO Shells in the Orion A Molecular Cloud. <b>2018</b> , 862, 121	12
963	The curious case of II Lup: a complex morphology revealed with SAM/NACO and ALMA. 2018, 480, 1006-1021	5
962	Confirmation of the link between central star binarity and extreme abundance discrepancy factors in planetary nebulae. <b>2018</b> , 480, 4589-4613	42
961	X-ray radiative transfer in protoplanetary disks. <i>Astronomy and Astrophysics</i> , <b>2018</b> , 609, A91 5.1	15
960	The most metal-poor Galactic globular cluster: the first spectroscopic observations of ESO280-SC06. <b>2018</b> , 477, 4565-4576	17
959	A Universal SpinMass Relation for Brown Dwarfs and Planets. <b>2018</b> , 859, 153	23
958	The Evolution of Protoplanetary Disks: Probing the Inner Disk of Very Low Accretors. <b>2018</b> , 861, 73	9
957	The Kinematics of Extended Ly Æmission in a Low-mass, Low-metallicity Galaxy at $z = 2.3$ . <b>2018</b> , 862, L10	22
956	Dust Attenuation, Bulge Formation, and Inside-out Quenching of Star Formation in Star-forming Main Sequence Galaxies atz~ 2. <b>2018</b> , 859, 56	60
955	Icy Grains from the Nucleus of Comet C/2013 US 10 (Catalina). <b>2018</b> , 862, L16	12
954	Behavioral Characteristics and CO+CO2Production Rates of Halley-type Comets Observed byNEOWISE. <b>2018</b> , 155, 164	2

953	On Cepheid Distance Scale Bias Due to Stellar Companions and Cluster Populations. 2018, 861, 36		22
952	The ALHAMBRA survey: 2D analysis of the stellar populations in massive early-type galaxies at z Astronomy and Astrophysics, <b>2018</b> , 609, A20	5.1	12
951	Subsonic islands within a high-mass star-forming infrared dark cloud. <i>Astronomy and Astrophysics</i> , <b>2018</b> , 611, L3	5.1	15
950	The CARMENES Search for Exoplanets around M Dwarfs: A Low-mass Planet in the Temperate Zone of the Nearby K2-18. <b>2018</b> , 155, 257		33
949	The H.E.S.S. Galactic plane survey. Astronomy and Astrophysics, 2018, 612, A1	5.1	143
948	The Millimeter Continuum Size <b>E</b> requency Relationship in the UZ Tau E Disk. <b>2018</b> , 861, 64		22
947	ALMA Resolves C i Emission from the Pictoris Debris Disk. <b>2018</b> , 861, 72		22
946	Variability of Red Supergiants in M31 from the Palomar Transient Factory. <b>2018</b> , 859, 73		16
945	VISION - Vienna Survey in Orion. Astronomy and Astrophysics, 2018, 614, A65	5.1	11
944	A NIKA view of two star-forming infrared dark clouds: Dust emissivity variations and mass concentration. <i>Astronomy and Astrophysics</i> , <b>2018</b> , 615, A18	5.1	8
943	Optical Dimming of RW Aur Associated with an Iron-rich Corona and Exceptionally High Absorbing Column Density. <b>2018</b> , 156, 56		10
942	Diffuse interstellar bands B780 and B797 in the Antennae Galaxy as seen by MUSE. <i>Astronomy and Astrophysics</i> , <b>2018</b> , 615, A33	5.1	3
941	Dense Gas Kinematics and a Narrow Filament in the Orion A OMC1 Region Using NH3. <b>2018</b> , 861, 77		28
940	Ionized Gas Motions and the Structure of Feedback near a Forming Globular Cluster in NGC 5253. <b>2018</b> , 860, 47		11
939	The Solar Neighborhood. XLIII. Discovery of New Nearby Stars with 12018, 156, 49		5
938	The 1.4 mm Core of Centaurus A: First VLBI Results with the South Pole Telescope. <b>2018</b> , 861, 129		6
937	The discovery of WASP-151b, WASP-153b, WASP-156b: Insights on giant planet migration and the upper boundary of the Neptunian desert. <i>Astronomy and Astrophysics</i> , <b>2018</b> , 610, A63	5.1	29
936	The Dingle Dell meteorite: A Halloween treat from the Main Belt. <b>2018</b> , 53, 2212-2227		21

935	The Highly Polarized Dusty Emission Core of Cygnus A. <b>2018</b> , 861, L23	13
934	K 2 Ultracool Dwarfs Survey. IV. Monster Flares Observed on the Young Brown Dwarf CFHT-BD-Tau 4. <b>2018</b> , 861, 76	15
933	Where are the most ancient stars in the Milky Way?. <b>2018</b> , 480, 652-668	63
932	A Very High Energy ERay Survey toward the Cygnus Region of the Galaxy. <b>2018</b> , 861, 134	23
931	The primordial deuterium abundance at zabs´=´2.504 from a high signal-to-noise spectrum of Q1009+2956. <b>2018</b> , 477, 5536-5553	14
930	Expansion and Brightness Changes in the Pulsar-wind Nebula in the Composite Supernova Remnant Kes 75. <b>2018</b> , 856, 133	20
929	The Stellar Populations of Two Ultra-diffuse Galaxies from Optical and Near-infrared Photometry. <b>2018</b> , 858, 29	31
928	OSSOS. VII. 800+ Trans-Neptunian Objects⊞he Complete Data Release. <b>2018</b> , 236, 18	71
927	Galaxy Zoo: constraining the origin of spiral arms. <b>2018</b> , 478, 932-949	10
926	SDSS-IV MaNGA: the spatially resolved stellar initial mass function in ~400 early-type galaxies. <b>2018</b> , 477, 3954-3982	59
925	Understanding the LombBcargle Periodogram. <b>2018</b> , 236, 16	305
924	sunstardb: A Database for the Study of Stellar Magnetism and the Solar-stellar Connection. <b>2018</b> , 236, 19	2
923	High-precision pulsar timing and spin frequency second derivatives. <b>2018</b> , 478, 2359-2367	10
922	AAS WorldWide Telescope: A Seamless, Cross-platform Data Visualization Engine for Astronomy Research, Education, and Democratizing Data. <b>2018</b> , 236, 22	13
921	The connection between the peaks in velocity dispersion and star-forming clumps of turbulent galaxies. <b>2018</b> , 474, 522-535	13
920	Global photometric analysis of Galactic HII regions. <b>2018</b> , 18, 091	3
919	Multiple populations within globular clusters in early-type galaxies exploring their effect on stellar initial mass function estimates. <b>2018</b> , 478, 2368-2387	4
918	The Hunt for Intermediate-mass Black Holes in the JWST Era. <b>2018</b> , 861, 142	16

917	First Results of an ALMA Band 10 Spectral Line Survey of NGC 6334I: Detections of Glycolaldehyde (HC(O)CH2OH) and a New Compact Bipolar Outflow in HDO and CS. <b>2018</b> , 863, L35	24
916	Does black-hole growth depend on the cosmic environment?. <b>2018</b> , 480, 1022-1042	16
915	Varying driver velocity fields in photospheric MHD wave simulations. <b>2018</b> , 480, 2839-2845	3
914	The low-mass population of the Vela OB2 association from Gaia. <b>2018</b> , 480, L121-L125	10
913	Optical and Infrared Photometry of the nearby SN 2017cbv. <b>2018</b> , 863, 90	5
912	O/H-N/O: the curious case of NGC 4670. <b>2018</b> , 476, 3793-3815	14
911	Investigating Galactic Supernova Remnant Candidates Using LOFAR. 2018, 860, 133	11
910	ASASSN-15nx: A Luminous Type II Supernova with a <b>P</b> erfectILinear Decline. <b>2018</b> , 862, 107	15
909	Blue Straggler Stars beyond the Milky Way. II. A Binary Origin for Blue Straggler Stars in Magellanic Cloud Clusters. <b>2018</b> , 862, 133	4
908	Stellar Populations in the Outer Disk and Halo of the Spiral Galaxy M101. <b>2018</b> , 862, 99	10
907	Stellar Streams Discovered in the Dark Energy Survey. <b>2018</b> , 862, 114	141
906	The geometric distance and binary orbit of PSR B1259B3. <b>2018</b> , 479, 4849-4860	23
905	The Next Generation Fornax Survey (NGFS). III. Revealing the Spatial Substructure of the Dwarf Galaxy Population Inside Half of Fornax's Virial Radius. <b>2018</b> , 859, 52	25
904	The Swift/BAT AGN Spectroscopic Survey. IX. The Clustering Environments of an Unbiased Sample of Local AGNs. <b>2018</b> , 858, 110	33
903	The APOGEE-2 Survey of the Orion Star-forming Complex. I. Target Selection and Validation with Early Observations. <b>2018</b> , 236, 27	16
902	The ALMA-PILS survey: 3D modeling of the envelope, disks and dust filament of IRAS 16293\(\textit{U}\)422.  Astronomy and Astrophysics, <b>2018</b> , 612, A72	30
901	The role of spiral arms in Milky Way star formation. <b>2018</b> , 479, 2361-2373	10
900	The Sagittarius dwarf galaxy: where did all the gas go?. <b>2018</b> , 478, 5263-5277	18

## (2018-2018)

899	The R-Process Alliance: Discovery of the First Metal-poor Star with a Combined r- and s-process Element Signature. <b>2018</b> , 862, 174	16
898	A Keplerian Disk around Orion SrCI, a ~ 15 M ? YSO. <b>2018</b> , 860, 119	43
897	CO in Protostars (COPS): Herschel-SPIRE Spectroscopy of Embedded Protostars. 2018, 860, 174	12
896	Variability Timescale and Spectral Index of Sgr A* in the Near Infrared: Approximate Bayesian Computation Analysis of the Variability of the Closest Supermassive Black Hole. <b>2018</b> , 863,	62
895	Cosmic shear calibration with forward modeling. <b>2018</b> , 2018, 007-007	7
894	Discovery of a radio galaxy at z = 5.72. <b>2018</b> , 480, 2733-2742	33
893	Neutrino masses and beyond-IDM cosmology with LSST and future CMB experiments. 2018, 97,	31
892	Deep neutral hydrogen observations of Leo T with the Westerbork Synthesis Radio Telescope.  Astronomy and Astrophysics, <b>2018</b> , 612, A26  5.1	22
891	The VMC survey. Astronomy and Astrophysics, <b>2018</b> , 612, A115	6
890	Cluster kinematics and stellar rotation in NGC 419 with MUSE and adaptive optics. <b>2018</b> , 480, 1689-1695	37
889	Individual stellar haloes of massive galaxies measured to 100 kpc at 0.3′. <b>2018</b> , 475, 3348-3368	52
888	The Importance of the 13C(舟)16O Reaction in Asymptotic Giant Branch Stars. <b>2018</b> , 859, 105	28
887	Galaxy And Mass Assembly (GAMA): the effect of galaxy group environment on active galactic nuclei. <b>2018</b> , 475, 4223-4234	16
886	Connecting optical and X-ray tracers of galaxy cluster relaxation. 2018, 475, 4704-4716	12
885	The ASAS-SN catalogue of variable stars I: The Serendipitous Survey. 2018, 477, 3145-3163	146
884	The Circumstellar Disk and Asymmetric Outflow of the EX Lup Outburst System. <b>2018</b> , 859, 111	12
883	J plots: a new method for characterizing structures in the interstellar medium. 2018, 477, 1940-1948	4
882	K2-137 b: an Earth-sized planet in a 4.3-h orbit around an M-dwarf. <b>2018</b> , 474, 5523-5533	43

881	Ground-based detection of G star superflares with NGTS. 2018, 477, 4655-4664	15
880	Search for Gamma-Ray Emission from Local Primordial Black Holes with theFermiLarge Area Telescope. <b>2018</b> , 857, 49	10
879	Kinematic Distances: A Monte Carlo Method. <b>2018</b> , 856, 52	44
878	Starburst to Quiescent fromHST/ALMA: Stars and Dust Unveil Minor Mergers in Submillimeter Galaxies atz~ 4.5. <b>2018</b> , 856, 121	42
877	The SAMI Galaxy Survey: Gravitational Potential and Surface Density Drive Stellar Populations. I. Early-type Galaxies. <b>2018</b> , 856, 64	22
876	The Gaia IWISE Extragalactic Astrometric Catalog. <b>2018</b> , 236, 37	7
875	On the UV/Optical Variation in NGC 5548: New Evidence Against the Reprocessing Diagram. <b>2018</b> , 860, 29	10
874	ESASky: A science-driven discovery portal for space-based astronomy missions. <b>2018</b> , 24, 97-103	3
873	Using the Properties of Broad Absorption Line Quasars to Illuminate Quasar Structure. <b>2018</b> , 479, 4153-4171	6
872	The Emission and Distribution of Dust of the Torus of NGC 1068. <b>2018</b> , 859, 99	26
8 <sub>72</sub>	The Emission and Distribution of Dust of the Torus of NGC 1068. <b>2018</b> , 859, 99  First Observations of the Magnetic Field inside the Pillars of Creation: Results from the BISTRO Survey. <b>2018</b> , 860, L6	26
	First Observations of the Magnetic Field inside the Pillars of Creation: Results from the BISTRO	
871	First Observations of the Magnetic Field inside the Pillars of Creation: Results from the BISTRO Survey. <b>2018</b> , 860, L6  Anti-glitches in the Ultraluminous Accreting Pulsar NGC 300 ULX-1 Observed with NICER. <b>2019</b> ,	20
8 <sub>7</sub> 1	First Observations of the Magnetic Field inside the Pillars of Creation: Results from the BISTRO Survey. 2018, 860, L6  Anti-glitches in the Ultraluminous Accreting Pulsar NGC 300 ULX-1 Observed with NICER. 2019, 879, 130  Rotational and Rotational-Vibrational Raman Spectroscopy of Air to Characterize Astronomical	20
871 870 869	First Observations of the Magnetic Field inside the Pillars of Creation: Results from the BISTRO Survey. 2018, 860, L6  Anti-glitches in the Ultraluminous Accreting Pulsar NGC 300 ULX-1 Observed with NICER. 2019, 879, 130  Rotational and Rotational-Vibrational Raman Spectroscopy of Air to Characterize Astronomical Spectrographs. 2019, 123, 061101	20
871 870 869 868	First Observations of the Magnetic Field inside the Pillars of Creation: Results from the BISTRO Survey. 2018, 860, L6  Anti-glitches in the Ultraluminous Accreting Pulsar NGC 300 ULX-1 Observed with NICER. 2019, 879, 130  Rotational and Rotational-Vibrational Raman Spectroscopy of Air to Characterize Astronomical Spectrographs. 2019, 123, 061101  Four Small Planets Buried in K2 Systems: What Can We Learn for TESS?. 2019, 880, L5	20 13 2
871 870 869 868 867	First Observations of the Magnetic Field inside the Pillars of Creation: Results from the BISTRO Survey. 2018, 860, L6  Anti-glitches in the Ultraluminous Accreting Pulsar NGC 300 ULX-1 Observed with NICER. 2019, 879, 130  Rotational and Rotational-Vibrational Raman Spectroscopy of Air to Characterize Astronomical Spectrographs. 2019, 123, 061101  Four Small Planets Buried in K2 Systems: What Can We Learn for TESS?. 2019, 880, L5  The X-shooter GRB afterglow legacy sample (XS-GRB). Astronomy and Astrophysics, 2019, 623, A92  Multiplicity of Galactic Cepheids and RR Lyrae stars from Gaia DR2. Astronomy and Astrophysics,	20 13 2 5

863	The Independent Discovery of Planet Candidates around Low-mass Stars and Astrophysical False Positives from the First Two TESS Sectors. <b>2019</b> , 158, 81		6	
862	The REASONS Survey: Resolved Millimeter Observations of a Large Debris Disk around the Nearby F Star HD 170773. <b>2019</b> , 881, 84		12	
861	Non-LTE chemical abundances in Galactic open and globular clusters. <i>Astronomy and Astrophysics</i> , <b>2019</b> , 628, A54	5.1	21	
860	Searches after Gravitational Waves Using ARizona Observatories (SAGUARO): System Overview and First Results from Advanced LIGO/Virgo Third Observing Run. <b>2019</b> , 881, L26		27	
859	Novel method for component separation of extended sources in X-ray astronomy. <i>Astronomy and Astrophysics</i> , <b>2019</b> , 627, A139	5.1	12	
858	Molecular envelope around the HII region RCW 120. <b>2019</b> , 488, 5641-5650		9	
857	Hot Subdwarf Stars Observed in Gaia DR2 and LAMOST DR5. <b>2019</b> , 881, 7		13	
856	Reconstructing phenomenological distributions of compact binaries via gravitational wave observations. <b>2019</b> , 100,		68	
855	Spatially Resolved Metal Loss from M31. <b>2019</b> , 877, 120		13	
854	The large gamma-ray flare of the flat-spectrum radio quasar PKS 034627. <i>Astronomy and Astrophysics</i> , <b>2019</b> , 627, A140	5.1	5	
853	The Spur and the Gap in GD-1: Dynamical Evidence for a Dark Substructure in the Milky Way Halo. <b>2019</b> , 880, 38		67	
852	Extremely metal-poor galaxies with HST/COS: laboratories for models of low-metallicity massive stars and high-redshift galaxies. <b>2019</b> , 488, 3492-3506		32	
851	A Thousand Earths: A Very Large Aperture, Ultralight Space Telescope Array for Atmospheric Biosignature Surveys. <b>2019</b> , 158, 83		15	
850	Measuring Star Formation Histories, Distances, and Metallicities with Pixel Color Magnitude Diagrams. I. Model Definition and Mock Tests. <b>2019</b> , 876, 78		7	
849	The Curious Case of KOI 4: ConfirmingKepler®First Exoplanet Detection. <b>2019</b> , 157, 192		13	
848	Planetary Nebulae and How to Find Them: Color Identification in Big Broadband Surveys. <b>2019</b> , 879, 38		Ο	
847	Exploring the Origin of Multiwavelength Activities of High-redshift Flat-spectrum Radio Quasar PKS 1502+106 during 2014 2018. <b>2019</b> , 881, 125		7	
0.6				
846	The Magellanic System: the puzzle of the leading gas stream. <b>2019</b> , 488, 918-938		19	

845	ASKAP detection of periodic and elliptically polarized radio pulses from UV Ceti. 2019, 488, 559-571	17
844	The Detectability and Characterization of the TRAPPIST-1 Exoplanet Atmospheres with JWST. <b>2019</b> , 158, 27	84
843	Sulfur Chemistry in Protoplanetary Disks: CS and H2CS. <b>2019</b> , 876, 72	38
842	Organic Complexity in Protostellar Disk Candidates. <b>2019</b> , 3, 1564-1575	13
841	SHALOS: StatisticalHerschel-ATLAS lensed objects selection. <i>Astronomy and Astrophysics</i> , <b>2019</b> , 627, A31 <sub>5.1</sub>	9
840	k-means Aperture Optimization Applied to Kepler K2 Time Series Photometry of Titan. <b>2019</b> , 131, 084505	1
839	The impact of stellar feedback from velocity-dependent ionized gas maps <b>(la MUSE view of Haro 11. <b>2019</b>, 487, 3183-3198</b>	14
838	High-resolution radiative transfer modelling of M33. <b>2019</b> , 487, 2753-2770	15
837	Stochastic modelling of star-formation histories I: the scatter of the star-forming main sequence. <b>2019</b> , 487, 3845-3869	34
836	Synthetic molecular line observations of the first hydrostatic core from chemical calculations. <b>2019</b> , 487, 2853-2873	4
835	Extreme digitization for ground-based cosmic microwave background experiments. <b>2019</b> , 487, 3279-3287	
834	Photoevaporation of Jeans-unstable molecular clumps. <b>2019</b> , 487, 3377-3391	17
833	Black hole mass estimation for active galactic nuclei from a new angle. <b>2019</b> , 487, 3404-3418	22
832	Inferring the jet parameters of active galactic nuclei using Bayesian analysis of VLBI data with a non-uniform jet model. <b>2019</b> , 488, 939-953	2
831	Detection of the self-regulation of star formation in galaxy discs. <b>2019</b> , 487, L61-L66	5
830	HALO7D II: The Halo Velocity Ellipsoid and Velocity Anisotropy with Distant Main-sequence Stars. <b>2019</b> , 879, 120	9
829	Through thick or thin: multiple components of the magneto-ionic medium towards the nearby H ii region Sharpless 2½7 revealed by Faraday tomography. <b>2019</b> , 487, 4751-4767	8
828	Linking gas and galaxies at high redshift: MUSE surveys the environments of six damped Ly∃ systems at z B. <b>2019</b> , 487, 5070-5096	18

## (2019-2019)

827	UV background fluctuations and three-point correlations in the large-scale clustering of the Lyman Forest. <b>2019</b> , 487, 5346-5362	5
826	Morphology and star formation in IllustrisTNG: the build-up of spheroids and discs. <b>2019</b> , 487, 5416-5440	59
825	Identifying optical turbulence profiles for realistic tomographic error in adaptive optics. <b>2019</b> , 488, 213-221	6
824	NGC 326: X-shaped no more. <b>2019</b> , 488, 3416-3422	25
823	Towards Sentinel-1 SAR Analysis-Ready Data: A Best Practices Assessment on Preparing Backscatter Data for the Cube. <b>2019</b> , 4, 93	31
822	Contribution of Radio Halos to the Foreground for SKA EoR Experiments. <b>2019</b> , 879, 104	9
821	Col-OSSOS: The Colors of the Outer Solar System Origins Survey. <b>2019</b> , 243, 12	22
820	Possible Detection of Gamma-Rays from Epsilon Eridani. <b>2019</b> , 878, 8	5
819	A Comparison of the Chemical Composition of Main-sequence and Giant Stars in the Open Cluster NCC 752. <b>2019</b> , 878, 99	3
818	Characterization of a Sample of Southern M Dwarfs Using Harps and X-shooter Spectra. <b>2019</b> , 878, 134	8
817	The Fundamental Metallicity Relation Emerges from the Local Anti-correlation between Star Formation Rate and Gas-phase Metallicity that Exists in Disk Galaxies. <b>2019</b> , 878, L6	7
816	Constraining Compact Object Formation with 2M0521. <b>2019</b> , 878, L4	13
815	ASASSN-15pz: Revealing Significant Photometric Diversity among 2009dc-like, Peculiar SNe Ia. <b>2019</b> , 880, 35	14
814	The First Candidate Colliding-wind Binary in M33. <b>2019</b> , 880, 8	5
813	JCMT BISTRO Survey Observations of the Ophiuchus Molecular Cloud: Dust Grain Alignment Properties Inferred Using a Ricean Noise Model. <b>2019</b> , 880, 27	21
812	Optical Tomography of Chemical Elements Synthesized in Type Ia Supernovae. <b>2019</b> , 123, 041101	18
811	Stellar Evolution in Real Time: Models Consistent with the Direct Observation of a Thermal Pulse in T Ursae Minoris. <b>2019</b> , 879, 62	10
810	First stellar occultation by the Galilean moon Europa and upcoming events between 2019 and 2021. <i>Astronomy and Astrophysics</i> , <b>2019</b> , 626, L4	3

The study of unclassified B[e] stars and candidates in the Galaxy and Magellanic Clouds  $\Box$  2019, 488, 1090-1110  $\varsigma$ 809 Observational properties of ultra-diffuse galaxies in low-density environments: field UDGs are 808 30 predominantly blue and star forming. 2019, 488, 2143-2157 Two sub-millimetre bright protoclusters bounding the epoch of peak star-formation activity. 2019, 807 12 488, 1790-1812 The EDGE-CALIFA survey: exploring the star formation law through variable selection. 2019, 488, 1926-1940 806 17 eleanor: An Open-source Tool for Extracting Light Curves from the TESS Full-frame Images. 2019, 805 94 131.094502 Mass transport in galaxy discs limits black hole growth to sub-Eddington rates. 2019, 488, 2006-2017 804 The L 98-59 System: Three Transiting, Terrestrial-size Planets Orbiting a Nearby M Dwarf. 2019, 803 56 158, 32 Dust Production of Comet 21P/GiacobiniZinner throughout Its 2018 Apparition. 2019, 158, 7 802 5 The total mass of the Large Magellanic Cloud from its perturbation on the Orphan stream. 2019, 801 130 487, 2685-2700 Resolving the Decades-long Transient FIRST J141918.9+394036: An Orphan Long Gamma-Ray Burst 800 17 or a Young Magnetar Nebula?. 2019, 876, L14 Phat ELVIS: The inevitable effect of the Milky Way® disc on its dark matter subhaloes. 2019, 487, 4409-4423 799 49 The Extremely Luminous Quasar Survey in the Pan-STARRS 1 Footprint (PS-ELQS). 2019, 243, 5 798 14 Fundamental uncertainty levels of 21 cm power spectra from a delay analysis. 2019, 487, 5840-5853 797 12 The Measured Impact of Chromatic Atmospheric Effects on Barycentric Corrections: Results from 796 8 the EXtreme PREcision Spectrograph. 2019, 158, 40 Census of IOphiuchi candidate members from Gaia Data Release 2. Astronomy and Astrophysics, 26 5.1 795 2019, 626, A80 Star Clusters Across Cosmic Time. 2019, 57, 227-303 794 190 The physical and chemical structure of Sagittarius B2. Astronomy and Astrophysics, 2019, 630, A73 8 793 5.1 Forecasting super-sample covariance in future weak lensing surveys with SuperSCRAM. 2019, 2019, 004-004 792

791	simsurvey: estimating transient discovery rates for the Zwicky transient facility. 2019, 2019, 005-005	19
790	ALTSched: Improved Scheduling for Time-domain Science with LSST. <b>2019</b> , 131, 115002	4
789	Default Parallels: The Science Potential of JWST Parallel Observations during TSO Primary Observations. <b>2019</b> , 131, 114504	0
788	Localization of binary black hole mergers with known inclination. <b>2019</b> , 488, 4459-4463	9
787	New perspectives on the BOSS small-scale lensing discrepancy for the Planck IDM cosmology. <b>2019</b> , 488, 5771-5787	20
786	Discovery of a radio transient in M81. <b>2019</b> , 489, 1181-1196	4
785	NGTS-7Ab: an ultrashort-period brown dwarf transiting a tidally locked and active M dwarf. <b>2019</b> , 489, 5146-5164	29
784	Radio Galaxy Zoo: Knowledge Transfer Using Rotationally Invariant Self-organizing Maps. <b>2019</b> , 131, 108009	8
783	Performance of the Gemini Planet Imager Non-redundant Mask and Spectroscopy of Two Close-separation Binaries: HR 2690 and HD 142527. <b>2019</b> , 157, 249	0
782	The Case for a Large-scale Occultation Network. <b>2019</b> , 158, 19	1
781	A Hot Saturn Near (but Unassociated with) the Open Cluster NGC 1817. <b>2019</b> , 158, 62	1
780	Magnetic Inflation and Stellar Mass. III. Revised Parameters for the Component Stars of NSVS 07394765. <b>2019</b> , 158, 89	4
779	Three Red Suns in the Sky: A Transiting, Terrestrial Planet in a Triple M-dwarf System at 6.9 pc. <b>2019</b> , 158, 152	39
778	LRG-BEASTS: Transmission Spectroscopy and Retrieval Analysis of the Highly Inflated Saturn-mass Planet WASP-39b. <b>2019</b> , 158, 144	18
777	Probing an X-Ray Flare Pattern in Mrk 421 Induced by Multiple Stationary Shocks: A Solution to the Bulk Lorentz Factor Crisis. <b>2019</b> , 877, 26	7
776	The Rest-frame H-band Luminosity Function of Red-sequence Galaxies in Clusters at 1.0 2019, 880, 119	9
775	The HERA-19 Commissioning Array: Direction-dependent Effects. <b>2019</b> , 882, 58	12
774	The CGMIGRB Study. I. Uncovering the Circumgalactic Medium around GRB Hosts at Redshifts 216. <b>2019</b> , 884, 66	5

773	The Super Eight Galaxies: Properties of a Sample of Very Bright Galaxies at 7 2019, 882, 42	17
772	The Delay Times of Type Ia Supernova. <b>2019</b> , 882, 52	10
771	Hunting for the Dark Matter Wake Induced by the Large Magellanic Cloud. <b>2019</b> , 884, 51	62
770	T CrB: Radio Observations during the 20162017 Super-activelState. <b>2019</b> , 884, 8	1
769	Short-duration Stellar Flares in GALEX Data. <b>2019</b> , 883, 88	16
768	A Simplified, Lossless Reanalysis of PAPER-64. <b>2019</b> , 883, 133	59
767	Supermassive Black Hole Binary Candidates from the Pan-STARRS1 Medium Deep Survey. <b>2019</b> , 884, 36	27
766	Resolved ALMA Continuum Image of the Circumbinary Ring and Circumstellar Disks in the L1551 IRS 5 System. <b>2019</b> , 882, L4	9
765	Counter-rotation and High-velocity Outflow in the Parsec-scale Molecular Torus of NGC 1068. <b>2019</b> , 884, L28	36
764	Resolved scaling relations and metallicity gradients on sub-kiloparsec scales at z 🗈 . <b>2019</b> , 489, 224-240	11
763	Photon-weighted barycentric correction and its importance for precise radial velocities. <b>2019</b> , 489, 2395-2402	8
762	Studying the morphology of reionization with the triangle correlation function of phases. <b>2019</b> , 489, 1321-1337	12
761	Dark-age reionization and galaxy formation simulation IXIX. Predictions of infrared excess and cosmic star formation rate density from UV observations. <b>2019</b> , 489, 1357-1372	7
760	Exploring the M-dwarf LuminosityIIemperatureRadius relationships using Gaia DR2. <b>2019</b> , 489, 2615-2633	18
759	Bow shocks, bow waves, and dust waves []II. Diagnostics. <b>2019</b> , 489, 2142-2158	8
758	Secularly powered outflows from AGNs: the dominance of non-merger driven supermassive black hole growth. <b>2019</b> , 489, 4016-4031	14
757	Diffuse ionized gas and its effects on nebular metallicity estimates of star-forming galaxies. <b>2019</b> , 489, 4721-4733	21
756	horizon-AGN virtual observatory I. Template-free estimates of galaxy properties from colours. <b>2019</b> , 489, 4817-4835	10

755	The nature of faint radio galaxies at high redshifts. <b>2019</b> , 489, 5053-5075	6
754	A dwarf disrupting [Andromeda XXVII and the North West Stream. <b>2019</b> , 490, 2905-2917	1
753	Limits on a population of collisional-triples as progenitors of Type-Ia supernovae. <b>2019</b> , 490, 657-664	8
75 <sup>2</sup>	The VANDELS survey: the star-formation histories of massive quiescent galaxies at 1.0 %lt; ź %lt; 1.3. <b>2019</b> , 490, 417-439	37
751	Tentative detection of the circumgalactic medium of the isolated low-mass dwarf galaxy WLM. <b>2019</b> , 490, 467-477	6
750	Investigating the complex velocity structures within dense molecular cloud cores with GBT-Argus. <b>2019</b> , 490, 527-539	9
749	Cosmological Evidence Modelling: a new simulation-based approach to constrain cosmology on non-linear scales. <b>2019</b> , 490, 1870-1878	12
748	Dbserving unrelaxed clusters in dark matter simulations. <b>2019</b> , 490, 773-783	2
747	Illuminating the Tadpole® metamorphosis II. MUSE observations of a small globule in a sea of ionizing photons. <b>2019</b> , 490, 2056-2070	3
746	Towards the analysis of JWST exoplanet spectra: the effective temperature in the context of direct imaging. <b>2019</b> , 490, 2086-2090	
745	The multiphase gas structure and kinematics in the circumnuclear region of NGC 5728. <b>2019</b> , 490, 5860-5887	36
744	MOBSTER [III. HD 62658: a magnetic Bp star in an eclipsing binary with a non-magnetic [dentical twin[]2019, 490, 4154-4165	9
743	The rotational profiles of cluster galaxies. <b>2019</b> , 490, 5017-5032	2
742	The G332 molecular cloud ring: I. Morphology and physical characteristics. <b>2019</b> , 484, 2089-2118	1
741	Dissecting the active galactic nucleus in Circinus III. A thin dusty disc and a polar outflow on parsec scales. <b>2019</b> , 484, 3334-3355	28
740	On the triple-star origin of the planetary nebula Sh´2-71. <b>2019</b> , 489, 2195-2203	8
739	An unusually large gaseous transit in a debris disc. <b>2019</b> , 490, 5218-5227	2
738	Modern stellar spectroscopy caveats. <b>2019</b> , 486, 2075-2101	68

737	Investigation of the origin of the anomalous microwave emission in Lambda Orionis. 2019,		3
736	JCMT BISTRO Survey: Magnetic Fields within the Hub-filament Structure in IC 5146. <b>2019</b> , 876, 42		27
735	M-subdwarf Research. I. Identification, Modified Classification System, and Sample Construction. <b>2019</b> , 240, 31		9
734	A Blueprint of State-of-the-art Techniques for Detecting Quasi-periodic Pulsations in Solar and Stellar Flares. <b>2019</b> , 244, 44		19
733	Resolved and Integrated Stellar Masses in the SDSS-IV/MaNGA Survey. II. Applications of PCA-based Stellar Mass Estimates. <b>2019</b> , 883, 83		9
73²	Constraining Mass-transfer Histories of Blue Straggler Stars with COS Spectroscopy of White Dwarf Companions. <b>2019</b> , 885, 45		13
731	The first maps of 🛭 Ithe dust mass absorption coefficient 🗓 nearby galaxies, with DustPedia. <b>2019</b> , 489, 5256-5283		22
730	Resolved and Integrated Stellar Masses in the SDSS-iv/MaNGA Survey. I. PCA Spectral Fitting and Stellar Mass-to-light Ratio Estimates. <b>2019</b> , 883, 82		8
729	Disklet Coupling in the 2017/2018 Outburst of the Galactic Black Hole Candidate X-Ray Binary MAXI J1535B71. <b>2019</b> , 883, 198		35
728	Globular Cluster Intrinsic Iron Abundance Spreads. I. Catalog. <b>2019</b> , 245, 5		12
727	The SLUGGS survey: measuring globular cluster ages using both photometry and spectroscopy. <b>2019</b> , 490, 491-501		17
726	Analysis of Helium-rich White Dwarfs Polluted by Heavy Elements in the Gaia Era. <b>2019</b> , 885, 74		53
725	Dust properties and star formation of approximately a thousand local galaxies. <i>Astronomy and Astrophysics</i> , <b>2019</b> , 631, A38	5.1	10
724	Consistent radial velocities of classical Cepheids from the cross-correlation technique. <i>Astronomy and Astrophysics</i> , <b>2019</b> , 631, A37	5.1	6
723	Red and dead CANDELS: massive passive galaxies at the dawn of the Universe. <b>2019</b> , 490, 3309-3328		31
722	Learning the relationship between galaxies spectra and their star formation histories using convolutional neural networks and cosmological simulations. <b>2019</b> , 490, 5503-5520		11
721	The Sloan Digital Sky Survey Reverberation Mapping Project: Accretion and Broad Emission Line Physics from a Hypervariable Quasar. <b>2019</b> , 885, 44		20
720	A New Technique for Finding Galaxies Leaking Lyman-continuum Radiation: [S ii]-deficiency. <b>2019</b> , 885, 57		21

## (2022-2019)

719	SDSS-IV MaNGA: Evidence for Enriched Accretion onto Satellite Galaxies in Dense Environments. <b>2019</b> , 884, 156	13
718	A Warm Jupiter-sized Planet Transiting the Pre-main-sequence Star V1298 Tau. <b>2019</b> , 158, 79	36
717	Reflected Light Phase Curves in the TESS Era. <b>2019</b> , 158, 66	10
716	Signatures of Obliquity in Thermal Phase Curves of Hot Jupiters. <b>2019</b> , 158, 108	9
715	Studying Microlensing Events from New Horizons. <b>2019</b> , 158, 110	0
714	WEan: Comprehensive Time-series Detrending in Python. <b>2019</b> , 158, 143	54
713	Spectrophotometric Parallaxes with Linear Models: Accurate Distances for Luminous Red-giant Stars. <b>2019</b> , 158, 147	22
712	STRIDES: Automated uniform models for 30 quadruply imaged quasars.	O
711	The Upper Edge of the Neptune Desert Is Stable Against Photoevaporation. <b>2022</b> , 164, 234	0
710	ALMA Uncovers Highly Filamentary Structure toward the Sgr E Region. <b>2022</b> , 939, 58	Ο
709	iPTF Archival Search for Fast Optical Transients. <b>2022</b> , 45-60	0
708	Beamforming approaches towards detecting the 21-cm global signal from Cosmic Dawn with radio array telescopes. <b>2022</b> , 39,	О
707	WALLABY Pilot Survey: Public release of HI kinematic models for more than 100 galaxies from phase 1 of ASKAP pilot observations. <b>2022</b> , 39,	0
706	The X-ray angular power spectrum of extended sources in the eROSITA final equatorial depth survey.	O
705	Cold gas mass measurements for the era of large optical spectroscopic surveys. <b>2022</b> , 518, 353-367	0
704	Toward the Automated Detection of Light Echoes in Synoptic Surveys: Considerations on the Application of Deep Convolutional Neural Networks. <b>2022</b> , 164, 250	O
703	ALMACAL VIII: A pilot survey for untargeted extragalactic CO emission lines in deep ALMA calibration data.	0
702	High-resolution Hubble Space Telescope Imaging Survey of Local Star-forming Galaxies. I. Spatially Resolved Obscured Star Formation with H⊞nd Paschen-ℝecombination Lines. <b>2022</b> , 263, 17	O

701	Star-forming early-type galaxies and quiescent late-type galaxies in the local Universe.	Ο
700	LSST Survey Strategies and Brown Dwarf Parallaxes. <b>2022</b> , 263, 23	O
699	The GAPS Programme at TNG. XLI. The climate of KELT-9b revealed with a new approach to high-spectral-resolution phase curves.	0
698	Triage of the Gaia DR3 astrometric orbits. I. A sample of binaries with probable compact companions.	2
697	Optical <b>R</b> adio Position Offsets Are Inversely Correlated with AGN Photometric Variability. <b>2022</b> , 939, L32	0
696	Spinning up the Surface: Evidence for Planetary Engulfment or Unexpected Angular Momentum Transport?. <b>2022</b> , 940, 23	O
695	Two Remarkably Luminous Galaxy Candidates at z 🗓 0🗓 2 Revealed by JWST. <b>2022</b> , 940, L14	13
694	Empirical constraints on the turbulence in QSO host nebulae from velocity structure function measurements.	1
693	Isolated Massive Star Formation in G28.20-0.05. <b>2022</b> , 939, 120	0
692	Star formation in IC1396. Kinematics and subclusters structure reveled by Gaia.	О
691	Origin of highly r-process-enhanced stars in a cosmological zoom-in simulation of a Milky Way-like galaxy. <b>2022</b> , 517, 4856-4874	1
690	pySYD: Automated measurements of global asteroseismic parameters. <b>2022</b> , 7, 3331	1
689	NICMOS Kernel-phase Interferometry. I. Catalogue of Brown Dwarfs Observed in F110W and F170M. <b>2022</b> , 164, 244	0
688	Hadronic signatures from magnetically dominated baryon-loaded AGN jets.	1
687	A GMOS/IFU Study of Jellyfish Galaxies in Massive Clusters. <b>2022</b> , 940, 24	0
686	The Properties of Fast Yellow Pulsating Supergiants: FYPS Point the Way to Missing Red Supergiants. <b>2022</b> , 940, 27	O
685	Ultra-diffuse Galaxies as Extreme Star-forming Environments. II. Star Formation and Pressure Balance in H i-rich UDGs. <b>2022</b> , 939, 101	0
684	Bridging the GapII he Disappearance of the Intermediate Period Gap for Fully Convective Stars, Uncovered by New ZTF Rotation Periods. <b>2022</b> , 164, 251	0

683	Does absorption against AGN reveal supermassive black hole accretion?.	1
682	Interpreting molecular hydrogen and atomic oxygen line emission of T Tauri disks with photoevaporative disk-wind models.	O
681	Exploiting stellar explosion induced by the QCD phase transition in large-scale neutrino detectors. <b>2022</b> , 106,	0
680	Roaring Storms in the Planetary-mass Companion VHS 1256-1257 b: Hubble Space Telescope Multiepoch Monitoring Reveals Vigorous Evolution in an Ultracool Atmosphere. <b>2022</b> , 164, 239	O
679	First Results from the JWST Early Release Science Program Q3D: Turbulent Times in the Life of a z ~ 3 Extremely Red Quasar Revealed by NIRSpec IFU. <b>2022</b> , 940, L7	0
678	Is the star formation rate in z $\sim$ 6 quasars overestimated?.	O
677	GOALS-JWST: Resolving the Circumnuclear Gas Dynamics in NGC 7469 in the Mid-infrared. <b>2022</b> , 940, L5	0
676	Tracing Interstellar Heating: An ALCHEMI Measurement of the HCN Isomers in NGC 253. <b>2022</b> , 939, 119	O
675	On the Origin of the Strong Optical Variability of Emission-line Galaxies. <b>2022</b> , 940, 35	O
674	WATTS: Workflow and template toolkit for simulation. <b>2022</b> , 7, 4735	О
673	The Steady-State Multi-TeV Diffuse Gamma-Ray Emission Predicted with galprop and Prospects for the Cherenkov Telescope Array.	0
672	A Short Gamma-Ray Burst from a Protomagnetar Remnant. <b>2022</b> , 939, 106	O
671	Multi-gas phases in supernova remnant IC 443: Mapping shocked H2 with VLT/KMOS.	O
670	The Automated Photometry of Transients pipeline (AutoPhOT). <b>2022</b> , 667, A62	2
669	relensing: Reconstructing the mass profile of galaxy clusters from gravitational lensing.	0
668	JWST Imaging of Earendel, the Extremely Magnified Star at Redshift z = 6.2. <b>2022</b> , 940, L1	2
667	Extreme value statistics of the halo and stellar mass distributions at high redshift: are JWST results in tension with IDM?.	2
666	A New Stellar Companion to GJ 1292. <b>2022</b> , 6, 242	O

665	Mode Mixing and Rotational Splittings. I. Near-degeneracy Effects Revisited. <b>2022</b> , 940, 18	O
664	The demographics of obscured AGN from X-ray spectroscopy guided by multiwavelength information.	O
663	A Milliarcsecond-accurate Position for Sagittarius A*. <b>2022</b> , 940, 15	0
662	Efficient Interrogation of the Kinetic Barriers Demarcating Catalytic States of a Tyrosine Kinase with Optimal Physical Descriptors and Mixture Models.	O
661	Unveiling a new extragalactic structure hidden by the Milky Way.	1
660	The Velocity Dispersion Function for Massive Quiescent and Star-forming Galaxies at 0.6 < z 🗓 .0. <b>2022</b> , 939, 90	O
659	GMAG: An open-source python package for ground-based magnetometers. 9,	0
658	The Turndown of the Baryonic Tully <b>E</b> isher Relation and Changing Baryon Fraction at Low Galaxy Masses. <b>2022</b> , 940, 8	O
657	The ALMA Survey of 70 fb Dark High-mass Clumps in Early Stages (ASHES). VII. Chemistry of Embedded Dense Cores. <b>2022</b> , 939, 102	0
656	Seven Years of Coordinated Chandra NuSTAR Observations of SN 2014C Unfold the Extreme Mass-loss History of Its Stellar Progenitor. <b>2022</b> , 939, 105	O
655	A Q-band Line Survey toward Orion KL Using the Tianma Radio Telescope. <b>2022</b> , 263, 13	0
654	Stellar Chromospheric Activity Database of Solar-like Stars Based on the LAMOST Low-Resolution Spectroscopic Survey. <b>2022</b> , 263, 12	O
653	Opening the Era of Quasar-host Studies at High Redshift with JWST. <b>2022</b> , 939, L28	0
652	First r-process enhanced star confirmed as a member of the Galactic bulge.	Ο
651	Pixel Centroid Characterization with Laser Speckle and Application to the Nancy Grace Roman Space Telescope Detector Arrays. <b>2022</b> , 134, 115001	0
650	CLASSY IV. Exploring UV Diagnostics of the Interstellar Medium in Local High-z Analogs at the Dawn of the JWST Era*. <b>2022</b> , 939, 110	Ο
649	Potential scientific synergies in weak lensing studies between the CSST and Euclid space probes.	1
648	COOL-LAMPS. II. Characterizing the Size and Star Formation History of a Bright Strongly Lensed Early-type Galaxy at Redshift 1.02. <b>2022</b> , 940, 42	O

647	How do the dynamics of the Milky Way - Large Magellanic Cloud system affect gamma-ray constraints on particle dark matter?.	0
646	Molecular Gas Reservoirs in Massive Quiescent Galaxies at $z\sim0.7$ Linked to Late-time Star Formation. <b>2022</b> , 940, 39	Ο
645	X-ray emission from a rapidly accreting narrow-line Seyfert 1 galaxy at z=6.56.	0
644	First Light And Reionisation Epoch Simulations (FLARES) VII: The star formation and metal enrichment histories of galaxies in the early Universe.	О
643	Morphological signatures of mergers in the TNG50 simulation and the Kilo-Degree Survey: the merger fraction from dwarfs to Milky Way-like galaxies.	O
642	Dwarf Galaxies with Central Cores in Modified Newtonian Dynamics Gravity. <b>2022</b> , 940, 46	O
641	First light and reionisation epoch simulations (FLARES) V: The redshift frontier.	2
640	Multiwavelength Observations of the Obscuring Wind in the Radio-quiet Quasar MR 2251-178. <b>2022</b> , 940, 41	O
639	Probing Galactic variations in the fine-structure constant using solar twin stars: Systematic errors. <b>2022</b> , 519, 1221-1237	3
638	Probing Galactic variations in the fine-structure constant using solar twin stars: methodology and results. <b>2022</b> , 519, 1238-1252	3
637	sympy2c: From symbolic expressions to fast C/C++ functions and ODE solvers in Python. <b>2023</b> , 42, 100666	0
636	Astronomical source detection in radio continuum maps with deep neural networks. <b>2023</b> , 42, 100682	Ο
635	A preference for cold dark matter over Superfluid Dark Matter in local Milky Way data. 2023, 39, 101140	0
634	The GLEAMing of the first supermassive black holes: II. A new sample of high-redshift radio galaxy candidates. <b>2022</b> , 39,	Ο
633	PyThea: An open-source software package to perform 3D reconstruction of coronal mass ejections and shock waves. 9,	1
632	How to interpret measurements of diffuse light in stacked observations of groups and clusters of galaxies. <b>2022</b> , 518, 3685-3701	Ο
631	Searching for Compact Objects in Binaries with Gaia DR3. <b>2022</b> , 940, 126	О
630	Spectral Evolution of Ultraluminous X-Ray Pulsar NGC 300 ULX-1. <b>2022</b> , 940, 138	O

629	A Ghost in Bolles: The Least-Luminous Disrupted Dwarf Galaxy. <b>2022</b> , 940, 127	0
628	Proper Motions, Orbits, and Tidal Influences of Milky Way Dwarf Spheroidal Galaxies. <b>2022</b> , 940, 136	4
627	Testing Velocity Kinks as a Planet Detection Method: Do Velocity Kinks in Surface Gas Emission Trace Planetary Spiral Wakes in the Midplane Continuum?. <b>2022</b> , 940, L43	0
626	Characterization and dynamics of the peculiar stream Jhelum. A tentative role for the Sagittarius dwarf galaxy.	O
625	Observations of 4U 1626日7 with the Imaging X-Ray Polarimetry Explorer. <b>2022</b> , 940, 70	0
624	A First Look into the Nature of JWST/MIRI 7.7 th Sources from SMACS 0723. <b>2022</b> , 940, L24	О
623	Diverse Properties of Molecular Gas in the Host Galaxies of Fast Radio Bursts. <b>2022</b> , 940, L34	Ο
622	APERO: A PipelinE to Reduce ObservationsDemonstration with SPIRou. 2022, 134, 114509	1
621	Probing Patchy Reionization with the Void Probability Function of Ly Emitters. 2022, 940, 102	1
620	GOALS-JWST: Unveiling Dusty Compact Sources in the Merging Galaxy IIZw096. <b>2022</b> , 940, L6	O
619	Identifying the 3FHL Catalog. VI. Swift Observations of 3FHL Unassociated Objects with Source Classification via Machine Learning. <b>2022</b> , 940, 139	0
618	The Role of Filamentary Structures in the Formation of Two Dense Cores, L1544 and L694-2. <b>2022</b> , 940, 112	1
617	Two decades of optical timing of the shortest-period binary star system HM Cancri. <b>2022</b> , 518, 5123-5139	0
616	A targeted search for repeating fast radio bursts with the MWA. <b>2022</b> , 518, 4278-4289	O
615	The dark side of galaxy stellar populations [II. The dependence of star-formation histories on halo mass and on the scatter of the main sequence. <b>2022</b> , 518, 6325-6339	0
614	MUSE-ALMA Haloes IVIII. Statistical study of circumgalactic medium gas. <b>2022</b> , 519, 931-947	1
613	Revisiting the Magnetic Field Distribution of Normal Pulsars: Implications for the Multiple Origins for Neutron Stars. <b>2022</b> , 134, 114201	0
612	Flexible Models for Galaxy Star Formation Histories Both Shift and Scramble the Optical ColorMass-to-light Ratio (M/L) Relationship. <b>2022</b> , 940, 88	О

611	Observational Inference on the Delay Time Distribution of Short Gamma-Ray Bursts. <b>2022</b> , 940, L18	1
610	A New Period Determination Method for Periodic Variable Stars. <b>2022</b> , 134, 114507	O
609	Structure in the Magnetic Field of the Milky Way Disk and Halo Traced by Faraday Rotation. <b>2022</b> , 940, 75	O
608	Preemergence Signatures of Horizontal Divergent Flows in Solar Active Regions. <b>2022</b> , 940, 109	O
607	Testing the Limits of AGN Feedback and the Onset of Thermal Instability in the Most Rapidly Star-forming Brightest Cluster Galaxies. <b>2022</b> , 940, 140	1
606	Tracing PAH Emission in EOrionis Using COBE/DIRBE Data. <b>2022</b> , 940, 59	O
605	A Machine-learning Approach to Enhancing eROSITA Observations. <b>2022</b> , 940, 60	O
604	The nature of 500 micron risers []I. Multiplicities and environments of sub-mm faint dusty star-forming galaxies. <b>2022</b> , 519, 709-728	O
603	Mock galaxy surveys for HST and JWST from the IllustrisTNG simulations. <b>2022</b> , 518, 6318-6324	0
602	Deep LearningBased Fast Spectral Inversion of H⊞and Ca ii 8542 Line Spectra. <b>2022</b> , 940, 147	O
601	Chasing ICM cooling and AGN feedback from the macro to the meso scales in the galaxy cluster ZwCl 235.	О
600	Near-infrared Extragalactic Background Light Fluctuations on Nonlinear Scales. <b>2022</b> , 940, 115	O
599	Horizons: nuclear astrophysics in the 2020s and beyond. <b>2022</b> , 49, 110502	1
598	Rocky Histories: The Effect of High Excitations on the Formation of Rocky Planets. <b>2022</b> , 940, 144	O
597	An Electron-scattering Time Delay in Black Hole Accretion Disks. <b>2022</b> , 940, L22	Ο
596	The MOSDEF survey: probing resolved stellar populations at $z \sim 2$ Using a new bayesian-defined morphology metric called patchiness. <b>2022</b> , 518, 4214-4237	О
595	Detection of Intracluster Globular Clusters in the First JWST Images of the Gravitational Lens Cluster SMACS J0723.3 $\blacksquare$ 327 at z = 0.39. <b>2022</b> , 940, L19	О
594	Magnetic activity and parameters of 43 flare stars in the GWAC archive.	O

593	A Segmented PeriodIuminosity Relation for Nearby Extragalactic Delta Scuti Stars. 2022, 940, L25	О
592	The Gaia-ESO Survey: Old super-metal-rich visitors from the inner Galaxy.	O
591	Assessing the physical reality of Milky Way open cluster candidates. 2022, 518, 6216-6222	O
590	A 16 hr Transit of Kepler-167 e Observed by the Ground-based Unistellar Telescope Network. <b>2022</b> , 940, L39	O
589	Plasma lensing near the eclipses of the Black Widow pulsar B1957+20. <b>2022</b> , 519, 121-135	O
588	The Disk Population in a Distant Massive Protocluster. <b>2022</b> , 940, 124	O
587	Simulated Bars May Be Shorter but Are Not Slower Than Those Observed: TNG50 versus MaNGA. <b>2022</b> , 940, 61	2
586	PRODIGE - Envelope to disk with NOEMA. II. Small-scale temperature structure and streamer feeding the SVS13A protobinary based on CH3CN and DCN.	O
585	Limiting the accretion disc light in two mass transferring hot subdwarf binaries. 2022, 519, 148-156	O
584	King Ghidorah Supercluster: Mapping the light and dark matter in a new supercluster at $z=0.55$ using the subaru hyper suprime-cam. <b>2022</b> , 519, L45-L50	O
583	Collimation of the Relativistic Jet in the Quasar 3C 273. <b>2022</b> , 940, 65	O
582	Tracking ALMA System Temperature with Water Vapor Data at High Frequency. <b>2022</b> , 134, 125001	O
581	The X-Ray Polarimetry View of the Accreting Pulsar Cen X-3. <b>2022</b> , 941, L14	O
580	SPYGLASS. II. The Multigenerational and Multiorigin Star Formation History of Cepheus Far North. <b>2022</b> , 941, 49	O
579	Evidence for the Disruption of a Planetary System During the Formation of the Helix Nebula. <b>2023</b> , 165, 22	O
578	JWST PEARLS. Prime Extragalactic Areas for Reionization and Lensing Science: Project Overview and First Results. <b>2023</b> , 165, 13	1
577	A long-duration gamma-ray burst with a peculiar origin. <b>2022</b> , 612, 232-235	1
576	Robust Inference of Neutron-star Parameters from Thermonuclear Burst Observations. <b>2022</b> , 263, 30	O

575	Dust Hot Spots at 10 au Scales around the Class 0 Binary IRAS 16293\(\bar{1}\)422 A: A Departure from the Passive Irradiation Model. <b>2022</b> , 941, L23	O
574	What Are Those Tiny Things? A First Study of Compact Star Clusters in the SMACS0723 Field with JWST. <b>2022</b> , 941, L11	O
573	Mapping Dark Matter with Extragalactic Stellar Streams: The Case of Centaurus A. <b>2022</b> , 941, 19	2
572	Atomic Gas Scaling Relations of Star-forming Galaxies at z 🛭 . <b>2022</b> , 941, L6	O
571	ArtPop: A Stellar Population and Image Simulation Python Package. 2022, 941, 26	O
570	Observing circumplanetary disks with METIS.	O
569	Fraction of stars in clusters for the LEGUS dwarf galaxies.	О
568	Two substellar survivor candidates: one found and one missing. <b>2022</b> , 519, 1381-1395	O
567	Emission Line Galaxies in the SHARDS Hubble Frontier Fields. II. Limits on Lyman-continuum Escape Fractions of Lensed Emission Line Galaxies at Redshifts 2 < z < 3.5. <b>2022</b> , 941, 181	O
566	PHANGS-JWST First Results: Spurring on Star Formation: JWST Reveals Localized Star Formation in a Spiral Arm Spur of NGC 628. <b>2022</b> , 941, L27	1
565	The Origin of High-energy Emission in the Young Radio Source PKS 1718图9. <b>2022</b> , 941, 52	O
564	Probing quasar lifetimes with proximate 21-centimetre absorption in the diffuse intergalactic medium at redshifts z 🖟.	O
563	Concerning Colour: The Effect of Environment on Type Ia Supernova Colour in the Dark Energy Survey.	1
562	Ultraviolet spectropolarimetry: conservative and nonconservative mass transfer in OB interacting binaries. <b>2022</b> , 367,	O
561	Ultraviolet Spectropolarimetry: on the origin of rapidly rotating B stars. 2022, 367,	0
560	DUVET: Spatially Resolved Observations of Star Formation Regulation via Galactic Outflows in a Starbursting Disk Galaxy. <b>2022</b> , 941, 163	O
559	A Catalog of Candidate Double and Lensed Quasars from Gaia and WISE Data. <b>2023</b> , 264, 4	O
558	Extreme Nature of Four Blue-excess Dust-obscured Galaxies Revealed by Optical Spectroscopy. <b>2022</b> , 941, 195	O

557	GOALS-JWST: Tracing AGN Feedback on the Star-forming Interstellar Medium in NGC 7469. <b>2022</b> , 941, L36	О
556	Has the dust clump in the debris disk of Beta Pictoris moved?.	O
555	V-LoTSS: The circularly polarised LOFAR Two-metre Sky Survey.	О
554	Properties of Redlen cadmium zinc telluride with respect to x-ray spectroscopy. 2022, 8,	О
553	CO(J = $1\overline{D}$ ) Mapping Survey of 64 Galaxies in the Fornax Cluster with the ALMA Morita Array. <b>2022</b> , 263, 40	О
552	Accretion Variability of the Multiple T Tauri System VW Cha. <b>2022</b> , 941, 177	Ο
551	A Long Time Ago in a Galaxy Far, Far Away: A Candidate $z\sim 12$ Galaxy in Early JWST CEERS Imaging. <b>2022</b> , 940, L55	8
550	The PhotoDissociation Region Toolbox: Software and Models for Astrophysical Analysis. <b>2023</b> , 165, 25	Ο
549	Characterizing Observed Extra Mixing Trends in Red Giants using the Reduced Density Ratio from Thermohaline Models. <b>2022</b> , 941, 164	О
548	The Impact of Initial <b>E</b> inal Mass Relations on Black Hole Microlensing. <b>2022</b> , 941, 116	1
547	Deep Narrowband Photometry of the M101 Group: Strong-line Abundances of 720 H ii Regions. <b>2022</b> , 941, 182	О
546	The Astrometric Animation of Water Masers toward the Mira Variable BX Cam. <b>2022</b> , 941, 105	Ο
545	The First Interferometric Measurements of NH2D/NH3 Ratio in Hot Corinos. 2022, 941, 75	О
544	Analysis of Eclipsing Binary Stars and Identification of Exoplanets Using Transit Timing Variation Using data from TESS. <b>2022</b> , 2381, 012106	О
543	Radial velocity confirmation of a hot super-Neptune discovered by TESS with a warm Saturn-mass companion.	0
542	Dark matter halos and scaling relations of extremely massive spiral galaxies from extended H i rotation curves. <b>2022</b> , 518, 6340-6354	О
541	Constraining the physical properties of the first lensed z $\sim$ 9 $\Box$ 16 galaxy candidates with JWST.	2
540	Photometric detection of internal gravity waves in upper main-sequence stars. <b>2022</b> , 668, A134	Ο

539	A dichotomy in group II Herbig disks. ALMA gas disk height measurements show both shadowed large vertically  extended disks and compact flat disks.	O
538	The Possible Tidal Demise of Kepler First Planetary System. <b>2022</b> , 941, L31	O
537	Measured spinBrbit alignment of ultra-short-period super-Earth 55 Cancri e.	O
536	The size $f$ has and other structural parameter (n, $g$ , Rz) relations for local bulges/spheroids from multicomponent decompositions.	O
535	First semi-empirical test of the white dwarf mass-radius relationship using a single white dwarf via astrometric microlensing.	O
534	Ultra-diffuse Galaxies as Extreme Star-forming Environments. I. Mapping Star Formation in H i-rich UDGs. <b>2022</b> , 941, 11	O
533	Characterization of Population III Stars with Stellar Atmosphere and Evolutionary Modeling and Predictions of their Observability with the JWST. <b>2023</b> , 165, 2	1
532	Evidence for the volatile-rich composition of a 1.5-Earth-radius planet.	O
531	Spectroscopic Mapping of Io® Surface with HST/STIS: SO2 Frost, Sulfur Allotropes, and Large-scale Compositional Patterns. <b>2022</b> , 3, 272	O
530	Meta-analysis of Photometric and Asteroseismic Measurements of Stellar Rotation Periods: The LombBcargle Periodogram, Autocorrelation Function, and Wavelet and Rotational Splitting Analysis for 92 Kepler Asteroseismic Targets. <b>2022</b> , 941, 175	O
529	AGN Selection and Demographics in GOODS-S/HUDF from X-Ray to Radio. 2022, 941, 191	1
528	Brighter and More Massive Galaxies in the Vicinity of LyENebulae. <b>2022</b> , 941, 180	O
527	Testing the Retrieval of Inner Disk Water Enrichment with Spitzer/IRS and JWST/MIRI. 2022, 941, 187	0
526	Overcoming Separation Between Counterparts Due to Unknown Proper Motions in Catalogue Cross-Matching.	O
525	Moving groups across Galactocentric radius with Gaia DR3. <b>2022</b> , 519, 432-444	1
524	Tidally locked rotation of the dwarf planet (136199) Eris discovered via long-term ground-based and space photometry.	O
523	Velocity-coherent substructure in TMC-1: inflow and fragmentation. <b>2022</b> , 519, 285-299	O
522	Spectroscopic Confirmation of a Population of Isolated, Intermediate-mass Young Stellar Objects. <b>2023</b> , 165, 3	O

521	An Atmospheric Retrieval of the Brown Dwarf Gliese 229B. <b>2022</b> , 940, 164	1
520	Occurrence Rate of Hot Jupiters Around Early-type M Dwarfs Based on Transiting Exoplanet Survey Satellite Data. <b>2023</b> , 165, 17	O
519	Can we constrain galaxy geometry parameters using spatially integrated SED fitting?.	Ο
518	Semi-analytic forecasts for Roman I the beginning of a new era of deep-wide galaxy surveys.	О
517	Constraining Sterile Neutrino Dark Matter in the Milky Way Halo with Swift-XRT. 2022, 941, 2	0
516	Occurrence rate of hot Jupiters orbiting red giant stars.	O
515	Searching for Converging Flows of Atomic Gas onto a Molecular Cloud. 2022, 941, 62	О
514	The Sensitivity of Eclipse Mapping to Planetary Rotation. <b>2023</b> , 165, 24	O
513	Optimising the shape of photometric redshift distributions with clustering cross-correlations.	0
512	CHANG-ES. XXVI. Insights into cosmic-ray transport from radio halos in edge-on galaxies.	O
511	Resolved Molecular Gas Observations of MaNGA Post-starbursts Reveal a Tumultuous Past. <b>2022</b> , 941, 93	1
510	·	0
	941, 93  Hard X-Ray Observations of the Hydrogen-poor Superluminous Supernova SN 2018hti with	
510	941, 93  Hard X-Ray Observations of the Hydrogen-poor Superluminous Supernova SN 2018hti with NuSTAR. 2022, 941, L16  An Ultra-deep Multiband Very Large Array (VLA) Survey of the Faint Radio Sky (COSMOS-XS): New	O
510	941, 93  Hard X-Ray Observations of the Hydrogen-poor Superluminous Supernova SN 2018hti with NuSTAR. 2022, 941, L16  An Ultra-deep Multiband Very Large Array (VLA) Survey of the Faint Radio Sky (COSMOS-XS): New Constraints on the Cosmic Star Formation History. 2022, 941, 10  TOI 560: Two Transiting Planets Orbiting a K Dwarf Validated with iSHELL, PFS, and HIRES RVs.	0
510 509 508	Hard X-Ray Observations of the Hydrogen-poor Superluminous Supernova SN 2018hti with NuSTAR. 2022, 941, L16  An Ultra-deep Multiband Very Large Array (VLA) Survey of the Faint Radio Sky (COSMOS-XS): New Constraints on the Cosmic Star Formation History. 2022, 941, 10  TOI 560: Two Transiting Planets Orbiting a K Dwarf Validated with iSHELL, PFS, and HIRES RVs. 2023, 165, 10	0 0
510 509 508 507	Hard X-Ray Observations of the Hydrogen-poor Superluminous Supernova SN 2018hti with NuSTAR. 2022, 941, L16  An Ultra-deep Multiband Very Large Array (VLA) Survey of the Faint Radio Sky (COSMOS-XS): New Constraints on the Cosmic Star Formation History. 2022, 941, 10  TOI 560: Two Transiting Planets Orbiting a K Dwarf Validated with iSHELL, PFS, and HIRES RVs. 2023, 165, 10  Powerful Yet Lonely: Is 3C 297 a High-redshift Fossil Group?. 2023, 264, 6  No Peaks without Valleys: The Stable Mass Transfer Channel for Gravitational-wave Sources in Light	o o o

503	CORINOS. I. JWST/MIRI Spectroscopy and Imaging of a Class 0 Protostar IRAS 15398 <b>B</b> 359. <b>2022</b> , 941, L13	О
502	FUMES. III. Ultraviolet and Optical Variability of M-dwarf Chromospheres. 2023, 165, 12	0
501	The Host Galaxies of Hybrid Morphology Radio Sources. <b>2022</b> , 941, 136	О
500	Herschel Optimized Tau and Temperature (HOTT) Maps: Uncertainty Analysis and Robust Parameter Extraction. <b>2022</b> , 941, 135	1
499	Hazy with a Chance of Star Spots: Constraining the Atmosphere of Young Planet K2-33b. <b>2023</b> , 165, 23	О
498	SPYGLASS. III. The FornaxHorologium Association and Its Traceback History within the Austral Complex. <b>2022</b> , 941, 143	1
497	Probabilistic mass-mapping with neural score estimation.	О
496	PACMAN: A pipeline to reduce and analyze Hubble Wide Field Camera 3 IR Grism data. <b>2022</b> , 7, 4838	O
495	Redshift Survey of 12 Moderate-redshift Clusters. <b>2022</b> , 6, 277	О
494	Towards the impact of GMC collisions on the star formation rate.	О
493	Detection of anisotropic satellite quenching in galaxy clusters up to z ~ 1. <b>2022</b> , 519, 13-25	1
492	Nature of the Galaxies On Top Of Quasars producing Mg îi absorption.	O
491	The Spectroscopic Classification of Astronomical Transients (SCAT) Survey: Overview, Pipeline Description, Initial Results, and Future Plans. <b>2022</b> , 134, 124502	1
490	On the ages of bright galaxies $\sim$ 500 Myr after the big bang: insights into star formation activity at z ? 15 with JWST. <b>2022</b> , 519, 157-171	3
489	RR Lyrae stars as probes of the outer Galactic halo: Chemical and kinematic analysis of a pilot sample.	O
488	BioNumPy: Fast and easy analysis of biological data with Python.	O
487	A comparative analysis of the chemical compositions of Gaia-Enceladus/Sausage and Milky Way satellites using APOGEE.	0
486	A close-in planet orbiting giant star HD´167768.	O

485	Classifying Unidentified X-Ray Sources in the Chandra Source Catalog Using a Multiwavelength Machine-learning Approach. <b>2022</b> , 941, 104	1
484	Understanding the role of morphology and environment in the dynamical evolution of isolated galaxy triplets.	O
483	Photometric Properties of Jupiter Trojans Detected by the Dark Energy Survey. <b>2022</b> , 3, 269	O
482	Time-variable Jet Ejections from RW Aur A, RY Tau, and DG Tau*. <b>2023</b> , 264, 1	O
481	ALMA Observations of the HD 110058 Debris Disk. <b>2022</b> , 940, 161	1
480	Metallicity Gradient of Barred Galaxies with TYPHOON.	O
479	A measurement of the distance to the Galactic centre using the kinematics of bar stars. <b>2022</b> , 519, 948-960	2
478	An Interpretable Machine-learning Framework for Modeling High-resolution Spectroscopic Data*. <b>2022</b> , 941, 200	1
477	Radio Transients and Variables in the Tenth Deeper, Wider, Faster Observing Run.	О
476	Kamodol model-agnostic satellite flythrough: Lowering the utilization barrier for heliophysics model outputs. 9,	O
475	LoTSS Jellyfish Galaxies. IV. Enhanced Star Formation on the Leading Half of Cluster Galaxies and Gas Compression in IC3949. <b>2022</b> , 941, 77	О
474	Grain Growth in the Dust Ring with a Crescent around the Very Low-mass Star ZZ Tau IRS with JVLA. <b>2022</b> , 941, 66	O
473	Planet engulfment signatures in twin stars. <b>2022</b> , 518, 5465-5474	1
472	Conditional H i Mass Functions and the H i-to-halo Mass Relation in the Local Universe. <b>2022</b> , 941, 48	O
471	ALMA Observations of CO Emission from Luminous Lyman-break Galaxies at $z = 6.0293$ B.2037. <b>2022</b> , 941, 74	О
47°	Interaction of a high-mass X-ray binary with the interstellar medium through stellar wind. The case of GX 301-2.	O
469	Colour gradients of low-redshift galaxies in the DESI Legacy Imaging Survey. <b>2022</b> , 518, 3999-4023	О
468	Satellite Constellation Avoidance with the Rubin Observatory Legacy Survey of Space and Time. <b>2022</b> , 941, L15	O

467	Constraints on Cosmological Parameters with a Sample of Type Ia Supernovae from JWST. <b>2022</b> , 941, 71	О
466	Prompt Emission and Early Optical Afterglow of Very-high-energy Detected GRB 201015A and GRB 201216C: Onset of the External Forward Shock. <b>2023</b> , 942, 34	O
465	Diverse Carbonates in Exoplanet Oceans Promote the Carbon Cycle. 2023, 942, L20	O
464	Astrometric Accelerations as Dynamical Beacons: Discovery and Characterization of HIP 21152 B, the First T-dwarf Companion in the Hyades*. <b>2023</b> , 165, 39	О
463	GOALS-JWST: Mid-infrared Spectroscopy of the Nucleus of NGC 7469. <b>2023</b> , 942, L37	1
462	TESS Giants Transiting Giants. III. An Eccentric Warm Jupiter Supports a Period <b>E</b> ccentricity Relation for Giant Planets Transiting Evolved Stars. <b>2023</b> , 165, 44	O
461	Star formation histories of UV-luminous galaxies at z ? 6.8: Implications for stellar mass assembly at early cosmic times.	1
460	Clustering dependence on Lyalpha luminosity from MUSE surveys at 3 <z<6.< td=""><td>О</td></z<6.<>	О
459	The PHANGSMUSE Nebular Catalogue.	O
458	TOI-1075 b: A Dense, Massive, Ultra-short-period Hot Super-Earth Straddling the Radius Gap. <b>2023</b> , 165, 47	O
457	Reflections on nebulae around young stars. A systematic search for late-stage infall of material onto Class II disks.	O
456	A deep radius valley revealed by Kepler short cadence observations. <b>2023</b> , 519, 4056-4073	1
455	Multi-probe analysis of the galaxy cluster CL J1226.9+3332. Hydrostatic mass and hydrostatic-to-lensing bias.	О
454	A Light in the Dark: Searching for Electromagnetic Counterparts to Black Hole <b>B</b> lack Hole Mergers in LIGO/Virgo O3 with the Zwicky Transient Facility. <b>2023</b> , 942, 99	O
453	The VLT/SPHERE view of the ATOMIUM cool evolved star sample. I. Overview: Sample characterization through polarization analysis.	О
452	Early Release Science of the Exoplanet WASP-39b with JWST NIRSpec G395H.	1
451	Early Release Science of the exoplanet WASP-39b with JWST NIRSpec PRISM.	1
450	UGC 4211: A Confirmed Dual Active Galactic Nucleus in the Local Universe at 230 pc Nuclear Separation. <b>2023</b> , 942, L24	1

449	Where are the missing symbiotic stars? Uncovering hidden Symbiotic Stars in public catalogues.	Ο
448	Cosmic-CoNN: A Cosmic-Ray Detection Deep-learning Framework, Data Set, and Toolkit. <b>2023</b> , 942, 73	Ο
447	On the Origin of the North Celestial Pole Loop. <b>2023</b> , 942, 70	0
446	The shocked molecular layer in RCW 120.	Ο
445	Multiwavelength scrutiny of X-ray sources in dwarf galaxies: ULXs versus AGN.	0
444	Ageing and quenching through the ageing diagram: predictions from simulations and observational constraints.	O
443	OzDES reverberation mapping program: H#ags from the 6-year survey.	O
442	The Roles of Morphology and Environment on the Star Formation RateBtellar Mass Relation in COSMOS from 0 < z < 3.5. <b>2023</b> , 942, 49	O
441	Light Curves of Trans-Neptunian Objects from the K2 Mission of the Kepler Space Telescope. <b>2023</b> , 264, 18	O
440	High-resolution X-ray spectra of RSOphiuchi (2006 and 2021): Revealing the cause of SSS variability.	O
439	The Target-selection Pipeline for the Dark Energy Spectroscopic Instrument. <b>2023</b> , 165, 50	1
438	A Low-mass, Pre-main-sequence Eclipsing Binary in the 40 Myr Columba Association Hundamental Stellar Parameters and Modeling the Effect of Star Spots. <b>2023</b> , 165, 46	O
437	Salt-bearing Disk Candidates around High-mass Young Stellar Objects. <b>2023</b> , 942, 66	O
436	Forecast of cosmological constraints with type Ia supernovae from the Chinese Space Station Telescope. <b>2023</b> , 66,	O
435	Impact of updated multipole Love numbers and f-Love universal relations in the context of binary neutron stars. <b>2023</b> , 107,	O
434	The Dark Energy Camera Plane Survey 2 (DECaPS2): More Sky, Less Bias, and Better Uncertainties. <b>2023</b> , 264, 28	1
433	A Candidate for the Least-massive Black Hole in the First 1.1 Billion Years of the Universe. <b>2023</b> , 942, L17	1
432	The Faraday Rotation Measure Grid of the LOFAR Two-metre Sky Survey: Data Release 2.	1

431	Detailed Chemical Abundances of Stars in the Outskirts of the Tucana II Ultrafaint Dwarf Galaxy*. <b>2023</b> , 165, 55	O
430	The Gaia view of the Cepheus OB2 association.	O
429	Optical/Pay blazar flare correlations: understanding the high-energy emission process using ASAS-SN and Fermi light curves.	O
428	Systems Approach to Polarization Calibration for the Daniel K. Inouye Solar Telescope (DKIST). <b>2023</b> , 298,	O
427	Precise physical conditions for the warm gas outflows in the nearby active galaxy IC 5063.	O
426	Rotational modulation in A and F stars: Magnetic stellar spots or convective core rotation?.	O
425	Twisted magnetic field in star formation processes of L1521 F revealed by submillimeter dual-band polarimetry using the James Clerk Maxwell Telescope.	O
424	A unique, ring-like radio source with quadrilateral structure detected with machine learning.	O
423	GRB´160410A: the first Chemical Study of the Interstellar Medium of a Short GRB.	О
422	PySME. Spectroscopy Made Easier.	O
421	Resolved near-UV hydrogen emission lines at 40-Myr super-Jovian protoplanet Delorme 1 (AB)b. <b>2023</b> , 669, L12	O
420	Constraints on the X-ray Luminosity Function of AGN at $z=5.7$ <b>b</b> .4 with the Extragalactic Serendipitous Swift Survey.	O
420 419		0
	Serendipitous Swift Survey.	
419	Serendipitous Swift Survey.  Modeling Strong Lenses from Wide-Field Ground-Based Observations in KiDS and GAMA.	0
419	Modeling Strong Lenses from Wide-Field Ground-Based Observations in KiDS and GAMA.  JWSTB PEARLS: A JWST/NIRCam View of ALMA Sources. 2023, 942, L19  Stellar Properties for a Comprehensive Collection of Star-forming Regions in the SDSS APOGEE-2	0
419 418 417	Modeling Strong Lenses from Wide-Field Ground-Based Observations in KiDS and GAMA.  JWSTB PEARLS: A JWST/NIRCam View of ALMA Sources. 2023, 942, L19  Stellar Properties for a Comprehensive Collection of Star-forming Regions in the SDSS APOGEE-2 Survey*. 2023, 165, 51	0 0

413	The origin of ultramassive White Dwarfs: Hints from Gaia EDR3.	0
412	Morpheus Reveals Distant Disk Galaxy Morphologies with JWST: The First AI/ML Analysis of JWST Images. <b>2023</b> , 942, L42	1
411	The value-added catalog of ASAS-SN eclipsing binaries II: Properties of extra-physics systems.	1
410	Digging into the Galactic Bulge: Stellar Population and Structure of the Poorly Studied Cluster NGC 6316. <b>2023</b> , 942, 104	O
409	Dependence of Chemical Abundance on the Cosmic-Ray Ionization Rate in IC 348. <b>2023</b> , 942, 101	O
408	Predictions on the stellar-to-halo mass relation in the dwarf regime using the empirical model for galaxy formation Emerge.	O
407	Kepler K2 and TESS Observations of Two Magnetic Cataclysmic Variables: The New Asynchronous Polar SDSS J084617.11+245344.1 and Paloma. <b>2023</b> , 165, 43	0
406	QUIJOTE scientific results IIX. Radio sources in the QUIJOTE-MFI wide survey maps. <b>2023</b> , 519, 3526-3545	2
405	Searches for Shapiro delay in seven binary pulsars using the MeerKAT telescope.	0
404	(Nearly) Model-independent Constraints on the Neutral Hydrogen Fraction in the Intergalactic Medium at $z \sim 5$ Using Dark Pixel Fractions in Ly $\oplus$ and Ly $\oplus$ Forests. <b>2023</b> , 942, 59	0
403	The State of the Molecular Gas in Post-starburst Galaxies. <b>2023</b> , 942, 25	0
402	Spatio-temporal comparisons of the hydrogen-alpha line width and ALMA 3 mm brightness temperature in the weak solar network. 9,	O
401	The Relationship between Age, Metallicity, and Abundances for Disk Stars in a Simulated Milky Way. <b>2023</b> , 942, 35	O
400	Constraining the Densities of the Three Kepler-289 Planets with Transit Timing Variations. <b>2023</b> , 165, 48	O
399	unTimely: a Full-sky, Time-domain unWISE Catalog. <b>2023</b> , 165, 36	0
398	The ASAS-SN catalogue of variable stars X: discovery of 116 000 new variable stars using G-band photometry. <b>2023</b> , 519, 5271-5287	2
397	Searching for New Supernova Remnant Candidates from the VTSS Survey. 2022, 43, 760-768	0
396	Implications of the Milky Way Travel Velocity for Dynamical Mass Estimates of the Local Group. <b>2023</b> , 942, 18	2

395	Interpreting ALMA non-detections of JWST super-early galaxies. 2022, 520, L16-L20	O
394	An Elusive Population of Massive Disk Galaxies Hosting Double-lobed Radio-loud Active Galactic Nuclei. <b>2022</b> , 941, 95	O
393	Extragalactic Magnetism with SOFIA (SALSA Legacy Program): The Magnetic Fields in the Multiphase Interstellar Medium of the Antennae Galaxies*. <b>2023</b> , 942, L13	0
392	Gas-rich, Field Ultra-diffuse Galaxies Host Few Gobular Clusters. <b>2023</b> , 942, L5	Ο
391	The SOFIA Massive (SOMA) Star Formation Survey. IV. Isolated Protostars. <b>2023</b> , 942, 7	0
390	A Localized Kinematic Structure Detected in Atomic Carbon Emission Spatially Coincident with a Proposed Protoplanet in the HD 163296 Disk. <b>2022</b> , 941, L24	Ο
389	Radio jetISM interaction and positive radio-mechanical feedback in Abell 1795. 2023, 519, 3338-3356	0
388	The Hand [O iii] <b>5</b> 007 Luminosity Functions of 1.2 < z < 1.9 Emission-line Galaxies from Hubble Space Telescope (HST) Grism Spectroscopy. <b>2023</b> , 943, 5	0
387	TESS©aia Light Curve: A PSF-based TESS FFI Light-curve Product. <b>2023</b> , 165, 71	0
386	A Green Bank Telescope Search for Narrowband Technosignatures between 1.1 and 1.9 GHz During 12 Kepler Planetary Transits. <b>2023</b> , 165, 61	O
385	Kepler-102: Masses and Compositions for a Super-Earth and Sub-Neptune Orbiting an Active Star. <b>2023</b> , 165, 74	0
384	Resolved SPLASH Chemodynamics in Andromedal PHAT Stellar Halo and Disk: On the Nature of the Inner Halo along the Major Axis. <b>2023</b> , 165, 75	O
383	A Systematic Search for Short-period Close White Dwarf Binary Candidates Based on Gaia EDR3 Catalog and Zwicky Transient Facility Data. <b>2023</b> , 264, 39	0
382	PyAutoGalaxy: Open-Source Multiwavelength Galaxy Structure & amp; Morphology. <b>2023</b> , 8, 4475	2
381	The McDonald Accelerating Stars Survey: Architecture of the Ancient Five-planet Host System Kepler-444. <b>2023</b> , 165, 73	0
380	Inner Habitable Zone Boundary for Eccentric Exoplanets. <b>2023</b> , 943, L1	0
379	A Standard Siren Measurement of the Hubble Constant Using Gravitational-wave Events from the First Three LIGO/Virgo Observing Runs and the DESI Legacy Survey. <b>2023</b> , 943, 56	0
378	Pixel-to-pixel Translation of Solar Extreme-ultraviolet Images for DEMs by Fully Connected Networks. <b>2023</b> , 264, 33	Ο

377	Revealing the milky way! most recent major merger with a Gaia EDR3 catalog of machine-learned line-of-sight velocities.	0
376	An increase in black hole activity in galaxies with kinematically misaligned gas.	O
375	Hot Subdwarf Stars Identified in LAMOST DR8 with Single-lined and Composite Spectra. 2023, 942, 109	О
374	Ghost in the Shell: Evidence for Past Active Galactic Nucleus Activities in NGC 5195 from a Newly Discovered Large-scale Ionized Structure. <b>2023</b> , 943, 28	1
373	VISIONS: The VISTA Star Formation Atlas. I. Survey overview.	0
372	JWST NIRCam Defocused Imaging: Photometric Stability Performance and How It Can Sense Mirror Tilts. <b>2023</b> , 135, 018001	Ο
371	Molecular clouds at the eastern edge of radio nebula W´50.	О
370	A Naive Bayes Classifier for identifying Class II YSOs.	Ο
369	The Contribution of Evolved Stars to Polycyclic Aromatic Hydrocarbon Heating and Implications for Estimating Star Formation Rates. <b>2023</b> , 943, 60	0
368	Nonequilibrium Ionization Modeling of Petschek-type Shocks in Reconnecting Current Sheets in Solar Eruptions. <b>2023</b> , 943, 111	O
367	The star-formation history in the last 10 billion years from CIB cross-correlations. <b>2023</b> , 520, 1895-1912	O
366	Modelling populations of kilonovae.	O
365	Estimating Molecular Gas Content in Galaxies from Polycyclic Aromatic Hydrocarbon Emission. <b>2023</b> , 943, 1	О
364	The Ionizing Spectra of Extremely Metal-poor O Stars: Constraints from the Only H ii Region in Leo P. <b>2023</b> , 943, 65	O
363	The Pan-STARRS1 z > 5.6 Quasar Survey. III. The z ြ Quasar Luminosity Function. <b>2023</b> , 943, 67	О
362	Speckle SpaceII ime Covariance in High-contrast Imaging. <b>2023</b> , 165, 59	Ο
361	An $\sim$ 600 pc View of the Strongly Lensed, Massive Main-sequence Galaxy J0901: A Baryon-dominated, Thick Turbulent Rotating Disk with a Clumpy Cold Gas Ring at z = 2.259. <b>2023</b> , 942, 98	O
<b>3</b> 60	CARMA-NRO Orion Survey: Unbiased Survey of Dense Cores and Core Mass Functions in Orion A. <b>2023</b> , 264, 35	O

359	A Highly Magnified Gravitationally Lensed Red QSO at $z=2.5$ with a Significant Flux Ratio Anomaly. <b>2023</b> , 943, 25	0
358	Constraining the physics of star formation from CIB-cosmic shear cross-correlations. <b>2023</b> , 520, 583-598	O
357	Catching a Milky Way open cluster in its last breath. 2023, 519, 6239-6245	O
356	The SOUX AGN Sample: SDSSIMM-Newton Optical, Ultraviolet and X-ray selected active galactic nuclei spanning a wide range of parameter space (Sample definition.	O
355	Molecular Mapping of DR Tau® Protoplanetary Disk, Envelope, Outflow, and Large-scale Spiral Arm. <b>2023</b> , 943, 107	Ο
354	Transit timing variation analysis of the low-mass brown dwarf KELT-1 b.	O
353	CLEAR: Spatially Resolved Emission Lines and Active Galactic Nuclei at 0.6 < z < 1.3. <b>2023</b> , 943, 37	O
352	Investigating the Narrow-line Region Dynamics in Nearby Active Galaxies. 2023, 943, 98	O
351	The complex multiscale structure in simulated and observed emission maps of the proto-cluster cloud G0.253+0.016 (The Brick) 2023, 520, 2245-2268	O
350	Photometric and Structural Parameters of Newly Discovered Nuclear Star Clusters in Local Volume Galaxies.	O
349	Simulated performance of the molecular mapping for young giant exoplanets with the Medium-Resolution Spectrometer of JWST/MIRI.	Ο
348	Multiwavelength Analysis of a Nearby Heavily Obscured AGN in NGC 449. <b>2023</b> , 135, 014102	O
347	Distance determination of molecular clouds in the first quadrant of the Galactic plane using deep learning: I. Method and results. <b>2023</b> , 75, 279-295	O
346	PHANGS-MUSE: Detection and Bayesian classification of ~40000 ionised nebulae in nearby spiral galaxies.	O
345	When Spectral Modeling Meets Convolutional Networks: A Method for Discovering Reionization-era Lensed Quasars in Multiband Imaging Data. <b>2023</b> , 943, 150	Ο
344	A Comparison of the Baryonic Tully-Fisher Relation in MaNGA and IllustrisTNG.	O
343	POSYDON: A General-purpose Population Synthesis Code with Detailed Binary-evolution Simulations. <b>2023</b> , 264, 45	1
342	The Influence of the Galactic Bar on the Dynamics of Globular Clusters. 2023, 11, 26	Ο

341	Identifying Habitable-zone Planet Systems Susceptible to Nearby Supernovae. 2023, 7, 21	O
340	Discovery of the luminous X-ray ignition eRASSt J234402.9-352640. I. Tidal disruption event or a rapid increase in accretion in an  active galactic nucleus?.	O
339	Probing the Stellar Wind of the WolfRayet Star in IC 10 X-1. <b>2023</b> , 944, 52	O
338	Using Neural Networks to Differentiate Newly Discovered BL Lacertae Objects and FSRQs among the 4FGL Unassociated Sources Employing Gamma-Ray, X-Ray, UV/Optical, and IR Data. <b>2023</b> , 943, 167	O
337	Correcting bandwidth depolarization by extreme Faraday rotation. 2023, 520, 4822-4835	O
336	Temporal spectrum of spatial correlations between GNSS station position time series. 2023, 97,	O
335	An optimal envelope ejection efficiency for merging neutron stars.	0
334	Comet-like Activity Discovered on Quasi-Hilda Asteroid 2009 DQ118. <b>2023</b> , 7, 42	O
333	Star Formation Laws and Efficiencies across 80 Nearby Galaxies. <b>2023</b> , 945, L19	0
332	Temporal variation of the photometric magnetic activity for the Sun and Kepler solar-like stars. <b>2023</b> , 672, A56	O
331	The Evryscope Fast Transient Engine: Real-time Detection for Rapidly Evolving Transients. <b>2023</b> , 265, 63	0
330	ALMA ACA study of the H2S/OCS ratio in low-mass protostars. <b>2023</b> , 672, A122	O
329	Searching for Compact Object Candidates from LAMOST Time-domain Survey of Four K2 Plates. <b>2023</b> , 165, 187	0
328	Zwicky Transient Facility and Globular Clusters: The PeriodIluminosity and PeriodIWesenheit Relations for SX Phoenicis Variables in the gri Band. <b>2023</b> , 165, 190	O
327	Stellar Escape from Globular Clusters. I. Escape Mechanisms and Properties at Ejection. 2023, 946, 104	0
326	Tracking the Enigmatic Globular Cluster Ultracompact X-Ray Binary X1850\(\mathbb{D}\)87: Extreme Radio Variability in the Hard State. <b>2023</b> , 946, 88	O
325	TEMGYM Advanced [NanoMi lens characterisation. <b>2023</b> , 169, 103450	0
324	Characterising SMSS J2157B602, the most luminous known quasar, with accretion disc models. <b>2023</b> , 521, 3682-3698	O

323	ExoPSI: A Planet Similarity Python toolkit.	О
322	[C ii] Haloes in ALPINE galaxies: smoking-gun of galactic outflows?. <b>2023</b> , 519, 4608-4621	Ο
321	Massive galaxy formation caught in action at $z \sim 5$ with JWST. <b>2023</b> , 670, L11	0
320	DeepZipper. II. Searching for Lensed Supernovae in Dark Energy Survey Data with Deep Learning. <b>2023</b> , 943, 19	O
319	Mini-moons from horseshoes: A physical characterization of 2022 NX1 with OSIRIS at the 10.4 m Gran Telescopio Canarias. <b>2023</b> , 670, L10	О
318	Measuring the variability of directly imaged exoplanets using vector Apodizing Phase Plates combined with ground-based differential spectrophotometry. <b>2023</b> , 520, 4235-4257	O
317	Rethinking data-driven point spread function modeling with a differentiable optical model. <b>2023</b> , 39, 035008	О
316	Neutron star mass estimates from gamma-ray eclipses in spider millisecond pulsar binaries. <b>2023</b> , 7, 451-462	O
315	Models of Rotating Infall for the B335 Protostar. <b>2023</b> , 943, 90	0
314	Revealing the Progenitor of SN 2021zby through Analysis of the TESS Shock-cooling Light Curve. <b>2023</b> , 943, L15	O
313	Polarized Maser Emission with In-source Faraday Rotation. <b>2023</b> , 943, 123	0
312	Introducing the Condor Array Telescope. I. Motivation, Configuration, and Performance. <b>2023</b> , 135, 015002	0
311	Study of Radio Transients from the Quiet Sun during an Extremely Quiet Time. 2023, 943, 122	0
310	The AstroSat UV Deep Field North: The Far- and Near-ultraviolet Photometric Catalog. <b>2023</b> , 264, 40	O
309	The deconvolved distribution estimator: enhancing reionization-era CO line-intensity mapping analyses with a cross-correlation analogue for one-point statistics. <b>2023</b> , 520, 5305-5316	0
308	A puffy polar planet. <b>2023</b> , 671, A164	O
307	Discovery of a red backsplash galaxy candidate near M81. <b>2023</b> , 520, 4715-4729	0
306	Dusty-wind-clear JWST Super-early Galaxies. <b>2023</b> , 943, L27	1

305	Non-thermal broadening of IRIS Fe XXI line caused by turbulent plasma flows in the magnetic reconnection region during solar eruptions. 10,	0
304	MusE GAs FLOw and Wind (MEGAFLOW) IX. The impact of gas flows on the relations between the mass, star formation rate, and metallicity of galaxies. <b>2023</b> , 521, 546-557	O
303	M dwarf stars in the b294 field from the VISTA Variables in the VI Liltea (VVV). <b>2023</b> , 520, 4730-4739	О
302	Tidally perturbed gravity-mode pulsations in a sample of close eclipsing binaries. 2023, 671, A121	O
301	Hubble Space Telescope Transmission Spectroscopy for the Temperate Sub-Neptune TOI-270 d: A Possible Hydrogen-rich Atmosphere Containing Water Vapor. <b>2023</b> , 165, 84	0
300	Precision Ephemerides for Gravitational-wave Searches IIV. Corrected and refined ephemeris for Scorpius X-1. <b>2023</b> , 520, 5317-5330	O
299	TESS Hunt for Young and Maturing Exoplanets (THYME). IX. A 27 Myr Extended Population of Lower Centaurus Crux with a Transiting Two-planet System. <b>2023</b> , 165, 85	О
298	ALMA Resolves the First Strongly Lensed Optical/Near-IR-dark Galaxy. <b>2023</b> , 943, 151	O
297	Size and Spectroscopic Evolution of HectoMAP Quiescent Galaxies. 2023, 943, 149	0
296	EAGLE-like simulation models do not solve the entropy core problem in groups and clusters of galaxies. <b>2023</b> , 520, 3164-3186	O
295	On the Cosmic Evolution of AGN Obscuration and the X-Ray Luminosity Function: XMM-Newton and Chandra Spectral Analysis of the 31.3 deg2 Stripe 82X. <b>2023</b> , 943, 162	0
294	Modelling the accretion and feedback of supermassive black hole binaries in gas-rich galaxy mergers. <b>2023</b> , 520, 4463-4489	O
293	HOLISMOKES. <b>2023</b> , 671, A147	0
292	Gamma-Ray Emission from Galaxies Hosting Molecular Outflows. <b>2023</b> , 943, 168	O
291	Cutoff of transverse waves through the solar transition region. <b>2023</b> , 672, A105	0
<b>2</b> 90	TOI-561 b: A Low-density Ultra-short-period <b>R</b> ockylPlanet around a Metal-poor Star. <b>2023</b> , 165, 88	O
289	A New Physical Picture for Active Galactic Nuclei Lacking Optical Emission Lines. 2023, 943, 174	О
288	Understanding and predicting cadence effects in the characterization of exoplanet transits. <b>2023</b> , 520, 4103-4117	O

287	Dynamically constraining the length of the Milky way bar. <b>2023</b> , 520, 4779-4792	1
286	A 0.9% calibration of the Galactic Cepheid luminosity scale based on Gaia DR3 data of open clusters and Cepheids. <b>2023</b> , 672, A85	О
285	Constraints on Stellar Flare Energy Ratios in the NUV and Optical from a Multiwavelength Study of GALEX and Kepler Flare Stars. <b>2023</b> , 944, 5	o
284	The Planck clusters in the LOFAR sky. <b>2023</b> , 672, A41	O
283	Probing the Earliest Phases in the Formation of Massive Galaxies with Simulated HST+JWST Imaging Data from Illustris. <b>2023</b> , 944, 3	0
282	First on-sky demonstration of a scintillation correction technique using tomographic wavefront sensing. <b>2023</b> , 520, 4134-4146	О
281	Breaking bad degeneracies with Love relations: Improving gravitational-wave measurements through universal relations. <b>2023</b> , 107,	О
280	Universal gravity-driven isothermal turbulence cascade in disk galaxies. <b>2023</b> , 672, A193	O
279	TESS Discovery of Twin Planets near 2:1 Resonance around Early M Dwarf TOI 4342. <b>2023</b> , 165, 93	0
278	The SPIRou legacy survey. <b>2023</b> , 672, A52	O
277	White Dwarfs with Infrared Excess from LAMOST Data Release 5. <b>2023</b> , 944, 23	0
277 276	White Dwarfs with Infrared Excess from LAMOST Data Release 5. <b>2023</b> , 944, 23  Far-ultraviolet Dust Extinction and Molecular Hydrogen in the Diffuse Milky Way Interstellar Medium. <b>2023</b> , 944, 33	0
	Far-ultraviolet Dust Extinction and Molecular Hydrogen in the Diffuse Milky Way Interstellar	
276	Far-ultraviolet Dust Extinction and Molecular Hydrogen in the Diffuse Milky Way Interstellar Medium. <b>2023</b> , 944, 33	O
276 275	Far-ultraviolet Dust Extinction and Molecular Hydrogen in the Diffuse Milky Way Interstellar Medium. 2023, 944, 33  Enhanced Star Formation Efficiency in the Central Regions of Nearby Quasar Hosts. 2023, 944, 30  Identifying Exoplanets with Deep Learning. V. Improved Light-curve Classification for TESS	0
276 275 274	Far-ultraviolet Dust Extinction and Molecular Hydrogen in the Diffuse Milky Way Interstellar Medium. 2023, 944, 33  Enhanced Star Formation Efficiency in the Central Regions of Nearby Quasar Hosts. 2023, 944, 30  Identifying Exoplanets with Deep Learning. V. Improved Light-curve Classification for TESS Full-frame Image Observations. 2023, 165, 95  DESI Observations of the Andromeda Galaxy: Revealing the Immigration History of Our Nearest	0 0
276 275 274 273	Far-ultraviolet Dust Extinction and Molecular Hydrogen in the Diffuse Milky Way Interstellar Medium. 2023, 944, 33  Enhanced Star Formation Efficiency in the Central Regions of Nearby Quasar Hosts. 2023, 944, 30  Identifying Exoplanets with Deep Learning. V. Improved Light-curve Classification for TESS Full-frame Image Observations. 2023, 165, 95  DESI Observations of the Andromeda Galaxy: Revealing the Immigration History of Our Nearest Neighbor. 2023, 944, 1	0 0 1

269	Do Central Compact Objects have Carbon Atmospheres?. <b>2023</b> , 944, 36	O
268	TOI-836: A super-Earth and mini-Neptune transiting a nearby K-dwarf. <b>2023</b> , 520, 3649-3668	O
267	The e-TidalGCs project. Modeling the extra-tidal features generated by Galactic globular clusters.	0
266	The redshift evolution of the S0 fraction forz< 1 in COSMOS. 2023, 520, 5885-5902	O
265	The hot Neptune WASP-166 b with ESPRESSO IIII. A blue-shifted tentative water signal constrains the presence of clouds. <b>2023</b> , 521, 1233-1252	О
264	DSPS: Differentiable stellar population synthesis. <b>2023</b> , 521, 1741-1756	O
263	Constraints on S8 from a full-scale and full-shape analysis of redshift-space clustering and galaxygalaxy lensing in BOSS. <b>2023</b> , 520, 5373-5393	О
262	Efficient computation of the super-sample covariance for stage IV galaxy surveys. 2023, 671, A115	O
261	Catalog of Magnetic White Dwarfs with Hydrogen Dominated Atmospheres. 2023, 944, 56	O
260	The Hubble Space Telescope UV Legacy Survey of Galactic Globular Clusters. XXIV. Differences in Internal Kinematics of Multiple Stellar Populations. <b>2023</b> , 944, 58	1
259	Metal Mixing in the r-process Enhanced Ultrafaint Dwarf Galaxy Reticulum II*. 2023, 165, 100	0
258	Scattered polarized radiation of extrasolar circumplanetary rings. 2023, 671, A113	O
257	ExoClock Project. III. 450 New Exoplanet Ephemerides from Ground and Space Observations. <b>2023</b> , 265, 4	0
256	Galaxy Populations in Groups and Clusters: Evidence for a Characteristic Stellar Mass Scale at M * $\sim$ 109.5 M ?. <b>2023</b> , 944, 75	O
255	The TESS Grand Unified Hot Jupiter Survey. II. Twenty New Giant Planets*. 2023, 265, 1	О
254	A Lack of Variability between Repeated Spitzer Phase Curves of WASP-43b. <b>2023</b> , 165, 107	O
253	Discovery of Dust Emission Activity Emanating from Main-belt Asteroid 2015 FW412. <b>2023</b> , 7, 22	O
252	On the Spatial Distribution of 13CO Structures within 12CO Molecular Clouds. <b>2023</b> , 944, 91	O

251	Comparing the Locations of Supernovae to CO (211) Emission in Their Host Galaxies. 2023, 944, 110	O
250	Gaussian Process Modeling Blazar Multiwavelength Variability: Indirectly Resolving Jet Structure. <b>2023</b> , 944, 103	0
249	FEASTS: IGM Cooling Triggered by Tidal Interactions through the Diffuse H i Phase around NGC 4631. <b>2023</b> , 944, 102	О
248	Serendipitous Nebular-phase JWST Imaging of SN Ia SN 2021aefx: Testing the Confinement of 56Co Decay Energy. <b>2023</b> , 944, L28	О
247	A New Study on a Type Iax Stellar Remnant and its Probable Association with SN 1181. <b>2023</b> , 944, 120	О
246	The Solar System Notification Alert Processing System (SNAPS): Design, Architecture, and First Data Release (SNAPShot1). <b>2023</b> , 165, 111	Ο
245	PHANGSIIWST First Results: A Global and Moderately Resolved View of Mid-infrared and CO Line Emission from Galaxies at the Start of the JWST Era. <b>2023</b> , 944, L10	О
244	PHANGSIJWST First Results: Multiwavelength View of Feedback-driven Bubbles (the Phantom Voids) across NGC 628. <b>2023</b> , 944, L22	Ο
243	PHANGSIWST First Results: Mid-infrared Emission Traces Both Gas Column Density and Heating at 100 pc Scales. <b>2023</b> , 944, L9	О
242	PHANGSIIWST First Results: A Statistical View on Bubble Evolution in NGC 628. <b>2023</b> , 944, L24	О
241	PHANGSIIWST First Results: Duration of the Early Phase of Massive Star Formation in NGC 628. <b>2023</b> , 944, L20	0
240	Revising the properties of low mass eclipsing binary stars using TESS light curves. <b>2023</b> , 521, 3405-3420	Ο
239	PHANGSIIWST First Results: A Combined HST and JWST Analysis of the Nuclear Star Cluster in NGC 628. <b>2023</b> , 944, L25	0
238	PHANGSIJWST First Results: Dust-embedded Star Clusters in NGC 7496 Selected via 3.3 th PAH Emission. <b>2023</b> , 944, L26	O
237	The Bimodal Absorption System Imaging Campaign (BASIC). I. A Dual Population of Low-metallicity Absorbers at z < 1. <b>2023</b> , 944, 101	1
236	PHANGSIIWST First Results: The 21 th Compact Source Population. <b>2023</b> , 944, L21	O
235	PHANGSIJWST First Results: Stellar-feedback-driven Excitation and Dissociation of Molecular Gas in the Starburst Ring of NGC 1365?. <b>2023</b> , 944, L19	О
234	RC100: Rotation Curves of 100 Massive Star-forming Galaxies at $z = 0.6 \ 2.5$ Reveal Little Dark Matter on Galactic Scales. <b>2023</b> , 944, 78	O

233	PHANGSIIWST First Results: Rapid Evolution of Star Formation in the Central Molecular Gas Ring of NGC 1365. <b>2023</b> , 944, L15	О
232	A Census of the Low Accretors. II. Accretion Properties. <b>2023</b> , 944, 90	Ο
231	PHANGSIIWST First Results: The Dust Filament Network of NGC 628 and Its Relation to Star Formation Activity. <b>2023</b> , 944, L13	О
230	TDCOSMO. <b>2023</b> , 672, A20	O
229	PHANGSIIWST First Results: Destruction of the PAH Molecules in H ii Regions Probed by JWST and MUSE. <b>2023</b> , 944, L16	О
228	PHANGSIWST First Results: Tracing the Diffuse Interstellar Medium with JWST Imaging of Polycyclic Aromatic Hydrocarbon Emission in Nearby Galaxies. <b>2023</b> , 944, L8	O
227	Singular spectrum analysis of time series data from low-frequency radiometers, with an application to SITARA data. <b>2023</b> , 520, 6040-6052	О
226	New Active Asteroid 2015 VA108: A Citizen Science Discovery. <b>2023</b> , 7, 27	О
225	INSPIRE: INvestigating Stellar Population In RElics 🛭 V. The initial mass function slope in relics. <b>2023</b> , 521, 1408-1414	О
224	A Disk Wind Driving the Rotating Molecular Outflow in CB 26. <b>2023</b> , 944, 63	O
223	Detecting Exomoons from Radial Velocity Measurements of Self-luminous Planets: Application to Observations of HR 7672 B and Future Prospects. <b>2023</b> , 165, 113	О
222	Data-driven Cosmology from Three-dimensional Light Cones. <b>2023</b> , 944, 151	O
221	The Art of Measuring Physical Parameters in Galaxies: A Critical Assessment of Spectral Energy Distribution Fitting Techniques. <b>2023</b> , 944, 141	1
220	Milliarcsecond structures of variable-peaked spectrum sources. 2023, 40,	O
219	TOI-5205b: A Short-period Jovian Planet Transiting a Mid-M Dwarf. <b>2023</b> , 165, 120	0
218	WIYN Open Cluster Study. LXXXVII. Hubble Space Telescope Ultraviolet Detection of Hot White Dwarf Companions to Blue Lurkers in M67. <b>2023</b> , 944, 145	O
217	NEID Reveals That the Young Warm Neptune TOI-2076 b Has a Low Obliquity. 2023, 944, L41	О
216	A Swing of the Pendulum: The Chemodynamics of the Local Stellar Halo Indicate Contributions from Several Radial Merger Events. <b>2023</b> , 944, 169	0

215	Precise Empirical Determination of Metallicity Dependence of Near-infrared PeriodIluminosity Relations for RR Lyrae Variables. <b>2023</b> , 944, L51	О
214	JCMT BISTRO Observations: Magnetic Field Morphology of Bubbles Associated with NGC 6334. <b>2023</b> , 944, 139	О
213	Identification of Galaxy Shreds in Large Photometric Catalogs Using Convolutional Neural Networks. <b>2023</b> , 165, 123	0
212	Delayed Development of Cool Plasmas in X-Ray Flares from the Young Sun-like Star 🗓 Ceti. <b>2023</b> , 944, 163	О
211	GALFIT-ing AGN Host Galaxies in COSMOS: HST versus Subaru. <b>2023</b> , 944, 137	О
210	TOI-4562b: A Highly Eccentric Temperate Jupiter Analog Orbiting a Young Field Star. <b>2023</b> , 165, 121	O
209	Study of Variability in Long-term Multiwavelength Optical Lightcurves of Blazar AO 0235+164. <b>2023</b> , 265, 14	О
208	Interactions between the Jet and Disk Wind in Nearby Radio-intermediate Quasar III Zw 2. <b>2023</b> , 944, 187	O
207	A nearly constant CN/HCN line ratio in nearby galaxies: CN as a new tracer of dense gas. 2023, 521, 717-736	О
206	The Similar Seven: A Set of Very Alike Exoplanets to Test Correlations between System Parameters and Atmospheric Properties. <b>2023</b> , 944, L56	О
205	LyBcattering Models Trace Accretion and Outflow Kinematics in T Tauri Systems*. 2023, 944, 185	О
204	Tidal Disruption Events from Eccentric Orbits and Lessons Learned from the Noteworthy ASASSN-14ko. <b>2023</b> , 944, 184	О
203	NICMOS Kernel-phase Interferometry. II. Demographics of Nearby Brown Dwarfs. <b>2023</b> , 165, 130	О
202	Measuring the Obliquities of the TRAPPIST-1 Planets with MAROON-X. <b>2023</b> , 165, 129	O
201	Inferring More from Less: Prospector as a Photometric Redshift Engine in the Era of JWST. <b>2023</b> , 944, L58	О
200	ALMA confirmation of an obscured hyperluminous radio-loud AGN at $z = 6.853$ associated with a dusty starburst in the 1.5 deg2 COSMOS field. <b>2023</b> , 520, 4609-4620	О
199	Kpc-scale properties of dust temperature in terms of dust mass and star formation activity. <b>2023</b> , 520, 5506-5520	0
198	SN 2020uem: a Possible Thermonuclear Explosion within a Dense Circumstellar Medium (II). The Properties of the CSM from Polarimetry and Light-curve Modeling. <b>2023</b> , 944, 204	1

197	Cyanopolyyne Chemistry in the L1544 Prestellar Core: New Insights from GBT Observations. <b>2023</b> , 944, 208	0
196	SN 2020uem: a Possible Thermonuclear Explosion within a Dense Circumstellar Medium. I. The Nature of Type IIn/Ia-CSM SNe from Photometry and Spectroscopy. <b>2023</b> , 944, 203	O
195	Multiple Shock Fronts in RBS 797: The Chandra Window on Shock Heating in Galaxy Clusters. <b>2023</b> , 944, 216	O
194	Long-term Quasiperiodicity in LMXB 4U 1636B36. <b>2023</b> , 944, 214	О
193	X3: A High-mass Young Stellar Object Close to the Supermassive Black Hole Sgr A*. <b>2023</b> , 944, 231	О
192	Probing Velocity Structures of Protostellar Envelopes: Infalling and Rotating Envelopes within Turbulent Dense Cores. <b>2023</b> , 944, 222	О
191	A Broad-line Quasar with Unexplained Extreme Velocity Offsets: Post-shock Outflow?. 2023, 944, 217	О
190	UOCS-IX. AstroSat/UVIT Study of the Open Cluster NGC 2818: Blue Stragglers, Yellow Stragglers, Planetary Nebula, and their Membership. <b>2023</b> , 945, 11	0
189	HESS J1809🛮 93: A halo of escaped electrons around a pulsar wind nebula?. <b>2023</b> , 672, A103	0
188	CO Excitation in High-z Main-sequence Analogues: Resolved CO(4B)/CO(3D) Line Ratios in DYNAMO Galaxies. <b>2023</b> , 945, 9	o
187	Detecting Long-period Variability in the SDSS Stripe 82 Standards Catalog. 2023, 165, 138	O
186	A kinematic calibration of the O-rich Mira variable period ge relation from Gaia. 2023, 521, 1462-1478	o
185	WALLABY Pilot Survey: hydra cluster galaxies UV and H imorphometrics. 2023, 521, 1502-1517	0
184	COSMOS2020: Discovery of a Protocluster of Massive Quiescent Galaxies at $z = 2.77$ . <b>2023</b> , 945, L9	O
183	A Distance Measurement to M33 Using Optical Photometry of Mira Variables. <b>2023</b> , 165, 137	О
182	CLASS Survey Description: Coronal-line Needles in the SDSS Haystack. <b>2023</b> , 265, 21	O
181	First Look at z > 1 Bars in the Rest-frame Near-infrared with JWST Early CEERS Imaging. <b>2023</b> , 945, L10	O
180	Localizing Sources of Variability in Crowded TESS Photometry. <b>2023</b> , 165, 141	О

179	Near-infrared and Optical Nebular-phase Spectra of Type Ia Supernovae SN 2013aa and SN 2017cbv in NGC 5643. <b>2023</b> , 945, 27	О
178	The Local Cluster Survey II: disc-dominated cluster galaxies with suppressed star formation. <b>2023</b> , 521, 4614-4629	О
177	A Study of the Pulsation Properties of 57 Non-Blazhko Ab-type RR Lyrae Stars with Homogeneous Metallicities from the LAMOST <b>K</b> epler/K2 Survey. <b>2023</b> , 945, 18	0
176	The Mid-infrared Molecular Inventory toward Orion IRc2. <b>2023</b> , 945, 26	О
175	Hunting for C-rich long-period variable stars in the Milky Way® bar-bulge using unsupervised classification of GaiaBP/RP spectra. <b>2023</b> , 521, 2745-2764	O
174	LOTUS: A (Non-) LTE Optimization Tool for Uniform Derivation of Stellar Atmospheric Parameters. <b>2023</b> , 165, 145	О
173	Solar-MACH: An open-source tool to analyze solar magnetic connection configurations. 9,	О
172	Inferencing Progenitor and Explosion Properties of Evolving Core-collapse Supernovae from Zwicky Transient Facility Light Curves. <b>2023</b> , 945, 46	О
171	VERITAS and Fermi-LAT Constraints on the Gamma-Ray Emission from Superluminous Supernovae SN2015bn and SN2017egm. <b>2023</b> , 945, 30	0
170	A Measurement of the Cosmic Optical Background and Diffuse Galactic Light Scaling from the R < 50 au New Horizons-LORRI Data. <b>2023</b> , 945, 45	o
169	gyre_tides: Modeling Binary Tides within the GYRE Stellar Oscillation Code. 2023, 945, 43	0
168	Does the HCN/CO Ratio Trace the Star-forming Fraction of Gas? I. A Comparison with Analytical Models of Star Formation. <b>2023</b> , 945, 42	o
167	Flares, Rotation, Activity Cycles, and a Magnetic StarPlanet Interaction Hypothesis for the Far-ultraviolet Emission of GJ 436. <b>2023</b> , 165, 146	0
166	Examining the decline in the C iv content of the Universe over $4.3?z?6.3$ using the E-XQR-30 sample. <b>2023</b> , 521, 314-331	1
165	RR Lyrae Mid-infrared Period[luminosity[Metallicity and Period[Wesenheit[Metallicity Relations Based on Gaia DR3 Parallaxes. <b>2023</b> , 945, 83	O
164	The Pan-STARRS1 z > 5.6 Quasar Survey. II. Discovery of 55 Quasars at 5.6 < z < 6.5. <b>2023</b> , 265, 29	o
163	Beyond the bulgefialo conspiracy? Density profiles of early-type galaxies from extended-source strong lensing. <b>2023</b> , 521, 6005-6018	0
162	An APEX Study of Molecular Outflows in FUor-type Stars. <b>2023</b> , 945, 80	О

161	BICEP/Keck. XVI. Characterizing Dust Polarization through Correlations with Neutral Hydrogen. <b>2023</b> , 945, 72	О
160	Simulations for Planning Next-generation Exoplanet Radial Velocity Surveys. 2023, 165, 151	1
159	New insights into the rotational evolution of near-solar age stars from the open cluster M 67. <b>2023</b> , 672, A159	O
158	X-ray Time Lag Evaluation of MAXI J1820+070 with a Differential Cross-correlation Analysis. <b>2023</b> , 945, 92	O
157	A candidate magnetic helium-core white dwarf in the globular cluster NGC 6397. <b>2023</b> , 521, 5026-5032	O
156	Sidestepping the inversion of the weak-lensing covariance matrix with Approximate Bayesian Computation. <b>2023</b> , 43, 100705	O
155	HectoMAP: The Complete Redshift Survey (Data Release 2). <b>2023</b> , 945, 94	O
154	A Measurement of Circumgalactic Gas around Nearby Galaxies Using Fast Radio Bursts. <b>2023</b> , 945, 87	О
153	DAHe white dwarfs from the DESI Survey. <b>2023</b> , 521, 4976-4994	1
152	The Differential Assembly History of the Centers and Outskirts of Main-sequence Galaxies at z $\sim$ 2.3. <b>2023</b> , 945, 97	O
151	Robust clustering of the local Milky Way stellar kinematic substructures with Gaiae DR3. 2023, 521, 2623-2648	O
150	Detecting and characterizing pulsar haloes with the Cherenkov telescope array. <b>2023</b> , 521, 3793-3809	O
149	Extending the extinction law in 30 Doradus to the infrared with JWST. 2023, 671, L14	O
148	NGTS clusters survey IIV. Search for Dipper stars in the Orion Nebular Cluster. 2023, 521, 1700-1726	O
147	The PEPSI Exoplanet Transit Survey (PETS). II. A Deep Search for Thermal Inversion Agents in KELT-20 b/MASCARA-2 b with Emission and Transmission Spectroscopy*. <b>2023</b> , 165, 157	O
146	Circumstellar Medium Interaction in SN 2018lab, A Low-luminosity Type IIP Supernova Observed with TESS. <b>2023</b> , 945, 107	O
145	Examining the Rotation Period Distribution of the 40 Myr Tucana⊞orologium Association with TESS. <b>2023</b> , 945, 114	0
144	Characterization of a Set of Small Planets with TESS and CHEOPS and an Analysis of Photometric Performance. <b>2023</b> , 165, 134	O

143	JWST Low-resolution MIRI Spectral Observations of SN 2021aefx: High-density Burning in a Type Ia Supernova. <b>2023</b> , 945, L2	2
142	Planet engulfment detections are rare according to observations and stellar modelling. 2023, 521, 2969-2987	О
141	Evidence for AGN-regulated Cooling in Clusters at z $\sim$ 1.4: A Multiwavelength View of SPT-CL J0607-4448. <b>2023</b> , 944, 164	O
140	Testing nonparametrically for dependence between nonstationary time series with very few replicates.	О
139	A Catalog of 71 Coronal Line Galaxies in MaNGA: [Ne v] Is an Effective AGN Tracer. <b>2023</b> , 945, 127	O
138	Spatially Resolved Stellar Populations of 0.3 < z < 6.0 Galaxies in WHL 013708 and MACS 0647+70 Clusters as Revealed by JWST: How Do Galaxies Grow and Quench over Cosmic Time?. 2023, 945, 117	О
137	Resolving the Emission Regions of the Crab Pulsar Giant Pulses. II. Evidence for Relativistic Motion. <b>2023</b> , 945, 115	0
136	Measurement of Telescope Transmission Using a Collimated Beam Projector. <b>2023</b> , 135, 035001	Ο
135	Application of Deep Reinforcement Learning to Major Solar Flare Forecasting. 2023, 265, 34	O
134	The Calar Alto CAFOS direct imaging first data release. <b>2023</b> , 521, 3127-3149	O
133	Multi-scale Physical Properties of NGC 6334 as Revealed by Local Relative Orientations between Magnetic Fields, Density Gradients, Velocity Gradients, and Gravity. <b>2023</b> , 945, 160	О
132	Evidence for Black Holes in Green Peas from WISE Colors and Variability. 2023, 945, 157	O
131	Why weak lensing cluster shapes are insensitive to self-interacting dark matter. 2023, 521, 3172-3185	Ο
130	Comet P/2021 HS (PANSTARRS) and the Challenge of Detecting Low-activity Comets. <b>2023</b> , 4, 47	О
130	Comet P/2021 HS (PANSTARRS) and the Challenge of Detecting Low-activity Comets. <b>2023</b> , 4, 47  The MUSE Ultra Deep Field (MUDF). III. Hubble Space Telescope WFC3 Grism Spectroscopy and Imaging. <b>2023</b> , 265, 40	0
	The MUSE Ultra Deep Field (MUDF). III. Hubble Space Telescope WFC3 Grism Spectroscopy and	
129	The MUSE Ultra Deep Field (MUDF). III. Hubble Space Telescope WFC3 Grism Spectroscopy and Imaging. 2023, 265, 40  Firefly: A Browser-based Interactive 3D Data Visualization Tool for Millions of Data Points. 2023,	1

125	Neutrino follow-up with the Zwicky transient facility: results from the first 24 campaigns. <b>2023</b> , 521, 5046-5063	0
124	GPU-based framework for detecting small Solar system bodies in targeted exoplanet surveys. <b>2023</b> , 521, 4568-4578	О
123	Fast transitions of X-ray variability in the black hole transient GX 339臣: comparison with MAXI J1820+070 and MAXI J1348日30. <b>2023</b> , 521, 3570-3584	O
122	TOI-1695 b: A Water World Orbiting an Early-M Dwarf in the Planet Radius Valley. 2023, 165, 167	O
121	Data Combination: Interferometry and Single-dish Imaging in Radio Astronomy. <b>2023</b> , 135, 034501	O
120	The Messy Nature of Fiber Spectra: StartQuasar Pairs Masquerading as Dual Type 1 AGNs. <b>2023</b> , 945, 167	О
119	JWST PEARLS: Dust Attenuation and Gravitational Lensing in the Backlit-galaxy System VV 191. <b>2023</b> , 165, 166	O
118	Two new white dwarfs with variable magnetic Balmer emission lines. <b>2023</b> , 522, 693-699	О
117	High-resolution Transmission Spectroscopy of the Terrestrial Exoplanet GJ 486b. 2023, 165, 170	O
116	Ground-based Optical Transmission Spectroscopy of the Nearby Terrestrial Exoplanet LTT 1445Ab. <b>2023</b> , 165, 169	O
115	A Candidate Relativistic Tidal Disruption Event at 340 Mpc. <b>2023</b> , 945, 142	О
114	The origin of optical emission lines in the soft state of X-ray binary outbursts: the case of MAXI J1820+070. <b>2023</b> , 521, 4190-4206	О
113	Applying the Metallicity-dependent Binary Fraction to Double White Dwarf Formation: Implications for LISA. <b>2023</b> , 945, 162	O
112	Addressing Systematics in the Traceback Age of the Pictoris Moving Group. 2023, 946, 6	O
111	Introducing TIGRESS-NCR. I. Coregulation of the Multiphase Interstellar Medium and Star Formation Rates. <b>2023</b> , 946, 3	O
110	A Systematic View of Ten New Black Hole Spins. <b>2023</b> , 946, 19	О
109	New Recurrently Active Main-belt Comet 2010 LH15. <b>2023</b> , 7, 60	О
108	Correlating Changes in Spot Filling Factors with Stellar Rotation: The Case of LkCa 4. <b>2023</b> , 946, 10	O

Towards the systematic detection of active asteroid candidates: A photometric method. 2023, 521, 6075-6088 o 107 On the impact of spectral template uncertainties in synthetic stellar populations. 2023, 521, 4995-5012 106 Hydrodynamic Simulations of a Relativistic Jet Interacting with the Intracluster Medium: 105  $\circ$ Application to Cygnus A. 2023, 11, 51 IC 5146 Dark Streamer: The First Reliable Candidate of Edge Collapse, Hub-filament Systems, and 104 Intertwined Sub-filaments. 2023, 946, 22 Measuring Galactic dark matter through unsupervised machine learning. 2023, 521, 5100-5119 103 O The multiwavelength view of shocks in the fastest nova V1674 Her. 2023, 521, 5453-5472 102 Searching for Supernovae in HETDEX Data Release 3\*. 2023, 946, 31 101 O Bayesian Implications for the Primordial Black Holes from NANOGrav® Pulsar-Timing Data Using 100 the Scalar-Induced Gravitational Waves. 2023, 9, 157 Impact of Rubin Observatory Cadence Choices on Supernovae Photometric Classification. 2023,  $\circ$ 99 265, 43 3D radiative transfer modelling and virial analysis of starless cores in the B10 region of the Taurus 98 molecular cloud. 2023, 521, 4579-4597 Stirred but not shaken: a multiwavelength view of HD 16743 debris disc. 2023, 521, 5940-5951 97 0 Photometric Catalogue for Space and Ground Night-Time Remote-Sensing Calibration: RGB 96  $\circ$ Synthetic Photometry from Gaia DR3 Spectrophotometry. 2023, 15, 1767 CEERS Epoch 1 NIRCam Imaging: Reduction Methods and Simulations Enabling Early JWST Science O 95 Results. 2023, 946, L12 The First Survey of Quiet Sun Features Observed in Hard X-Rays with NuSTAR. 2023, 298, 94 O The Quest for the Missing Dust. II. Two Orders of Magnitude of Evolution in the Dust-to-gas Ratio 93  $\circ$ Resolved within Local Group Galaxies. 2023, 946, 42 Outlook for detecting the gravitational-wave displacement and spin memory effects with current 92 and future gravitational-wave detectors. 2023, 107, Revising Properties of Planet Bost Binary Systems. III. There Is No Observed Radius Gap for Kepler 91 O Planets in Binary Star Systems\* . 2023, 165, 177 CEERS Key Paper. III. The Diversity of Galaxy Structure and Morphology at z = 3D with JWST. 2023, 90 946, L15

89	The Optical Light Curve of GRB 221009A: The Afterglow and the Emerging Supernova. 2023, 946, L22	0
88	Limit on Supernova Emission in the Brightest Gamma-Ray Burst, GRB 221009A. <b>2023</b> , 946, L25	О
87	Crowdsourced Doppler measurements of time standard stations demonstrating ionospheric variability. <b>2023</b> , 15, 1403-1418	0
86	Elemental Abundances of Kepler Objects of Interest in APOGEE DR17. 2023, 165, 178	O
85	Dynamics of Molecular Gas in the Central Region of the Quasar I Zwicky 1. <b>2023</b> , 946, 45	O
84	TOI-2525 b and c: A Pair of Massive Warm Giant Planets with Strong Transit Timing Variations Revealed by TESS*. <b>2023</b> , 165, 179	O
83	Prediction and Verification of Parker Solar Probe Solar Wind Sources at 13.3 'R?. 2023, 128,	0
82	GRB 221009A: Discovery of an Exceptionally Rare Nearby and Energetic Gamma-Ray Burst. <b>2023</b> , 946, L24	0
81	The First JWST Spectrum of a GRB Afterglow: No Bright Supernova in Observations of the Brightest GRB of all Time, GRB 221009A. <b>2023</b> , 946, L28	0
80	Abell 1201: detection of an ultramassive black hole in a strong gravitational lens. <b>2023</b> , 521, 3298-3322	O
79	Forming intracluster gas in a galaxy protocluster at a redshift of 2.16. <b>2023</b> , 615, 809-812	O
78	StarHorse results for spectroscopic surveys and Gaia DR3: Chrono-chemical populations in the solar vicinity, the genuine thick disk, and young alpha-rich stars.	O
77	UVIT Observations of the Small Magellanic Cloud: Point-source Catalog. 2023, 946, 65	O
76	COOLIIAMPS. III. Discovery of a 25.?9 Separation Quasar Lensed by a Merging Galaxy Cluster* ´. <b>2023</b> , 946, 63	О
75	First BISTRO Observations of the Dark Cloud Taurus L1495A-B10: The Role of the Magnetic Field in the Earliest Stages of Low-mass Star Formation. <b>2023</b> , 946, 62	0
74	Time-resolved Optical Polarization Monitoring of the Most Variable Brown Dwarf. 2023, 165, 181	0
73	The SAMIBornax Dwarfs Survey [III. Evolution of [Fe] in dwarfs, from Galaxy Clusters to the Local Group. <b>2023</b> , 522, 130-150	О
72	L-dwarf Detection from SDSS Images using Improved Faster R-CNN. <b>2023</b> , 165, 184	O

71	Implications for the Formation of (155140) 2005 UD from a New Convex Shape Model. 2023, 4, 56	O
70	Bubble in the Whale: Identifying the Optical Counterparts and Extended Nebula for the Ultraluminous X-Ray Sources in NGC 4631. <b>2023</b> , 946, 72	O
69	Multiclass classification of Fermi-LAT sources with hierarchical class definition. 2023, 521, 6195-6209	O
68	A cosmic stream of atomic carbon gas connected to a massive radio galaxy at redshift 3.8. <b>2023</b> , 379, 1323-1326	1
67	The most luminous, merger-free AGNs show only marginal correlation with bar presence. <b>2023</b> , 522, 211-225	O
66	The clumpy structure of ? Eridani debris disc revisited by ALMA. <b>2023</b> , 521, 6180-6194	O
65	HST viewing of spectacular star-forming trails behind ESO 137-001. <b>2023</b> , 522, 173-194	0
64	TESS Observations of the Pleiades Cluster: A Nursery for 🖾 cuti Stars. <b>2023</b> , 946, L10	O
63	SN 2020jgb: A Peculiar Type Ia Supernova Triggered by a Helium-shell Detonation in a Star-forming Galaxy. <b>2023</b> , 946, 83	0
62	Coherent radio bursts from known M-dwarf planet-host YZ Ceti.	О
62	Coherent radio bursts from known M-dwarf planet-host YZ Ceti.  Search for a Black Hole Binary in Gaia DR3 Astrometric Binary Stars with Spectroscopic Data. <b>2023</b> , 946, 79	0
	Search for a Black Hole Binary in Gaia DR3 Astrometric Binary Stars with Spectroscopic Data. <b>2023</b> ,	
61	Search for a Black Hole Binary in Gaia DR3 Astrometric Binary Stars with Spectroscopic Data. <b>2023</b> , 946, 79  Abundance Ratios of OH/CO and HCO+/CO as Probes of the Cosmic-Ray Ionization Rate in Diffuse	0
61	Search for a Black Hole Binary in Gaia DR3 Astrometric Binary Stars with Spectroscopic Data. 2023, 946, 79  Abundance Ratios of OH/CO and HCO+/CO as Probes of the Cosmic-Ray Ionization Rate in Diffuse Clouds'. 2023, 946, 91  Observed UV Continuum Slopes (#of Galaxies at z = 0.400.75 in the GOODS-North Field. 2023,	0
61 60 59	Search for a Black Hole Binary in Gaia DR3 Astrometric Binary Stars with Spectroscopic Data. 2023, 946, 79  Abundance Ratios of OH/CO and HCO+/CO as Probes of the Cosmic-Ray Ionization Rate in Diffuse Clouds'. 2023, 946, 91  Observed UV Continuum Slopes (Fof Galaxies at z = 0.400.75 in the GOODS-North Field. 2023, 946, 90  A declining major merger fraction with redshift in the local Universe from the largest-yet catalogue	0 0
61 60 59 58	Search for a Black Hole Binary in Gaia DR3 Astrometric Binary Stars with Spectroscopic Data. 2023, 946, 79  Abundance Ratios of OH/CO and HCO+/CO as Probes of the Cosmic-Ray Ionization Rate in Diffuse Clouds'. 2023, 946, 91  Observed UV Continuum Slopes (∰of Galaxies at z = 0.400.75 in the GOODS-North Field. 2023, 946, 90  A declining major merger fraction with redshift in the local Universe from the largest-yet catalogue of major and minor mergers in SDSS. 2023, 522, 1-28	O O O
61 60 59 58	Search for a Black Hole Binary in Gaia DR3 Astrometric Binary Stars with Spectroscopic Data. 2023, 946, 79  Abundance Ratios of OH/CO and HCO+/CO as Probes of the Cosmic-Ray Ionization Rate in Diffuse Clouds'. 2023, 946, 91  Observed UV Continuum Slopes (Flof Galaxies at z = 0.400.75 in the GOODS-North Field. 2023, 946, 90  A declining major merger fraction with redshift in the local Universe from the largest-yet catalogue of major and minor mergers in SDSS. 2023, 522, 1-28  Spectral performance of the Microchannel X-ray Telescope on board the SVOM mission.  Dark Energy Survey Year 3 results: Constraints on extensions to CDM with weak lensing and	O O O

53	A hard look at the X-ray spectral variability of NGC 7582. <b>2023</b> , 522, 1169-1182	О
52	Metal line emission from galaxy haloes at z 🗈 . <b>2023</b> , 522, 535-558	O
51	pyTANSPEC: A data reduction package for TANSPEC. <b>2023</b> , 44,	0
50	Constraining IDM with density-split clustering. <b>2023</b> , 522, 606-625	O
49	Local stellar formation history from the 40 pc white dwarf sample. <b>2023</b> , 522, 1643-1661	O
48	Modelling the cosmological LymanWerner background radiation field in the early Universe. <b>2023</b> , 522, 330-349	O
47	Cosmological constraints from galaxy clusters and groups in the eROSITA final equatorial depth survey. <b>2023</b> , 522, 1601-1642	О
46	Galaxy and Mass Assembly (GAMA): Low-redshift Quasars and Inactive Galaxies Have Similar Neighbors´. <b>2023</b> , 946, 116	O
45	UVIT view of NGC 5291: Ongoing star formation in tidal dwarf galaxies at $\sim 0.35\mathrm{kpc}$ resolution. <b>2023</b> , 522, 1196-1207	O
44	AGN STORM 2. III. A NICER View of the Variable X-Ray Obscurer in Mrk 817. <b>2023</b> , 947, 2	O
43	Chemical Modeling of Orion Nebula Cluster Disks: Evidence for Massive, Compact Gas Disks with Interstellar Gas-to-dust Ratios. <b>2023</b> , 947, 7	O
42	Distances to Nearby Molecular Clouds Traced by Young Stars. <b>2023</b> , 265, 59	O
41	Validation and Testing of the CROBAR 3D Coronal Reconstruction Method with a MURaM Simulation. <b>2023</b> , 947, 5	О
40	Revealing the Interior Structure of Icy Moons with a Bayesian Approach to Magnetic Induction Measurements. <b>2023</b> , 4, 62	O
39	Shocks and Photoionization of the Inner 650 au Jet of the Interacting Binary Star R Aquarii from Multiwavelength Hubble Space Telescope Observations. <b>2023</b> , 947, 11	O
38	CosmoDRAGoN simulations Dynamics and observable signatures of radio jets in cosmological environments. <b>2023</b> , 40,	O
37	TIC 219006972: a compact, coplanar quadruple star system consisting of two eclipsing binaries with an outer period of 168′d. <b>2023</b> , 522, 90-101	О
36	Evolutionary and Observational Properties of Red Giant Acoustic Glitch Signatures. <b>2023</b> , 947, 22	O

35	A systematic survey of millimetre-wavelength flaring variability of young stellar objects in the Orion Nebula Cluster. <b>2023</b> , 522, 56-69	Ο
34	Strong Variability in AzV 493, an Extreme Oe-type Star in the SMC. <b>2023</b> , 947, 27	O
33	Nuclear Activity in the Low-metallicity Dwarf Galaxy SDSS J0944-0038 : A Glimpse into the Primordial Universe. <b>2023</b> , 946, L38	О
32	Saying Hallo to M94's Stellar Halo: Investigating the Accretion History of the Largest Pseudobulge Host in the Local Universe. <b>2023</b> , 947, 21	Ο
31	Unveiling the nature of infrared bright, optically dark galaxies with early JWST data. 2023, 522, 449-456	O
30	Spatially-resolved chemodynamics of the starburst dwarf galaxy CGCG 007-025: Evidence for recent accretion of metal-poor gas.	O
29	Search for X-Ray Quasiperiodicity of Six AGNs Using the Gaussian Process Method. 2023, 946, 52	0
28	Calibrating X-Ray Binary Luminosity Functions via Optical Reconnaissance. II. The High-mass XLF and Globular Cluster Population of X-Ray Binaries in the Low Star-forming Spiral M81. <b>2023</b> , 947, 31	Ο
27	A LAMOST Spectroscopic Study of T Tauri Stars in the Orion OB1a Subassociation. 2023, 165, 205	О
26	Overview of the DESI Milky Way Survey. <b>2023</b> , 947, 37	1
26 25	Overview of the DESI Milky Way Survey. <b>2023</b> , 947, 37  X-Ray Cluster Cosmology. <b>2023</b> , 1-52	0
25	X-Ray Cluster Cosmology. <b>2023</b> , 1-52	0
25	X-Ray Cluster Cosmology. <b>2023</b> , 1-52  X-Ray-luminous Supernovae: Threats to Terrestrial Biospheres. <b>2023</b> , 947, 42	0
25 24 23	X-Ray Cluster Cosmology. 2023, 1-52  X-Ray-luminous Supernovae: Threats to Terrestrial Biospheres. 2023, 947, 42  IXPE Observations of the Quintessential Wind-accreting X-Ray Pulsar Vela X-1. 2023, 947, L20  SPT-CL J2215B537: A Massive Starburst at the Center of the Most Distant Relaxed Galaxy Cluster.	0 0
25 24 23 22	X-Ray Cluster Cosmology. 2023, 1-52  X-Ray-luminous Supernovae: Threats to Terrestrial Biospheres. 2023, 947, 42  IXPE Observations of the Quintessential Wind-accreting X-Ray Pulsar Vela X-1. 2023, 947, L20  SPT-CL J2215B537: A Massive Starburst at the Center of the Most Distant Relaxed Galaxy Cluster. 2023, 947, 44  The SSA22 H i Tomography Survey (SSA22-HIT). I. Data Set and Compiled Redshift Catalog. 2023,	o o o
25 24 23 22 21	X-Ray-luminous Supernovae: Threats to Terrestrial Biospheres. 2023, 947, 42  IXPE Observations of the Quintessential Wind-accreting X-Ray Pulsar Vela X-1. 2023, 947, L20  SPT-CL J2215B537: A Massive Starburst at the Center of the Most Distant Relaxed Galaxy Cluster. 2023, 947, 44  The SSA22 H i Tomography Survey (SSA22-HIT). I. Data Set and Compiled Redshift Catalog. 2023, 165, 208  Predicting light curves of RR Lyrae variables using artificial neural network based interpolation of a	0 0 0

17	Target-of-Opportunity Observation Detectability of Kilonovae with WFST. 2023, 947, 59	О
16	Planet Eclipse Mapping with Long-term Baseline Drifts. <b>2023</b> , 165, 210	O
15	Searching for Gravitational-wave Counterparts Using the Transiting Exoplanet Survey Satellite. <b>2023</b> , 948, L3	O
14	Peeking beneath the precision floor II. Probing the chemo-dynamical histories of the potential globular cluster siblings, NGC 288 and NGC 362. <b>2023</b> , 522, 4404-4420	O
13	CHIME/FRB Discovery of 25 Repeating Fast Radio Burst Sources. <b>2023</b> , 947, 83	O
12	PACMan2: Next Steps in Proposal Review Management. <b>2023</b> , 165, 215	O
11	Phase Curves of Kuiper Belt Objects, Centaurs, and Jupiter-family Comets from the ATLAS Survey. <b>2023</b> , 4, 75	О
10	Detections of [C ii] 158 th and [O iii] 88 th in a Local Lyman Continuum Emitter, Mrk 54, and Its Implications to High-redshift ALMA Studies*. <b>2023</b> , 948, 3	O
9	CO or no CO? Narrowing the CO abundance constraint and recovering the H2O detection in the atmosphere of WASP-127 b using SPIRou. <b>2023</b> , 522, 5062-5083	О
8	Alignment and rotational disruption of dust grains in the Galactic Centre revealed by polarized dust emission. <b>2023</b> , 522, 4196-4214	O
7	A search for transients in the Reionization Lensing Cluster Survey (RELICS): three new supernovae. <b>2023</b> , 522, 4718-4727	0
6	A framework to measure the properties of intergalactic metal systems with two-point flux statistics. <b>2023</b> , 522, 5980-5995	O
5	Statistical properties of Hipparcos 2, caveats on its use, and a recalibration of the intermediate astrometric data. <b>2023</b> , 2, 218-230	O
4	Physical properties of the slow-rotating near-Earth asteroid (2059) Baboquivari from one apparition. <b>2023</b> , 232, 105698	O
3	The LyReference Sample. XIV. LyImaging of 45 Low-redshift Star-forming Galaxies and Inferences on Global Emission. <b>2023</b> , 266, 15	О
2	Spatially Resolved Properties of Galaxies at 5 < z < 9 in the SMACS 0723 JWST ERO Field. <b>2023</b> , 948, 126	O
1	Testing AGN outflow and accretion models with C îv and He îi emission line demographics in z D quasars.	О